Identification of Factors Controlling the Development of Subsidence Impacts Forecasting Methodology of the I-70 Alignment over Longwall Mining of the Tunnel Ridge Mine, Washington County, Pennsylvania

FINAL REPORT

26 February 2021

Anthony Iannacchione, Luis Vallejo, Julie Vandenbossche, Mingzhou Li, Emily Adelsohn, and Robert Winn

Civil and Environmental Engineering,
Swanson School of Engineering,
University of Pittsburgh

COMMONWEALTH OF PENNSYLVANIA

DEPARTMENT OF TRANSPORTATION

CONTRACT # 4400018535
WORK ORDER # PIT 016

1. Report No. FHWA-PA-016-PITT WO 016	**2. Government Accession No.**	**3. Recipient's Catalog No.**

4. Title and Subtitle Identification of Factors Controlling the Development of Subsidence Impacts Forecasting Methodology to the I-70 Alignment over Longwall Mining of the Tunnel Ridge Mine, Washington County, Pennsylvania	**5. Report Date** 26 February 2021 **6. Performing Organization Code**
7. Author(s) Anthony Iannacchione, Luis Vallejo, Julie Vandenbossche, Mingzhou Li, Emily Adelsohn, and Robert Winn	**8. Performing Organization Report No.**
9. Performing Organization Name and Address Civil and Environment Engineering Department, 742 Benedum Hall Swanson School of Engineering, 4800 O'Hara Street University of Pittsburgh, Pittsburgh, PA 15261	**10. Work Unit No. (TRAIS)** **11. Contract or Grant No.** **4400018535, PITT WO 016**
12. Sponsoring Agency Name and Address The Pennsylvania Department of Transportation Bureau of Planning and Research Commonwealth Keystone Building 400 North Street, 6th Floor Harrisburg, PA 17120-0064	**13. Type of Report and Period Covered** Final Report, Oct 2018 to Feb 2021 **14. Sponsoring Agency Code**

15. Supplementary Notes
University of Pittsburgh contact(s) – Dr(s) Anthony Iannacchione, ati2@pitt.edu; and Julie Vandenbossche, jmv7@pitt.edu
PennDOT contact – Roy Painter, ropainter@pa.gov

16. Abstract

In the winter of 2019, the Tunnel Ridge Mine extracted a longwall panel under I-70 in Washington County, PA. Additional longwall panels under other portions of the highway are planned in the future. The extraction of these panels can produce a subsidence basin with maximum surface drops from 4 to more than 5-ft, the majority of which occurs within one or two months of undermining the roadway. This project investigates the influence of longwall mining on highway alignments and associated slopes and embankments, evaluates how the highway deforms during undermining with a focus on determining its transient characteristics, utilizes models to better understand subsidence impacts to the highway alignment, and where possible, determines how other future highway alignments could be impacted.

17. Key Words Longwall coal mining, subsidence, subsidence induced movement, subsidence induced strain, roadway assets impacted by subsidence, highway subsidence, subsidence movement.	**18. Distribution Statement** No restrictions. This document is available from the National Technical Information Service, Springfield, VA 22161

19. Security Classif. (of this report)	**20. Security Classif. (of this page)**	**21. No. of Pages**	**22. Price**
Unclassified	Unclassified	700	

Form DOT F 1700.7 **(8-72)** **Reproduction of completed page authorized**

IDENTIFICATION OF FACTORS CONTROLLING THE DEVELOPMENT OF SUBSIDENCE IMPACTS FORECASTING METHODOLOGY TO THE I-70 ALIGNMENT OVER LONGWALL MINING OF THE TUNNEL RIDGE MINE, WASHINGTON COUNTY, PA

Final Contract Report
26 February 2021

The University of Pittsburgh Master Agreement
Contract No. 4400018535

Project Team

Anthony Iannacchione, Retired Associate Professor, Principal Investigator*
Luis Vallejo, Professor, Co-Principal Investigator
Julie Vandenbossche, Professor
Mingzhou Li, Graduate Research Student
Emily Adelsohn, Graduate Research Student
Robert Winn, Graduate Research Student
** - Email ati2@pitt.edu, Phone: 412-624-8289*

"This work was sponsored by the Pennsylvania Department of Transportation and the U.S. Department of Transportation, Federal Highway Administration."

Final Task Report

Authors of the Final Report
Anthony Iannacchione, Retired Associate Professor
Julie Vandenbossche, Professor
Robert Winn, Graduate Research Student

SECTION I – INTRODUCTION

Three task reports were delivered to PennDOT and are provided in Appendix I, II, and III. This final report provides a summary of the most important findings discussed in these three reports. The three task reports are constructed to summarize research activities prior to, during, and after the undermining of I-70 by Panel 15 of the Tunnel Ridge Mine.

Subsection Ia – Project Scope

1.0 Background

Longwall coal mining was introduced to Pennsylvania in the late 1960's. Since that time, almost 800 hundred longwall panels have extracted huge reserves of coal. Of this total, twenty-five panels have undermined parts of two interstate highways, I-70 and I-79. These twenty-five panels are located in four mines: Gateway, Eight-Four, Cumberland, and Emerald.

Over the last five decades, there has been a great deal of effort to understand how longwall subsidence basin formation impacts surface features, such as buildings, water supplies, streams and wetlands. Less is known as to how subsidence can impact interstates and even less about the embankments and cuts that carry these highway alignments. In some areas, careful monitoring of conditions and asphalt re-surfacing repaired the subsidence damage with only minimal impact to highway traffic. In other cases, bridges carrying I-79, as well as overpass structures, had to be replaced (Iannacchione, et al., 2011). Traffic delays were most noticeable during milling and paving activities. It should be stated that the University is not aware of any subsidence impacts causing a highway accident or injuring the traveling public.

2.0 Contract

The University of Pittsburgh (herein referred to as the 'University') submitted a proposal to Pennsylvania Department of Transportation (PennDOT) in May 2018. This proposal has the University studying data collected by PennDOT and its contractors during periods where an interstate was impacted by longwall subsidence. It also requires the University to assess the risk to other areas along Pennsylvania interstate alignments that might be impacted by longwall subsidence in the future.

The University received a notice to proceed with this effort on 3 October 2018. The contract is scheduled to end on 26 February 2021 at a cost of $516,348.30. The project is administered by Shelley Scott with Roy Painter as the technical advisor. This contract requires five task with the fifth task being the submission of a final report. This final report summarizes the most important information contained within the three tasks reports and also discusses considerations for the future.

Subsection Ib – Project Objective

Alliance Coal's Tunnel Ridge Mine has plans to undermine I-70 with the longwall mining method in both Pennsylvania and West Virginia over the next two decades. As of the writing of this report, three Tunnel Ridge longwall panels have undermined I-70; one, Panel 15, is largely in Pennsylvania with a small portion in West Virginia, and two others, Panels 16 and 17, are entirely in West Virginia. PennDOT took the initiative to full investigate Panel 15 in 2019 in preparation for future longwall mining under I-70 in the future. The objectives of this study are to:

1) Investigate the influence of longwall mining on highway alignments and associated slopes and embankments.
2) Evaluate how the highway deforms during undermining with a focus on determining its transient characteristics.
3) Utilize models to better understand subsidence impacts to the highway alignment, and where possible,
4) Determine how other future highway alignments could be impacted.

Subsection Ic – Overview

This project has two distinct study areas. The first has to do with detailed monitoring of the I-70 highway alignment during the undermining by longwall Panel 15 of the Tunnel Ridge Mine. The planning for this monitoring effort is discussed the Task 1 Report. Description and analysis of this data are reported in the Task 2 and 3 Reports. It should be noted that monitoring stopped a few months after Panel 15 passed under the study area. No attempt was made to monitor I-70 study area conditions when the adjacent Panel 16 was extracted in the fall of 2019.

Panel 15 lies less than one mile southwest of the West Alexander I-70 interchange. The initial study area is designated as the 3,300-ft of I-70 that spans the subsidence basin developed by the extraction of Panel 15 (Figure Ic.1). This subsidence basin consist of the 2,130-ft of I-70 above Panel 15, the adjacent gate road entries add another 520-ft (2 x 260-ft) of highway, and an additional 650-ft (2 x 325-ft) buffer zone over the unmined coal. The western end of this area lies ~700-ft into the State of West Virginia with the remaining 2,600-ft within the Commonwealth of Pennsylvania.

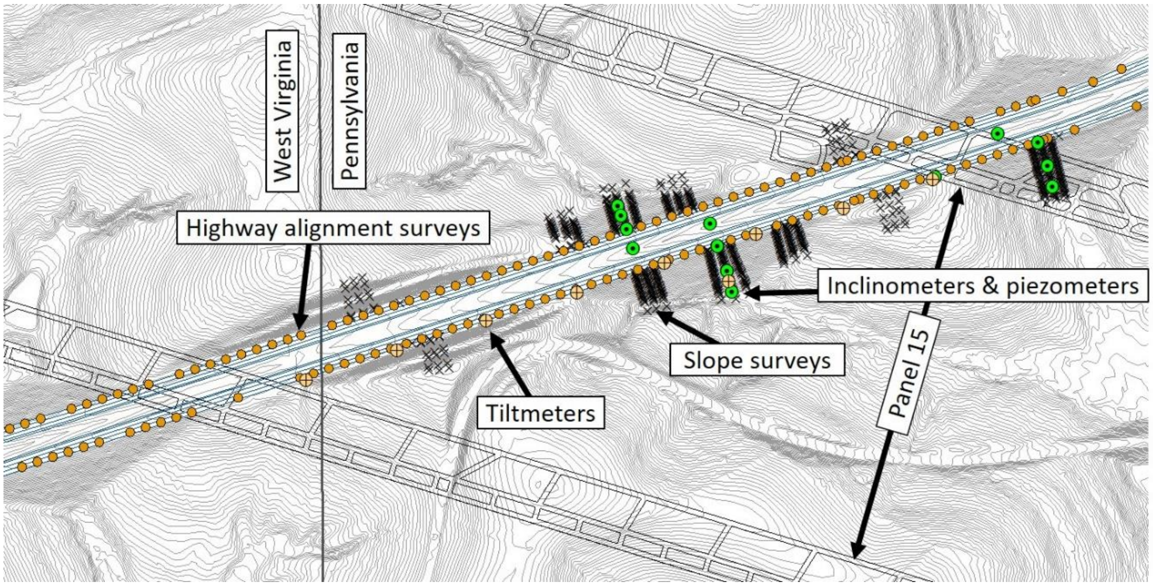

Figure Ic.1 - The initial study area and the location of monitoring instrumentation

The extended study area encompasses a portion of the Tunnel Ridge Mine reserves of the Pittsburgh Coalbed in western Pennsylvania (Figure Ic.2). A significant share of these reserves has the potential to be mined in the next two decades by the longwall mining method. The University was able to take the knowledge gained during the undermining of Panel 15, where a considerable array of monitoring equipment was assembled, to evaluate potential longwall mining subsidence impacts within the extended study area.

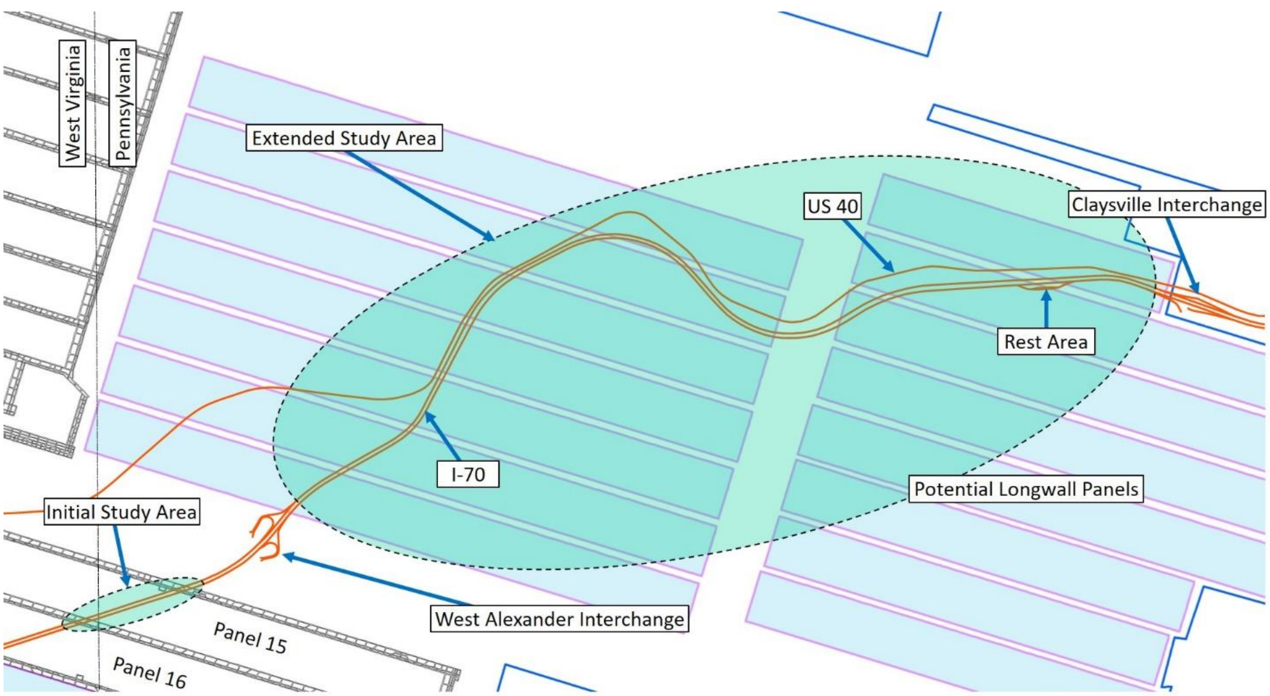

Figure Ic.2 – Extent of I-70 overlain by unmined portion of the Tunnel Ridge Mine reserves in Washington County, Pennsylvania. Also shown are the initial and extended study areas

SECTION II – SUMMARY OF FINDINGS

Three task reports were delivered to PennDOT and are provided in Appendix I, II, and III. This section provides a summary of the most important findings discussed in these three reports. The three task reports are constructed to summarize research activities prior to, during, and after the undermining of I-70 by Panel 15 of the Tunnel Ridge Mine.

Subsection IIa – Pre-Undermining Activities

1.0 Background

The Task 1 Report delivered to PennDOT on 2 July 2019 (see Appendix I) examined contract activities by the University of Pittsburgh prior to the undermining of I-70 by Panel 15 of the Tunnel Ridge Longwall Coal Mine. Panel 15 undermined a portion of I-70 in Pennsylvania in early 2019 approximately one mile southwest of the West Alexander I-70 interchange. This area is designated as the initial study area encompassing 3,300-ft of I-70 (Figure IIa.1). The western portion of the initial study area lies ~700-ft within the State of West Virginia and the remaining 2,600-ft within the Commonwealth of Pennsylvania.

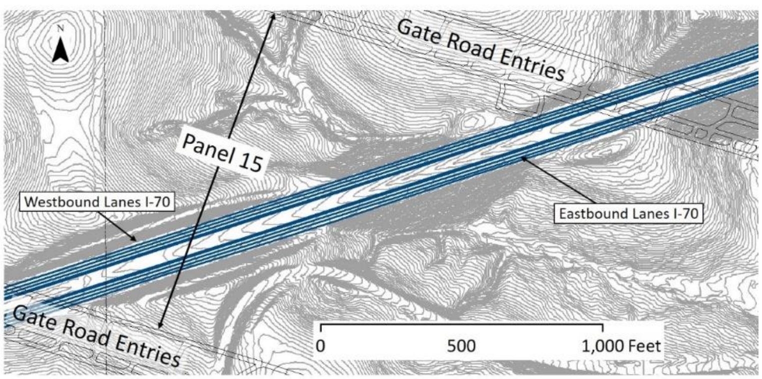

Figure IIa.1 – Characteristics of the initial study area encompassing the undermining of I-70 by Panel 15

2.0 History of Longwall Mining under Pennsylvania's Interstate Highways

Prior to the undermining of I-70 by Panel 15, twenty-five longwall panels have undermined Pennsylvania's Interstate highways (Table IIa.1). Five mines were involved starting in 1982 and ended in 2009. There has been a ten year span between the last undermining event at the Cumberland and Emerald Mines and the extraction of Panel 15 at the Tunnel Ridge Mine. The characteristics of the subsidence basin have significantly changed, first dominated by the subcritical subsidence basin type then by the supercritical type. Luo and Peng (1997) provided a widely used empirical formula for determining the width of a critical subsidence basin and the maximum vertical subsidence (Peng, Luo, and Zhang, 1995). The subcritical type basin never achieve the maximum subsidence for a particular overburden and extraction thickness. In the 1980's smaller panel widths produced subcritical subsidence basins with maximum vertical subsidence value of 3.2-ft. Once the critical panel width is exceeded, vertical subsidence achieve its maximum value for a particular overburden and extraction thickness. In the 1990's, panel widths across the basin exceeded the critical widths and are all of the supercritical type with an average maximum vertical subsidence value of 4.2-ft. As the shape and dimensions of the subsidence basin has change over time, so has its impact on overlying roadways.

Table IIa.1 – Characteristics of the twenty-five longwall panels that have undermined Pennsylvania's Interstate highways prior to 2019

Mine	Panel ID	Year Started	Panel Width, ft	Smax*, ft	Average Overburden, ft	Critical Panel Width, ft	Subsidence Basin Type
Gateway	0-Butt	1982	522	3.2	770	869	Subcritical
Gateway	1-Butt	1983	567	3.4	742	844	Subcritical
Gateway	2-Butt	1984	504	3.1	759	859	Subcritical
Gateway	3-Butt	1985	534	3.2	786	883	Subcritical
Gateway	4-Butt	1986	503	3.0	820	913	Subcritical
Gateway	7-Butt	1988	499	3.1	780	878	Subcritical
Gateway	8-Butt	1988	489	2.9	831	923	Subcritical
Gateway	9-Butt	1989	470	2.9	813	907	Subcritical
Mine 84	4-B	1986	612	4.1	556	680	Subcritical
Mine 84	4-C	1987	632	4.0	602	720	Subcritical
Mine 84	3-South	1999	1061	4.3	587	707	Supercritical
Mine 84	4-South	2000	1081	4.3	607	725	Supercritical
Cumberland	49	2003	1,270	4.1	741	843	Supercritical
Cumberland	50	2005	1,276	4.1	728	832	Supercritical
Cumberland	51	2005	1,276	4.2	709	815	Supercritical
Cumberland	52	2006	1,272	4.1	728	832	Supercritical
Cumberland	53	2007	1,271	4.2	693	801	Supercritical
Cumberland	54	2008	1,394	4.2	709	815	Supercritical
Cumberland	55	2008	1,394	4.2	713	818	Supercritical
Cumberland	56	2009	1,388	4.2	716	821	Supercritical
Emerald	B-3	2005	1,438	4.1	739	841	Supercritical
Emerald	B-4	2006	1,440	4.1	755	855	Supercritical
Emerald	B-5	2006	1,439	4.1	739	841	Supercritical
Emerald	B-6	2008	1,429	4.2	659	771	Supercritical
Emerald	B-7	2009	1,428	4.1	725	829	Supercritical

* Maximum vertical subsidence is dependent on overburden and extraction thickness. The extraction thickness for these panels is estimated to be 7.25-ft

The types of impacts experienced during the undermining of I-79 by the Cumberland and Emerald Mines from 2003 until 2009 was documented in a report by Iannacchione, et al. (2011). Impacts consisted of compression bumps, transverse cracks, joint faulting, and lane-to-should separations occurred (Figure IIa.2). It is estimated that PennDOT spent over 19 million dollars from 2002 to 2008 to repair these impacts (Table IIa.6, Task 1 Report).

Figure IIa.2 – Examples of surface damage on I-79 caused by Emerald and Cumberland undermining a) compression bump, b) transverse crack, c) joint faulting, and d) lane-to-shoulder separation (Iannacchione, et al., 2011) (Figure IIa.10, Task 1 Report)

3.0 Investigation of Southwestern Pennsylvania Interstate Slope Instabilities

Landslides have been a significant problem for roadways in southwestern Pennsylvania. Landslide impacts to the region's roadways and approaches to mitigate these occurrences were discussed at an IRISE sponsored workshop in August of 2019 (Iannacchione, et al., 2019). Attendees generally agreed that landslide related damage to roadways was one of this region's most significant transportation issues. For example, Painter (2020) reported that PennDOT District 12 is currently tracking over 300 landslides. District 12 is comprised of Washington, Greene, Fayette, and Westmoreland Counties. Many of these landslides developed in the past and are highly susceptible to additional failure when subjected to conditions that upset equilibrium. Mining induced subsidence has been identified as one of these conditions. Therefore, particular attention was paid to monitoring slope instabilities during the course of this study.

4.0 Analysis of As-Built Conditions

I-70 from the Claysville Interchange to the West Virginia State line was constructed in the late 1950's early 1960's. The as-built files provided by PennDOT helped to identify both the basic design of the highway as well as the location of large cuts and fills along this alignment (Figure IIa.2). Approximately 2.6 of the 5.7 miles of roadway was constructed using cuts and 3.6 miles using fill methods. The largest areas of cuts and fills represent potential slope instabilities risks. Embankments, because they contain the thickest fill and longest slopes, represent the highest risk for slope instabilities.

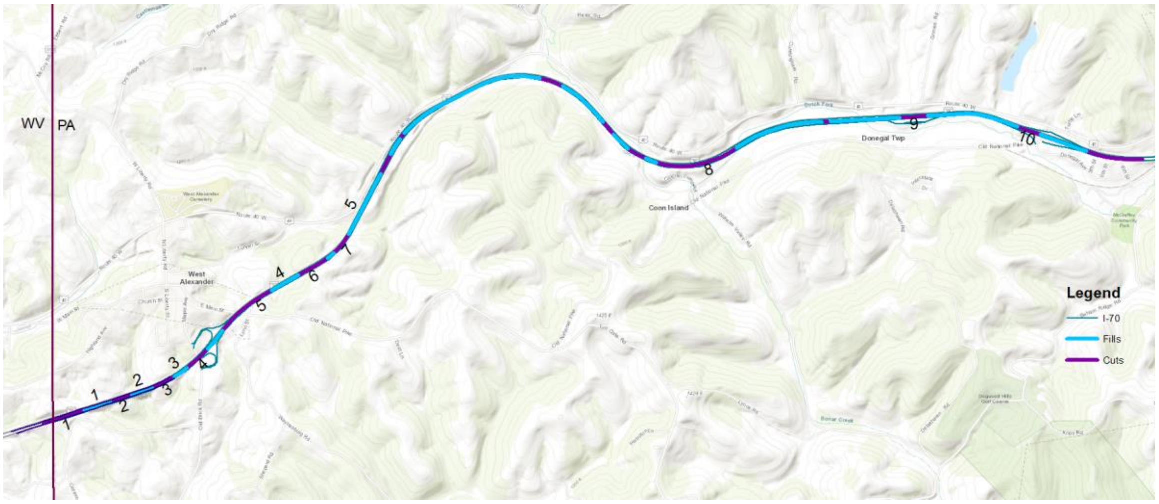

Figure IIa.2 – Cuts (purple) and Fills (blue) throughout study area with embankments and steep slopes numbered from left to right (Figure IIIa.1, Task 1 Report)

5.0 Location of Embankments

Six embankments were identified and basic characteristics determined (Figure IIa.3). Embankments #1 and #2 were expected to be within the subsidence basin formed during the mining of Panel 15. A decision was made to monitor both embankments. Embankment #3 was not planned to be undermined. Embankments #4, #5, and #6 are expected to be undermined in the future and would be studied during the post-undermining activity period.

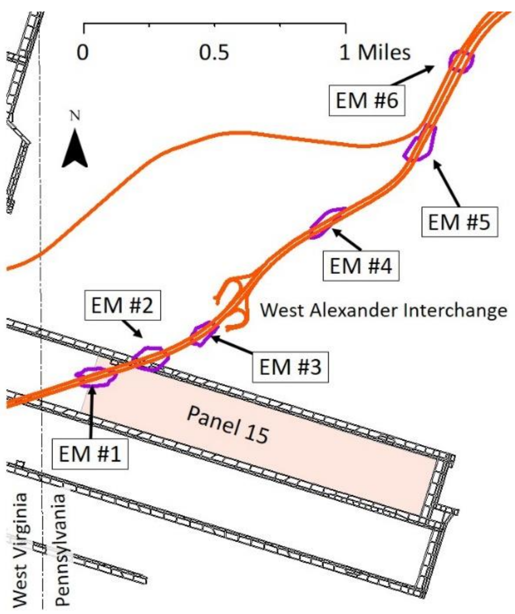

Figure IIa.3 – Six embankments were identified along the I-70 alignment between the Claysville Interchange and West Virginia State line

The as-built plans provided by PennDOT didn't contain details on the material properties comprising Embankments #1 and #2. Most of the boreholes were completed prior to construction of the embankments. Three important factors were identified within the as-built plans:

- The actual phreatic surface (height of groundwater) within the embankments was unknown,
- It was not clear if the colluvium soil that originally covered the surface was removed prior to adding the embankment fill, and
- The plans didn't indicate if the embankments were notched into bedrock (a common practice used in many similar projects today).

As a result, PennDOT decided to conduct a drilling program focused on answering some of these questions.

6.0 Evaluation of the Soil and Rock Laboratory Tests

Thirteen boreholes were drilled into Embankments #1 and #2 (Figure IIa.4). The embankment fill was subjected to standard soil laboratory tests including: Atterberg limits, grain size distribution curves, natural moisture content, optimum moisture content, dry unit weight, penetrometer tests to obtain the unconfined compression of soils, direct and Confined Undrained (CU) tri-axial testing to obtain the effective shear strength parameters (effective cohesion intercept, c, and effective friction angle, ϕ). A summary of these results is shown in (Table IIIb.2, Task 1 Report). In addition, three soil samples were collected from Embankment #1. All boreholes terminated in bedrock. The material properties of the bedrock showed a wide variety of types and strengths (Table III.b.4, Task 1 Report).

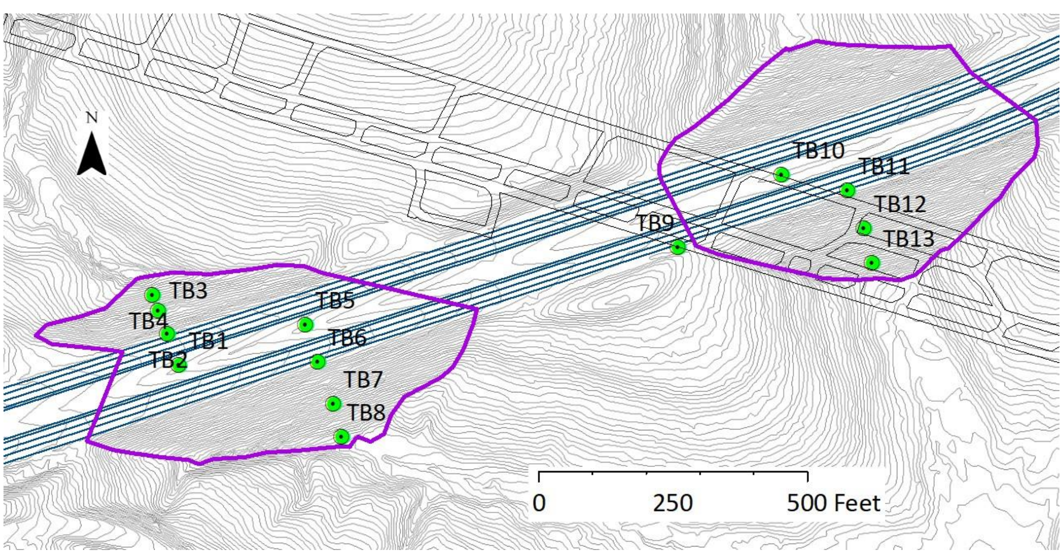

Figure IIa.4 – Location of boreholes drilled in Embankment #1 and #2.

The laboratory test found that Embankments #1 and #2 are composed mainly of soils of low plasticity (CL = clay of low plasticity and ML = silt of low plasticity and mixtures of silty clay with gravel). The values of the effective cohesion intercept, c, are generally low and range in values between 28.8 and 633.6-psf. The value of the effective angle of internal friction, ϕ, range in value between 23.2 and 33.5-deg. It should be noted that higher concentrations of gravels have been found to increase the strength of the CL and ML soils (Vallejo and Lobo-Guerrero, 2005). In particular, gravel acts to reinforce the soil structure producing higher value of the friction angle, ϕ. Thus, the presence of the gravel in the soils may enhance the stability of the embankments.

Perhaps the most important material properties identified with the laboratory testing was the strain hardening behavior of samples collected from Embankment #1. From the Consolidated-Undrained (CU) tests, plots are provided that relate the value of the deviator stress ($\Delta\sigma = \sigma_1 - \sigma_3$) with the axial strain (ε) in the samples subjected to tri-axial compression (Figures IIa.5). One sample identified as a brown elastic silt with sand soil (USCS description) behaves under tri-axial compression conditions as a strain hardening material (Figure IIa.5a). Another sample identified as a reddish crown sandy fat clay soil (USCS description) behaves as an elastic-plastic material (Figure IIa.5b). These findings are important for investigating embankment stability using the Finite Element approach.

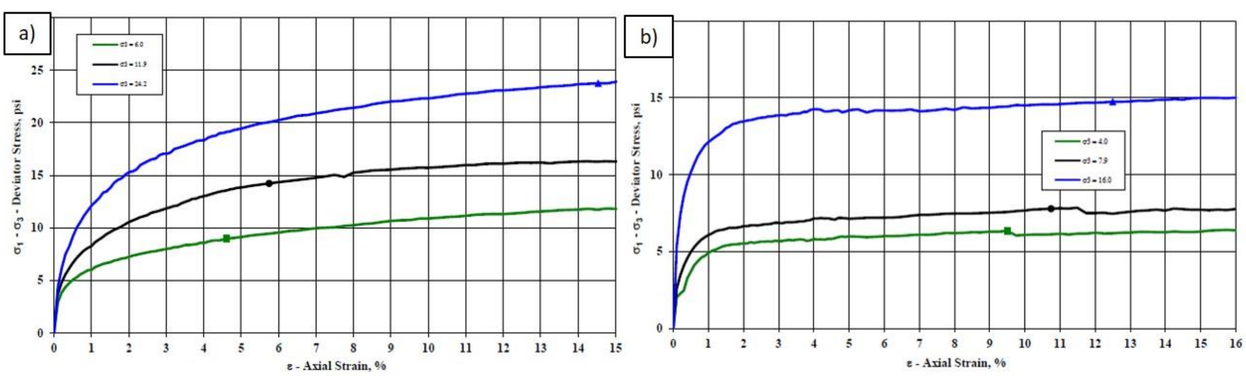

Figure IIa.5 – a) CU tri-axial compression test (ASTM D4767-11) on cohesive soils at a depth of 6.5 to 8.5-ft below the top of TB-8 (Figure IIIb.2, Task 1 Report); b) remolded, side and double drained, CU tri-axial compression test from near the surface of Embankment #1 (HS-2)

7.0 Initial Prediction of Panel 15 Final Subsidence Basin Characteristics using Empirical/Profile Methods

The University used two different methods to initially predict the characteristics of the final subsidence basin associated with the mining of Panel 15. The empirical relationships used in this study were developed by West Virginia University's Department of Mining Engineering in the mid-1990's (Peng, Luo, Zhang, 1995). These empirical relationships are used within a profile function to more fully characterize the Panel 15 subsidence basin.

Approximately 40 case studies from West Virginia and Pennsylvania longwall mines in the Pittsburgh Coalbed were used to develop fundamental relationships between vertical subsidence and overburden and extraction thickness for supercritical panels (see previous discussion). The most significant of these relationships are the determination of the maximum vertical subsidence and the location of the inflection point:

$a = 0.6760821 * 0.9997678^{h} = 0.6760821 * 0.9997678^{675} = 0.578$ [Eq. IVb.1, Task 1 Report]

$S_{max} = a * m = 0.578 * 7.25 \rightarrow S_{max} = 4.2\ ft$ [Eq. IVb.2, Task 1 Report]

$d = 0.45439 * h * e^{-0.000914*h} = 0.45439 * 675 * e^{-0.000914*675}$ [Eq. IVb.3, Task 1 Report]
d = 165-ft

Where:
a = Subsidence factor,
m = Extraction thickness, ft (7.25-ft)
Smax = Maximum vertical subsidence, ft
h = Overburden, ft (675-ft)
d = Distance from the inflection point to the edge of the solid coal, ft

The use of these empirical relationships and the profile function method produces a generalized prediction for the Panel 15 final subsidence basin (Figure IIa.6). For Panel 15 conditions, the inflection point would be located ~165-ft from the edge of longwall panel. The inflection point is associated with the maximum slope of the subsidence basin and the location where the surface will chance from extension to compression. The inflection point can be thought of as a line, or the inflection line, and projected behind the advancing longwall face to predict where the surface strains change from tension to compression.

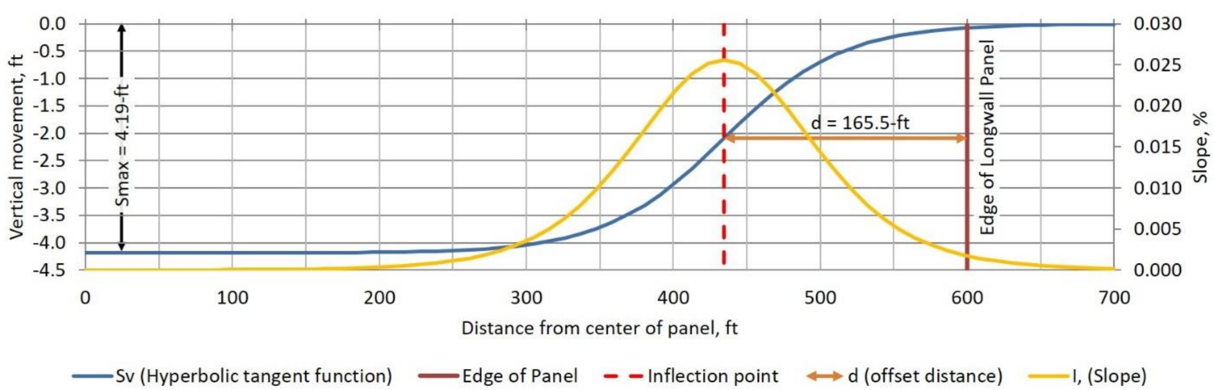

Figure IIa.6 – Generalized final subsidence basin sketched utilizing the profile function method and empirical relationships derived from Pittsburgh Coalbed data

8.0 Initial Prediction of Panel 15 Final Subsidence Basin Characteristics using the SDPS Model

The Surface Deformation Prediction System (SDPS) models was utilized to estimate parameters of the subsidence basin generated by the mining of Panel 15. The SDPS uses the influence function method and provides another technique to predict the final subsidence basin characteristics. The following assumptions were made for the SDPS analysis:

- Extraction thickness = 7.25-ft
- Supercritical Subsidence Factor = 64.2-pct
- Average overburden thickness is 675-ft
- Average percentage of hard rock is approximately 25-pct (typical for Pittsburgh Coalbed Longwall Mines)
- All pillars will remain rigid, minimizing vertical subsidence over the gate roads
- Surface is at a constant elevation (topography will be considered in the Task 3 Report activities)
- The longwall face progresses at an average rate of 115-ft/day

Under these conditions, the SDPS model predicts a maximum vertical subsidence of 4.65-ft and a maximum horizontal displacement of 1.63-ft (at the inflection point). The differences between the empirical/profile function and influence function (SDPS) methods shows the inherent uncertainty of predictive models and emphasize that the models will need to be calibrated to the specific behavior of Panel 15 once it is undermined.

9.0 A 3D Model Representative of the Initial Study Area Embankment Conditions Prior to Undermining

During Task 1 activities, the University and PennDOT decided to focus on investigating the potential for slope instabilities of embankments subjected to undermining. It was decided to begin constructing a numerical simulation that could take into account embankment material properties and geometry characteristics. This model would use stress-strain determinations to analyze slope stability prior-to, during, and after the formation of the planned subsidence basin. The University decided to utilize the ABAQUS Finite Element Method for this task.

Numerical simulations focused on Embankment #1 and the plan is to utilize actual field measurements collected during the undermining of Panel 15 to validate models. The field measurements will help to simulate the behavior of this embankment under both gravity loading and subsidence basin formation. The Shear Strength Reduction Method (SRM) will be utilize to estimate the factor of safety for Embankment #1 under these dramatically different conditions. Lastly, models would be investigated to identify the most likely location and characteristics of rupture surfaces within the embankment.

One of the first tasks was to use the soil profiled by Earth, Inc. (PennDOT subcontractor) from test borings and plotted the most important layers in 12 different cross sections. Material properties, including the shear strength parameters, were obtained from the laboratory test results discussed above. Figure IIa.7a shows the 3D geometric model. Material properties of the most significant soil layers (Figure IIa.7b) were identified and input into the University's Finite Element Model.

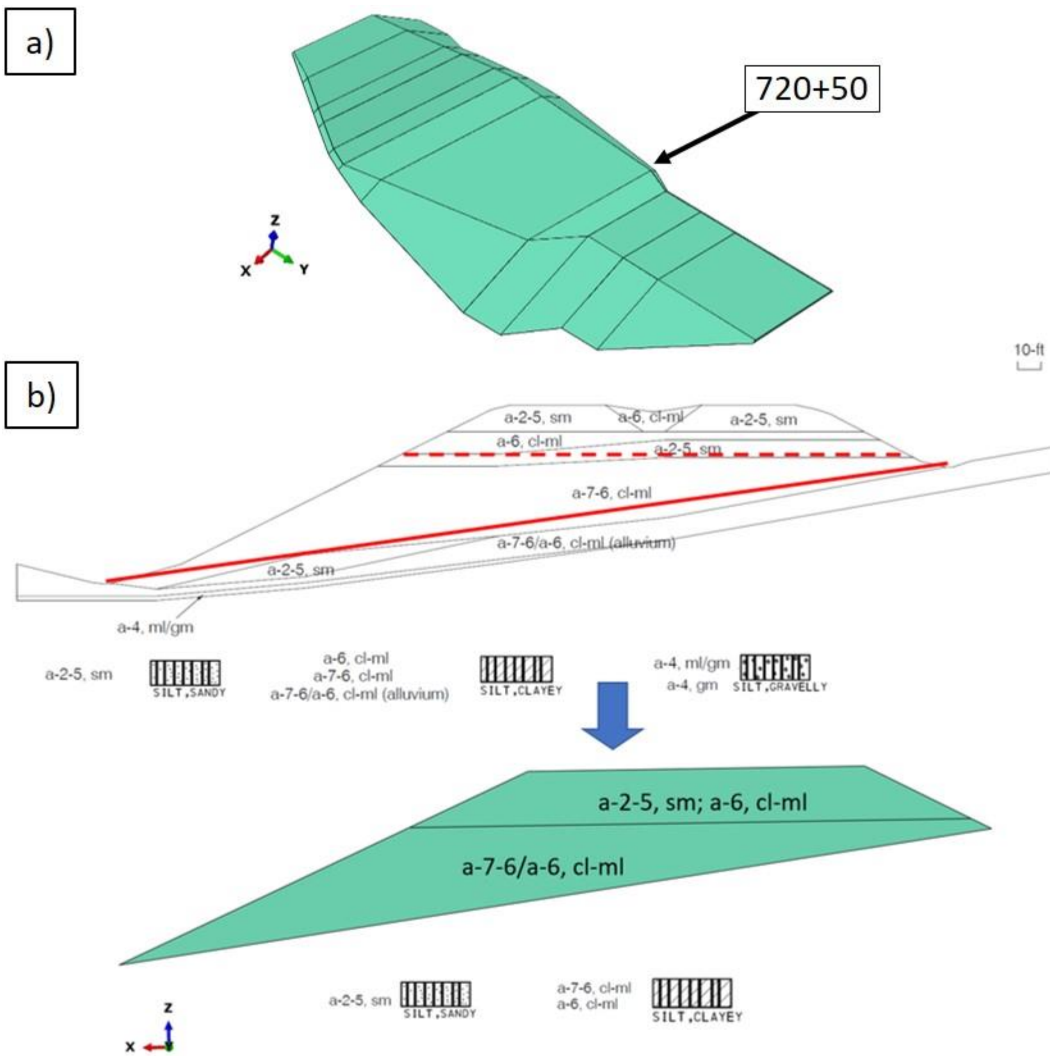

Figure IIa.7 – a) 3-D geometric model constructed from 12 control faces with the 48 points in ABAQUS; b) Cross-section 720+50 with identified soil types were used to identify broad layers with similar material properties.

After the initial finite element model was validated, the factor of safety for Embankment #1, prior to undermining, was determined by plotting the total displacement at the crest against the shear strength factor. This yielded the embankments pre-undermining factor of safety = 1.9 (Figure IIa.8). The obvious bending point can be observed in the plot where the total displacement begins to change dramatically. The shear strength reduction factor is located at the point of significant change to the factor of safety. The factor of safety of 1.9 indicates the embankment is stable prior to undermining.

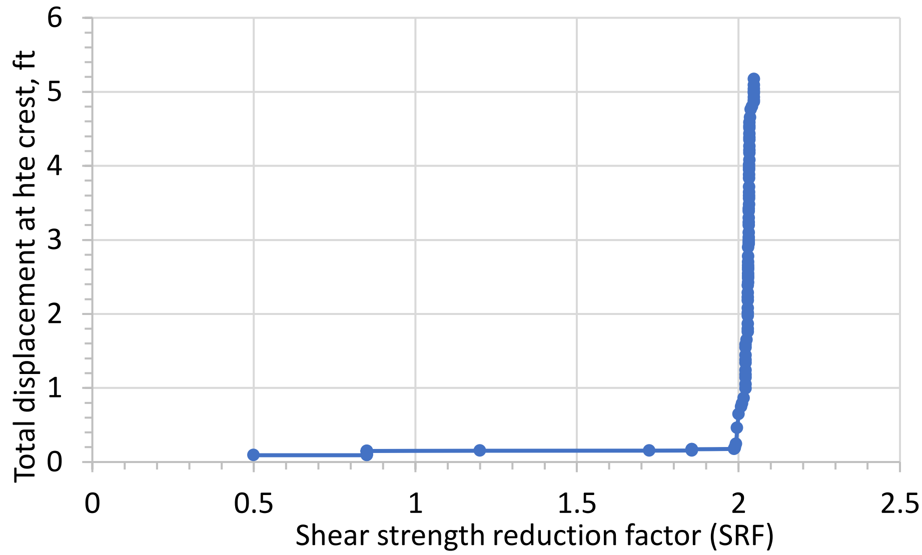

Figure IIa.8 - Determination of factor of safety by plotting the total displacement versus the shear strength reduction factor (Figure IVb.42, Task 1 Report)

10.0 Summary of Instrumentation Deployed and Detailed Plans to Monitor Highway Undermining

A total of 18 instruments were installed into Embankments #1 and #2 prior to undermining: nine tiltmeters, six inclinometers, and three piezometers. Over one-hundred highway alignment surveys and 500 slope survey points were established prior to undermining I-70. In addition, ten dynamics (moving) LiDAR surveys were schedule to occur prior-to, during, and after the undermining of I-70 above Panel 15. Additional information on all of these instruments is provided in Section V of the Task 1 Report.

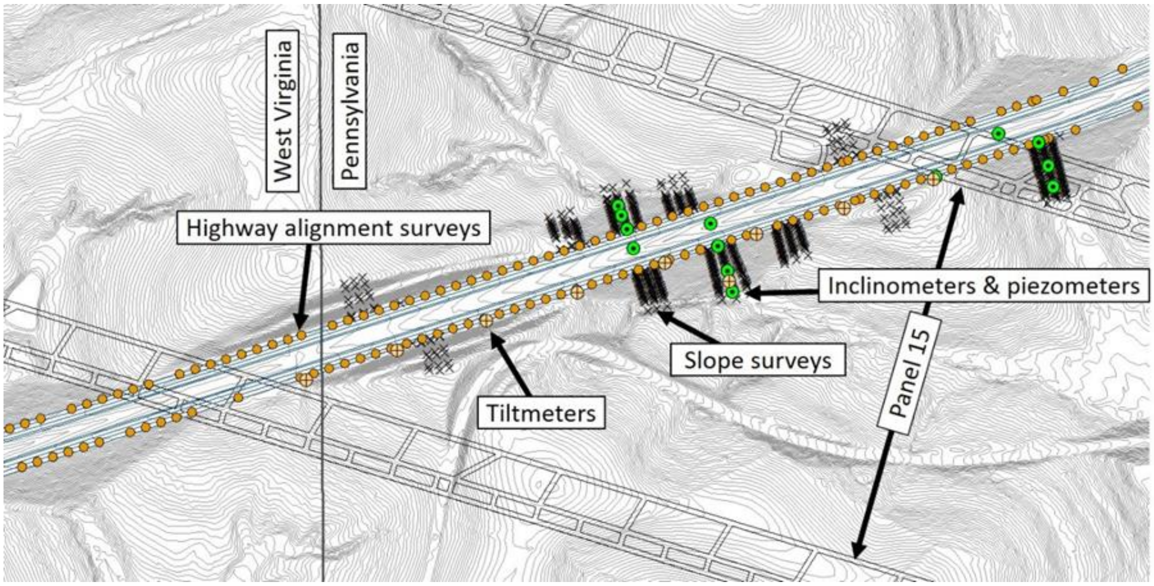

Figure IIa.9 – Location of tiltmeter, inclinometers, piezometers, highway alignment surveys, slope surveys along I-70 and above the predicted subsidence basin for Panel 15 (Figure Ic.1, Task 2 Report)

A detailed plan for observing subsidence impacts was established, addressing the number of surveys and the manner in which observations would be characterized, recorded, and reported. Lastly, protocols were established to assure the safety of University personnel involved in this activity.

Subsection IIb – Undermining Activities

Coal extraction for Panel 15 of the Tunnel Ridge longwall mine began on 28 October 2018 (mine survey coordinate 144+60) and cut the longwall chain and began recovering equipment on 1 May 2019 (0+0). Approximately one-half of Panel 15 is in Pennsylvania with the remainder in West Virginia. The panel is retreating towards West Virginia. I-70 was undermined from approximately 25 January until 20 February 2019. During this period, nine tiltmeters, six inclinometers, three piezometers, 147 highway alignment surveys, over 500 slope survey points, ten dynamics LiDAR surveys, and eleven field visits by the University were conducted and analyzed. The Task 2 Report provides data from these monitoring efforts and assesses important trends prior-to, during, and after the undermining of I-70 above Panel 15.

1.0 Background

Panel 15 lies less than one mile southwest of the West Alexander I-70 Interchange. This panel is currently part of an active underground coal mining permit approved by the PA DEP (Figure IIb.1). The most active monitoring period occurred from 25 January to 5 March 2019. During that period, traffic from the West Alexander Interchange to the West Virginia Welcome Center, was reduced to one lane in each direction with a speed limit of 45-mph. Four asphalt relief sections were installed prior to undermining ~300-ft from the gate road entries (~500-ft along the interstate). These is the areas where horizontal deformation is expected to be the highest. Lastly, an array of construction equipment was position close to the study area to mitigate any potential subsidence impact that may create a hazard for the passing traffic.

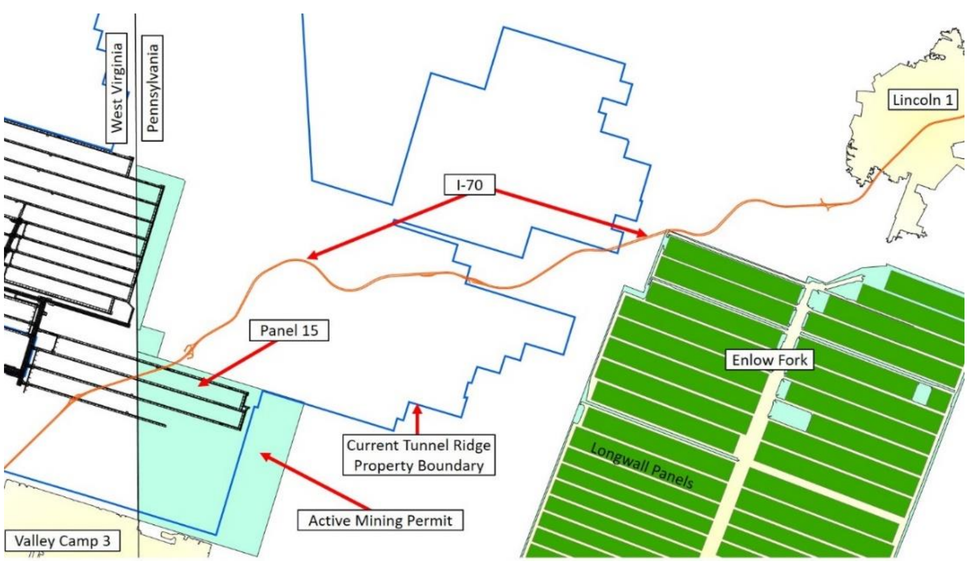

Figure IIb.1 - Location of Panel 15 with reference to adjacent underground coal mining activity and the alignment of the I-70 highway (Figure IIb.2, Task 2 Report)

2.0 Highway Alignment Surveys Data Analysis

The 147 highway alignment survey points were monitored every few days during the undermining of Panel 15. The highest vertical subsidence occurred over Embankment #1 with just over 5-ft of downward movement. It is also interesting to note that minor amounts of heave occurred over both Panel 15 gate road entries. The impact of the final subsidence basin can be seen in Figure IIIa.2. Note that the vertical subsidence is greater over the embankment than the adjacent cut.

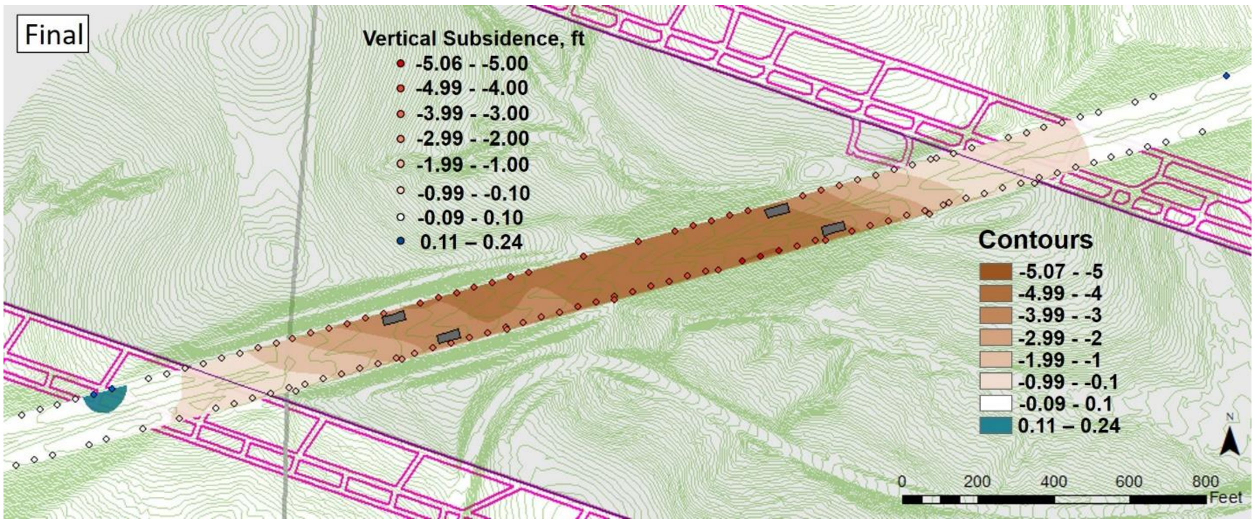

Figure IIb.2 – Final vertical subsidence as determined from the highway alignment surveys along the shoulder of I-70 over Panel 15

The horizontal deformations ranged from very little (0 to 0.25-ft) over the gate road entries to as much as 1.4-ft near eastern side of the subsidence basin close to the inflection point (Figure IIb.3). In addition to the final subsidence basin conditions, the Task 2 Report contains incremental displacements that documented the dynamic nature of the movement. Lastly, highway alignment surveys are used extensively in the Task 3 Report to examine the mechanisms contributing to the development of pavement distress features.

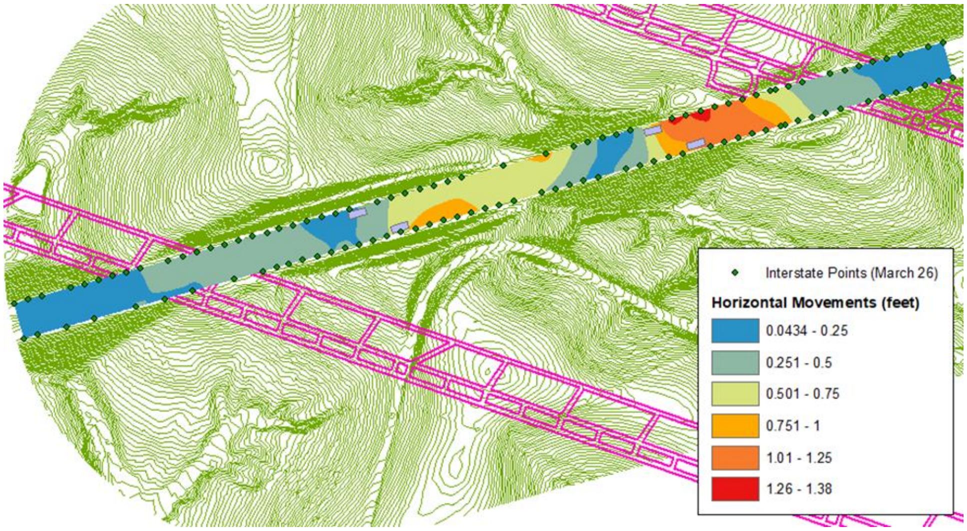

Figure IIb.3 – Final horizontal movement of highway surface due to mining of Panel 15 (Figure IIIa.4, Task 2 Report)

3.0 Embankment and Cut Slope Surveys

SPK Engineering installed 590 survey points to help characterize the movement of the slopes throughout the study area. These surveys have an accuracy of 0.03-ft in the vertical plane and 0.04-ft in the horizontal plane. The survey locations are shown in Figure IIb.4.

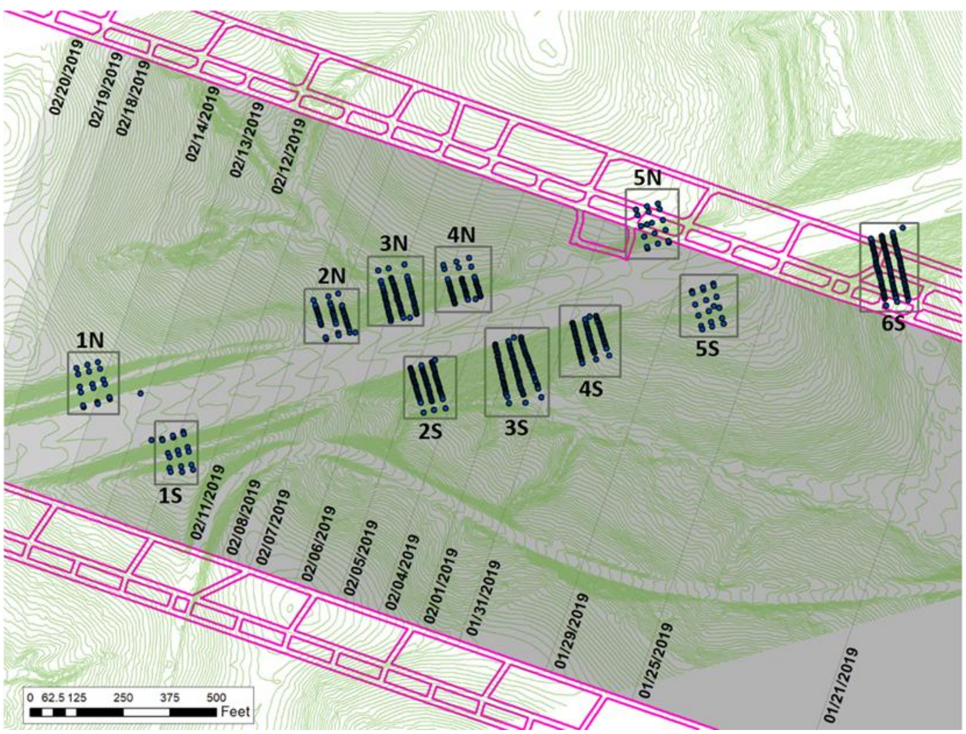

Figure IIb.4 – Slope survey locations and longwall face positions (Figure IIIb.1, Task 2 Report)

Minimal amounts of vertical subsidence occurred with Embankment #2 as it was located almost entirely over the gate road entries. The vertical movement in this area ranged from -0.06 to +0.22-ft, with the majority of the surface experiencing heave rather than subsidence. Figure IIb.5b displays the vertical movement from a selection of points, showing maximum heave developing when the longwall face is ~1,000-ft past the edge of Embankment #2.

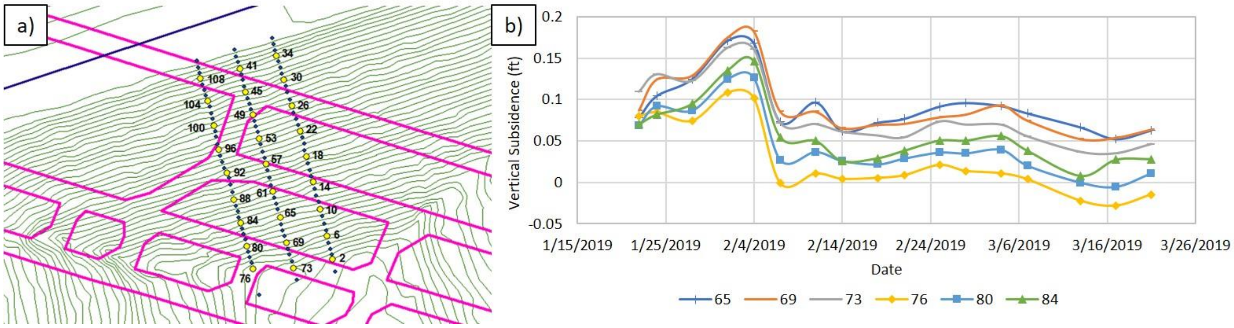

Figure IIb.5 – a) Selected SPK survey points located on Embankment #2 survey group 6S (Figure IIIb.2, Task 2 Report); and b) Vertical subsidence of select points within survey group 6S (Figure IIIb.3, Task 2 Report)

The northern portion of Embankment #1 is within the zone of maximum vertical subsidence (Figure IIb.6a). The vertical movement in this area ranged first from 0.44-ft of heave to a final subsidence of -4.91-ft (Figure IIb.6b). The heave initially occurred when the face was approaching the survey points and then reached maximum subsidence on 14 February when the face was ~700-ft passed the survey points. Perhaps one of the most revealing measurements is that the survey points located at the top of the embankment experienced almost 1-ft more subsidence than those located at the bottom of the embankment. This differential movement is likely due to factors other than subsidence, such as consolidation or spreading of the embankment.

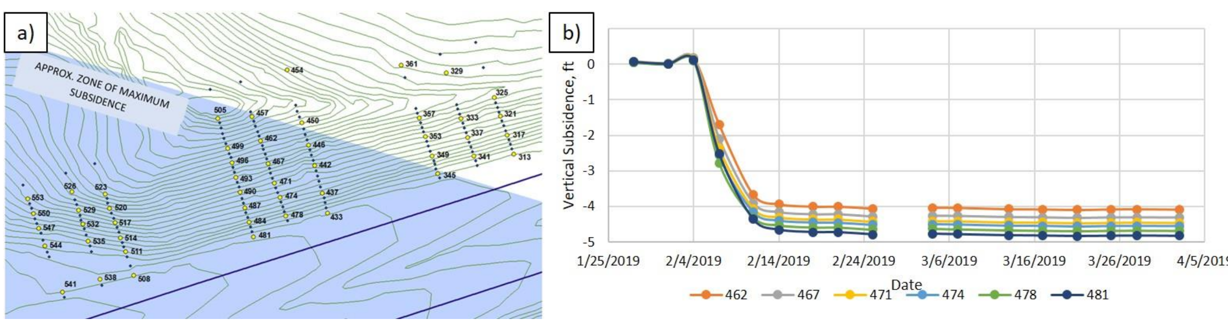

Figure IIb.6 – a) Selected SPK survey points located on north Embankment #1 survey groups 2N, 3N, and 4N (Figure IIIb.14, Task 2 Report); and b) Vertical subsidence of select points on north Embankment #1 survey group 3N (Figure IIIb.15, Task 2 Report)

The northwestern cut slope displayed distinctly different vertical subsidence characteristics than that found for the slopes of Embankment #1. For example, the maximum vertical subsidence within survey group 1N is approximately 4.4-ft compared to 4.9-ft for the north slope of Embankment #1 for an additional 0.5-ft of movement. The highest vertical subsidence occurred where the embankment fill is thickest. As the longwall face approached the western cut slope, a small amount of initial surface heave occurred. The maximum vertical subsidence was reached on 25 February when the face was approximately 700-ft passed the survey points (Figure IIb.7).

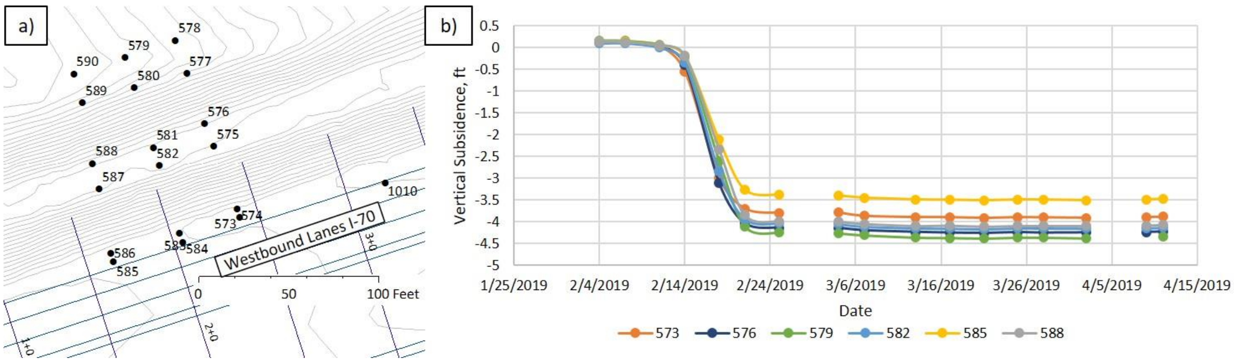

Figure IIb.7 – a) Selected SPK survey points located on north western cut slope survey group 1N (Figure IIIb.26, Task 2 Report); and b) Vertical subsidence of select points on north western cut slope survey group 1N (Figure IIIb.27, Task 2 Report)

4.0 Comparison of Highway Alignment and Slope Surveys

The final vertical subsidence from the slope surveys of I-70 associated with undermining Panel 15 is shown in Figure IIb.8. These data correspond very well with the vertical movements established using the highway alignment survey data (Figure IIb.2).

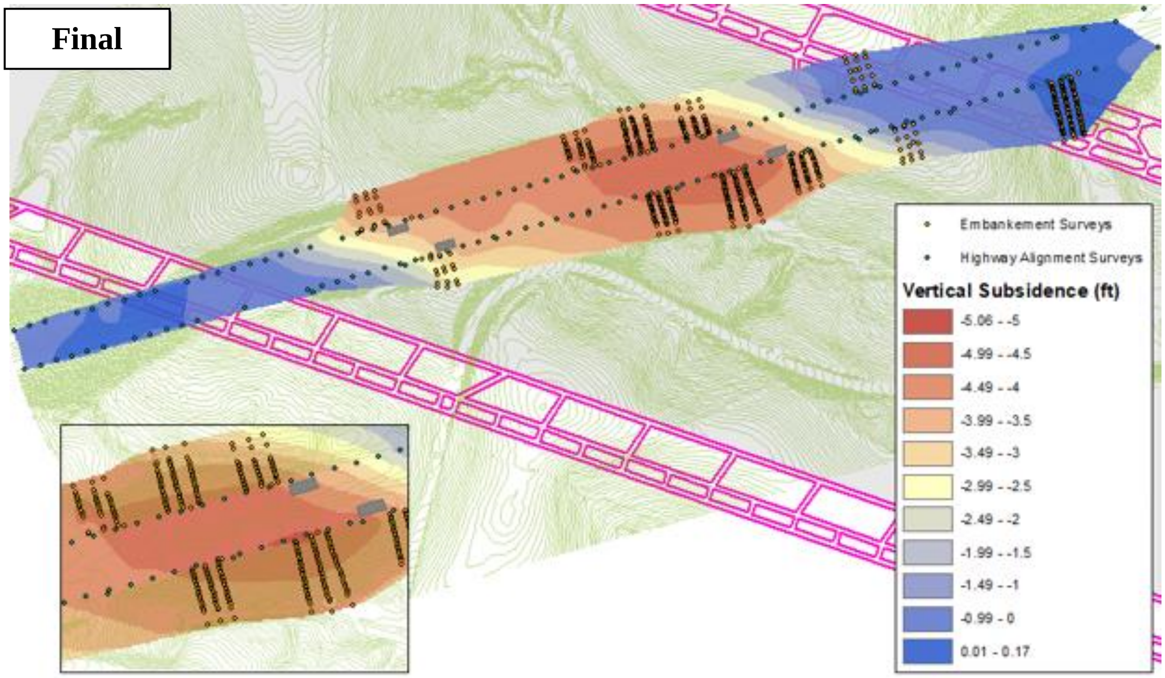

Figure IIb.8 – Final vertical movement of I-70 caused by Panel 15 subsidence as measured by the slope survey points (Figure IVa.1, Task 2 Report)

The final vertical movement for both the slope survey and the highway alignment points are combined to analyze the movement of the highway surface and the adjacent slopes in the horizontal plane. Figure IIb.9 shows the final horizontal movement throughout the study area.

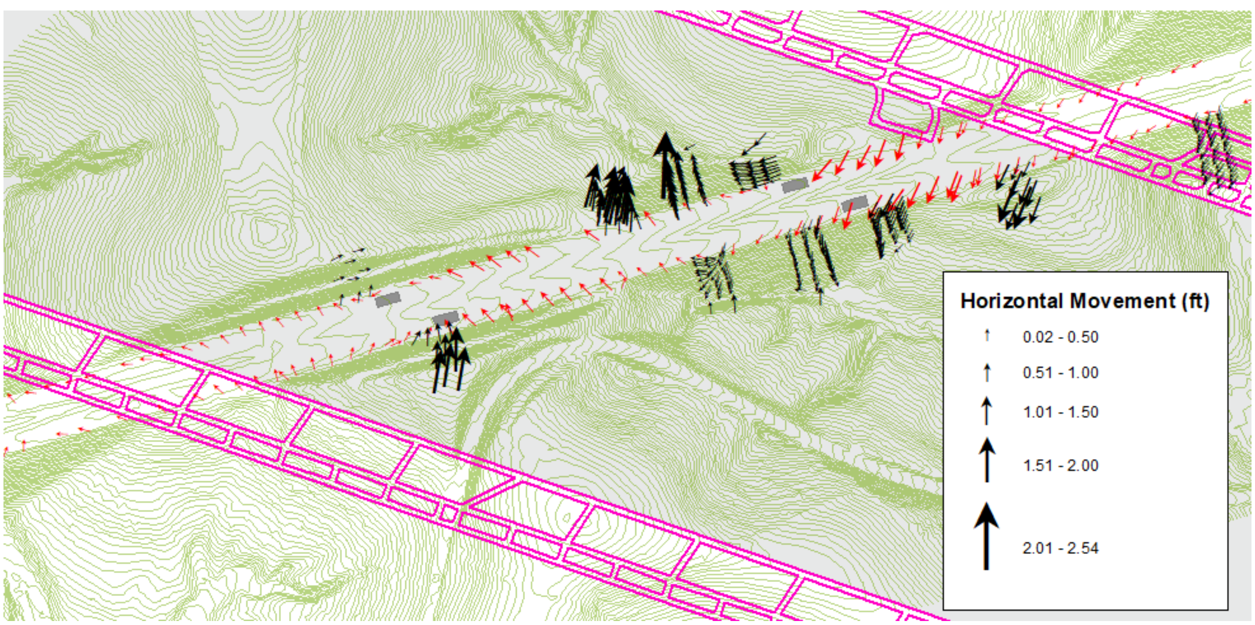

Figure IIb.9 – Final horizontal movement of I-70 caused by Panel 15 subsidence as measured by the highway alignment and slope survey points (Figure IVa.2, Task 2 Report)

Section IVa2.2 (Horizontal Movement over Time, Task 2 Report) provides an important perspective on how the surface, both on the highway shoulder and the cuts and slope within alignment, moves in response to the developing subsidence basin. This is a dynamic process, where the ground above the extraction zone adjusts to the developing subsidence basin by tilting/moving toward its center. It is also important to see how the highway shoulder and the cuts and fills adjacent to the highway can sometimes move in different directions and rates. This information was used in multiple analyses and is discussed in the Task 3 Report.

5.0 Observational Data

The University visited the site eleven times during undermining to observe the pavement surface, guiderails, berm, drains, and the slopes associated with road cuts and embankments. Techniques discussed by Miller and Bellinger (2014) to identify distress features formed the foundation for a set of observational protocol used by the University during site visits. During the most critical times, scroll maps of distress features and memorandum reports were provided to PennDOT as a means of supplying timely analysis and feedback. The scroll maps were particularly important during the most critical two week period in mid-February, when the highest frequency of distress development occurred. During this period, the University met with PennDOT personnel, either at the Taylorstown maintenance office or on-site to provide up-to-date scroll maps and discuss these observations.

Section IIIc of the Task 2 Report contains an inventory of detailed distress features that are categorized by location and the approximate time of occurrence. These observational data, and others supplied by PennDOT personnel, were used extensively in both the Task 2 (see below) and the Task 3 Reports (Section II). This data made it possible to relate the complex movements observed to the resulting type, severity, and quantity of distress that developed. For example, pavement separations, opening of contraction joints, and other distresses associated with surface extension are observed to occur most frequently when the active longwall face is directly under a point on the surface to when it is ~200-ft behind the moving longwall face. As the longwall face moved further away, blowup, compression bumps, and other distress features associated with surface compression became more prevalent. This transition from surface extension to compression is linked to the concept of the inflection point (see Section IIa.7).

One of the most important uses of the observational data is to compare it with monitoring data, especially in small increments in time. When this is done, it is possible to see a particular pattern of horizontal movement that is associated with specific types of distresses that develop along the highway.

For example, on 5 February 2019, sizable compression bumps and blowups occurred either within or adjacent to the asphalt relief sections (Figure IIb.10). The asphalt relief sections were designed by Roy Painter (PennDOT) to adsorb excessive levels of horizontal movement. Shear fractures occur near the edge of the shoulder nearest the travel lanes. All of these observations were used to better understand how horizontal movement influences the development of distress in the highway.

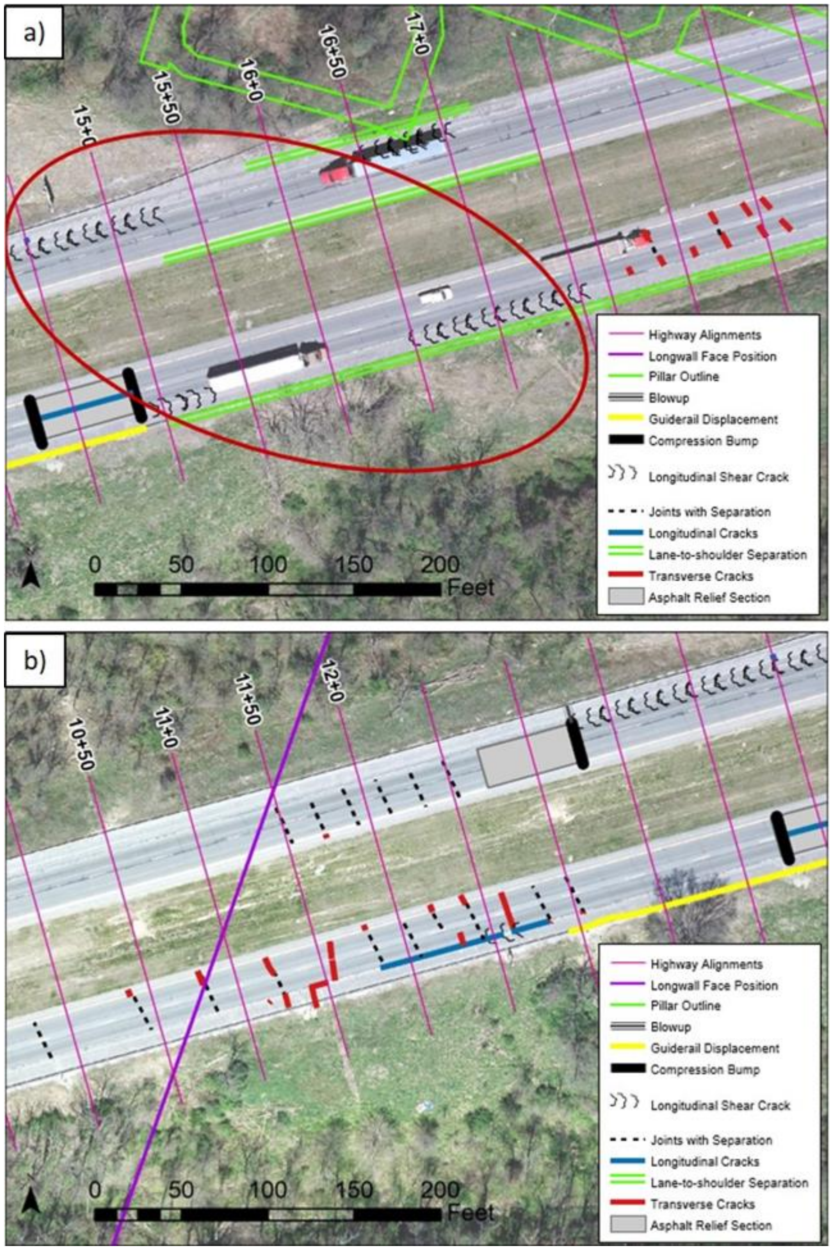

Figure IIb.10 – Highway observations in areas of large horizontal movements on 5 February 2019: a) 14+50 to 19+00; and b) 10+00 to 14+50 (Figure IVa.12, Task 2 Report)

Observations of distress features like those above were compared with actual measurement of horizontal movements (Section IVa.2.3, Task 2 Report). For example, the highway alignment survey measurements are found to deviate slightly from the slope surveys. This indicates the movement of the ground supporting the pavement might be different from the movement of the pavement, which the ground is supporting (Figure IIb.11). Perhaps this a result of the shape and scale of the highway structure (highway alignment surveys) in comparison to a point on the ground surface (slope survey). The point on the surface responds more quickly to ground movements whereas the connectivity of the pavement causes it to moves more in-mass. The differences in movement of the highway with respect to the original ground surface is also largely adsorbed by the individual pavement segments.

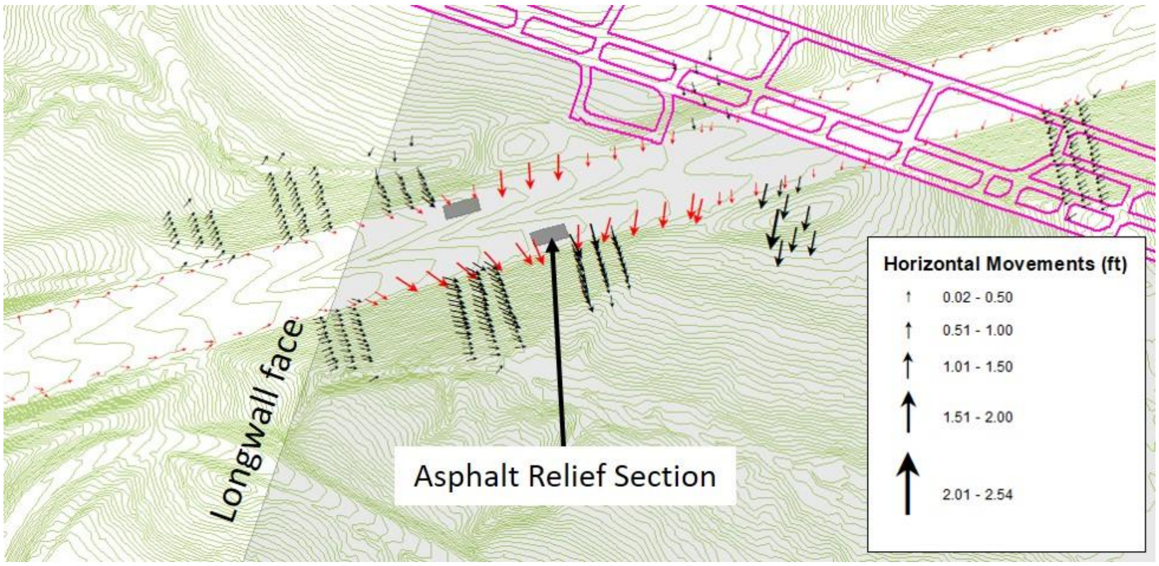

Figure IIb.11 – Cumulative horizontal movement (red highway alignment and black slope survey points) as of 5 February 2019

6.0 Inclinometer Data

Six inclinometers were installed by PennDOT contractors and readings were recorded every few days by PennDOT personnel. The locations and orientations of the borehole casings are shown in Figure IIb.12. The installation orientation shows the A+ direction pointing down the slope of the embankments and the B+ axis clockwise from the A+ orientation.

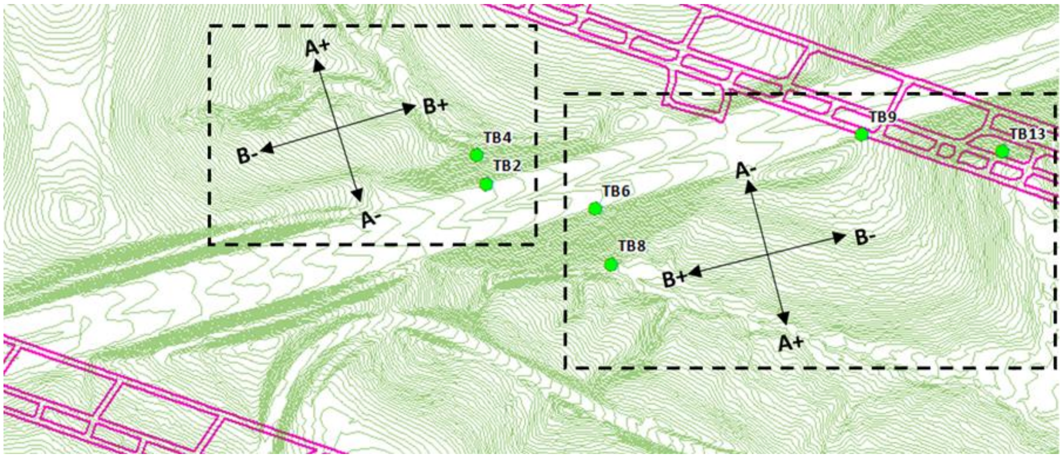

Figure IIb.12 - Locations and orientations of the inclinometers within the I-70 study area (Figure IIId.1, Task 2 Report)

The inclinometer data confirmed that movements began to occur within Embankment #1 either on the day of the undermining or on a subsequent day shortly after. This movement persisted until the longwall face was ~600 to 850-ft passed the instrument. In all cases, the largest movement occurred in the down-dip direction confirming that the slope were deformed outwards from the highway (Figure IIb.13). This outward, or spreading of the embankment, helps to explain the additional 0.5-ft of downward subsidence in areas of the thickest fill, i.e. the fill was consolidating. Of equal importance was that the inclinometers in the north and south slopes showed significant incremental movement associated with an interface between two fill layers near the bottom portions of the casings. The differential movement of the fill above and below the interface was a major point of concern until the longwall subsidence basin stabilized under Embankment #1.

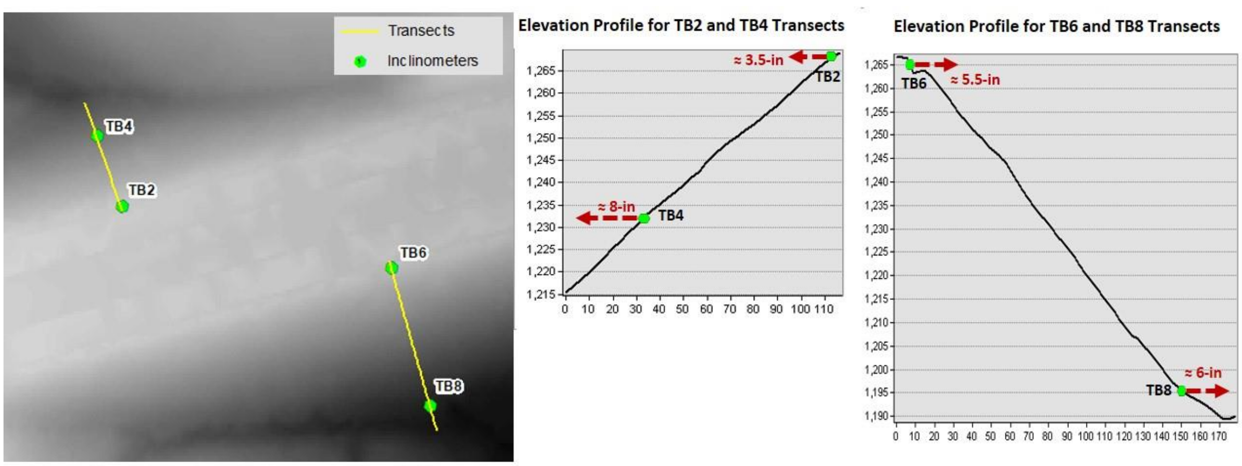

Figure IIb.13 - Depiction of the outward movements 2-ft below the surface that the inclinometer borehole casings experienced on Embankment #1. The lines represent the elevation of the transect for each inclinometer grouping (Figure IIId.3, Task 2 Report)

7.0 Tiltmeter Data

Eight tiltmeters were initially installed along the eastbound lane of I-70. A ninth tiltmeter was added to the lower portion of the south slope of Embankment #1. Visual signs of slope movements in this area required a monitoring point to help provide additional information. All instruments were programmed to take and record readings several times per hour. The vector representation of instrument tilt with respect to longwall face position for the three instruments active during the entire undermining period is shown in Figure IIb.14. TM-8, located on the edge of the Panel 15 subsidence basin, experienced a very small degree of tilt away from the basin. TM-6 and TM7 both tilted in the direction of the center of the subsidence basin. The severity of movement varied based on where in the basin the tiltmeter is placed. For example, TM-7 experienced the highest degree of tilt in the Y- direction. This could be expected as it is located very close to the inflection line (Figure IIa.6), which is where the highest surface slope angle is expected. In comparison, TM-6 experienced the highest degree of tilt on the X-axis, but ultimately settled with a smaller change in the Y- direction when compared to TM-7 (Figure IIb.14). These surface movements follow trends discussed in other sections of this report. Surface slope or tilt and horizontal movement are greatest near the inflection point. When the surface is located above the mid-panel area, it will tilt/move first towards the developing subsidence basin then move/tilt in the opposite direction once the longwall face has move away, eventually settling close to its original position.

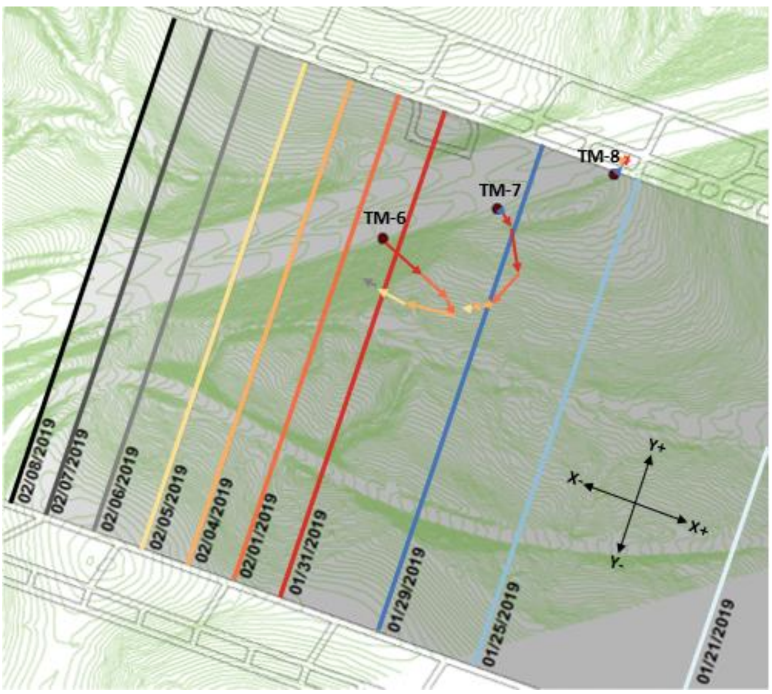

Figure IIb.14 - Location of three tiltmeters (TM-6, TM-7, TM-8) active during undermining along the eastbound lanes of I-70 and the vectors representation of instrument tilt with respect to longwall face position (Figure IIIe.6, Task 2 Report)

8.0 Piezometer Data

Three piezometers were installed in one within borehole labeled TB-12 for Embankment #2 and two separate boreholes, TB-7 (south slope) and TB-3 (north slope), for Embankment #1. TB-12 is above the Panel 15 gate road entries so it was only marginally affected by undermining (Figure IIb.15). Regardless, the water lever dropped ~10-ft from the time the longwall approached Embankment #2 until the lowest water level was recorded ~10-days after the longwall passed by TB-12. Water levels at TB-7 remained virtually unchanged until the longwall face was several hundred feet past the borehole. Water levels suddenly rose almost 3-ft over a few days and then dropped to between 1 and 2-ft above pre-undermining levels. There was some concern that the plug at the bottom of the hole at TB-7 was compromised and had allowed water to drain from the borehole. Conversely, a drop in water elevation of ~2-ft was observed at TB-3 just prior to the passage of the longwall face under the borehole and then it rapidly rebounded to ~3-ft above the original water level. All three piezometers exhibited different trends and are thought to be controlled by conditions within the borehole. Additional analyses of the piezometer data are provided in Sections Vd (Task 2 Report).

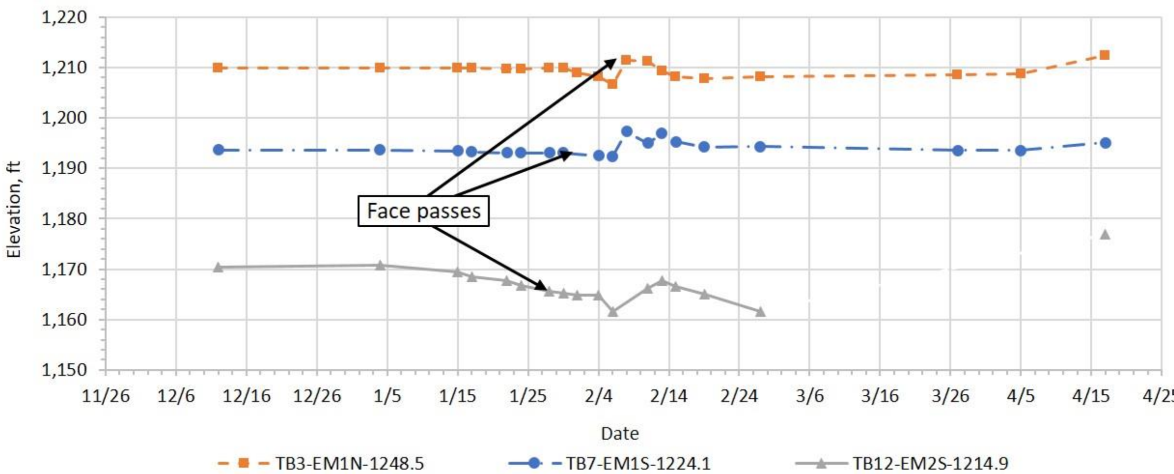

Figure IIb.15 - Variations in the embankment water levels due to longwall mining from 12 December 2018 to 17 April 2019 (Figure IIIf.2, Task 2 Report)

Rain events prior to the piezometer readings can dramatically influence results (Figure IIb.16). As such, it is helpful to analyze the rainfall data when utilizing the piezometer to observe the changes in the elevation of the phreatic surface. For example, there is a dramatic increase in the water level at TB-7 on 8 February 2019. It is not clear if this increase is the result of the two significant rain events that occurred in the two days prior to this date or the consolidation of the strata between the extraction zone and the bottom of Embankment #1. Other rain events of slightly less magnitude did not produce dramatic changes in water level.

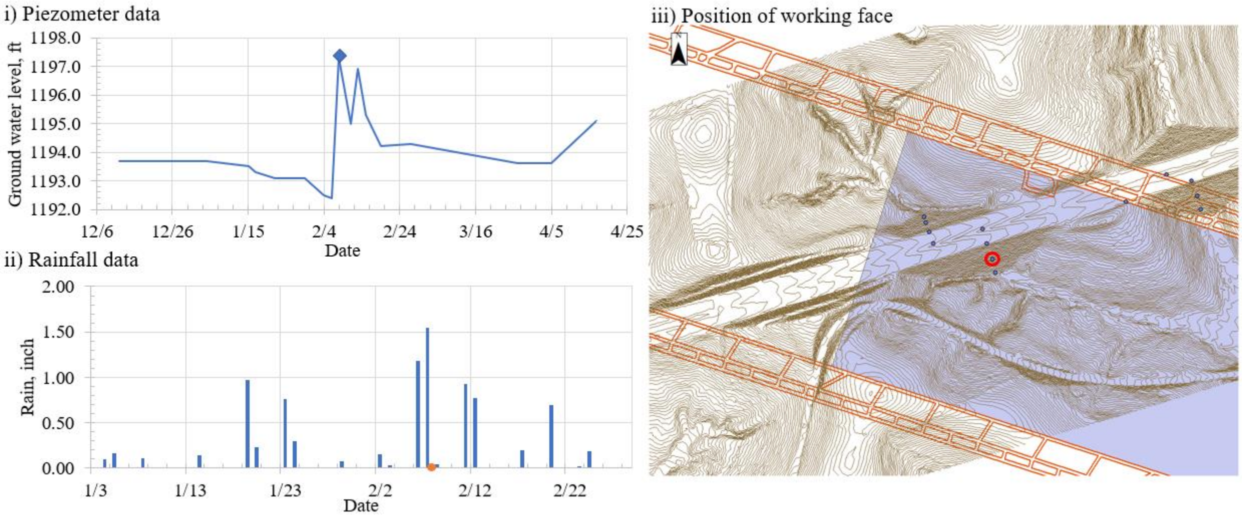

Figure IIb.16 – Plot of piezometer data (TB-7) and rainfall data when the longwall face had past under Embankment #1 on 8 February 2019 (Figure Vd.3h, Task 2 Report)

9.0 LiDAR Data

The accuracy of the LiDAR data and was found to be 0.4-in. A comparison between the LiDAR control points and the highway alignment points was also accomplished. The highway alignment points have an accuracy of 0.25-in, while the accuracy of the LiDAR control points is 0.4-in. This produces a combined accuracy of 0.65-in. See Section IIIg of the Task 2 Report for more details.

10.0 SDPS Model Calibration using Survey Data

The basic characteristics of the SDPS model of Panel 15 are provided in the Task 1 Report (Section IIa.8). The model predictions are compared to the measured observations obtained from the final survey (Figure IIb.13). By changing the percent hard rock from 25 to 30 (Figure IIb.17) a good agreement was achieved between the predicted and measured movements. The biggest discrepancy is in the area of Embankment #1. Here the vertical movement is influenced by consolidation and spreading of the embankment fill (discussed later in this report). This SDPS model considers the surface to be flat and cannot account for differences in material types.

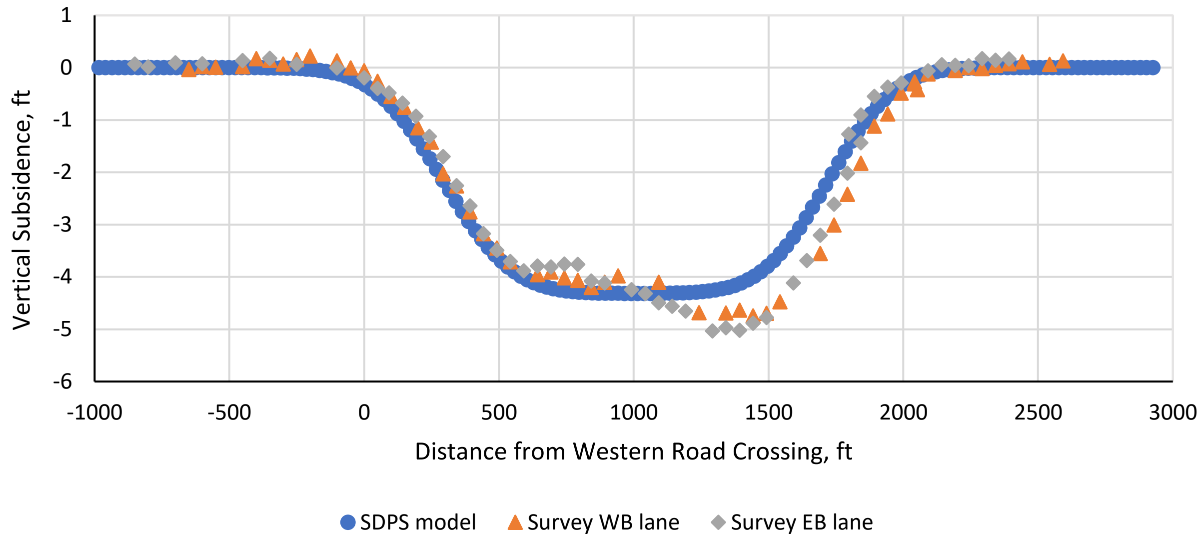

Figure IIb.17 – Vertical subsidence predicted using the SDPS model and measured along the highway (IVb.6, Task 2 Report)

The calibrated SDPS model predicts 0.34-ft less vertical subsidence than the initial SDPS model presented in the Task 1 Report. This was accomplished by increasing the percentage of hard rock in the overburden, resulting in slightly less subsidence on the surface. Comparing the results of the calibrated model and the observed results, it can be seen that the model fits the data well. The percent error between the vertical profile and the observed data is about 14.5-pct, which indicated a good correlation. Contrarily, the horizontal deformations did not fit the model profiles as well. The reasons for this are discussed in future sections. Table IIb.1 compares the vertical movements predicted using the initial and calibrated SDPS model and the highway alignment surveys.

To further test the validity of the SDPS calibrated model a comparison with an empirical/profile function model was conducted. This is especially important when applying this model to estimate future subsidence. This investigation found a good comparison between the two models (Figure IIb.18). The empirical/profile function model predicts very similar vertical movement as compared to the SPDS model but provides a more abrupt slope change. The subsidence profiles from these two models intersect at the inflection point. This point is located ~165-ft from the gate road entries. The influence of these properties, when making subsidence predictions, are addressed in the Task 3 Report.

Table IIb.1 – Comparison of subsidence predicted using SDPS models and measured along the highway (Table IVb.1, Task 2 Report).

		Distance from Western Panel Edge, ft	Vertical Subsidence, ft	EW Horizontal Deformation, ft	NS Horizontal Deformation, ft	Maximum Horizontal Strain, 1/1000
Initial Model	POI 1	0	-0.59	0.28	0.80	8.29
	POI 2	500	-4.27	0.20	0.59	-7.40
	POI 3	1000	-4.66	0.00	0.00	-0.04
	Max	--	0.00	0.53	1.54	8.48
	Min	--	-4.66	-0.53	-1.54	-8.48
Calibrated Model	POI 1	0	-0.32	0.17	0.50	6.38
	POI 2	500	-3.65	0.29	0.85	-7.66
	POI 3	1,000	-4.32	0.00	0.00	-0.13
	Max	--	0.00	0.49	1.43	8.03
	Min	--	-4.32	-0.49	-1.43	-8.02
Highway Alignment Survey	POI 1	0	-0.26	-0.32	0.07	--
	POI 2	500	-3.73	0.39	-0.04	--
	POI 3	1,000	-4.07	-0.54	0.39	--
	Max	--	0.22	0.63	0.39	--
	Min	--	-5.03	-1.14	-0.92	--

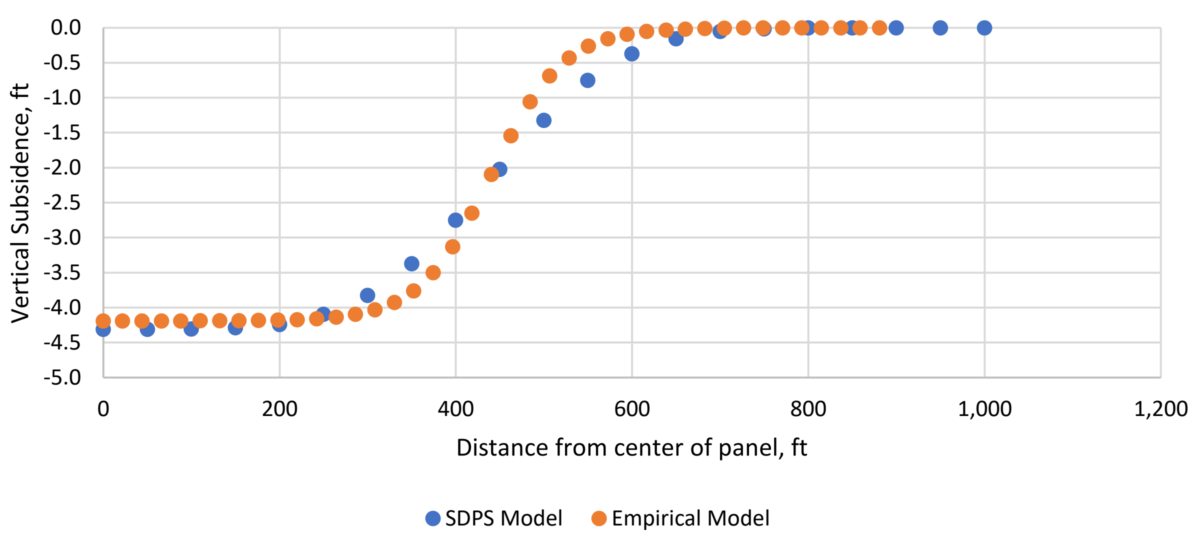

Figure IIb.18 – Comparison of vertical subsidence predicted using the calibrated SDPS and empirical/profile function models for one-half of Panel 15 (Figure IVc.2, Task 2 Report)

11.0 Embankment Behavior

The Task 1 Report discussed the characteristic and material properties of six boreholes drilled into Embankments #1 and #2. Work performed under the Task 2 Report explored the role of dispersed gravel on the stress-strain response of soil rock mixtures found within the embankment fills (Section Va.2, Task 2 Report). These material properties data are used to establish the input parameters for the numeral simulations.

Multiple sections of the Task 2 Report (Section IIIb and IVa) provides information on the vertical movement along the I-70 highway alignment over Panel 15. Figure IIb.19 shows vertical subsidence contours in the area of Embankment #1 generated using the slope surveys. The maximum subsidence (-5.5-ft) occurred on the top surface of the embankment. Measurably less subsidence, ranging from 3.9 to 4.2-ft, occurred along the bottom portions of Embankment #1. The difference is more than 1-ft and suggests that portions of the embankment consolidated as a result of the subsidence.

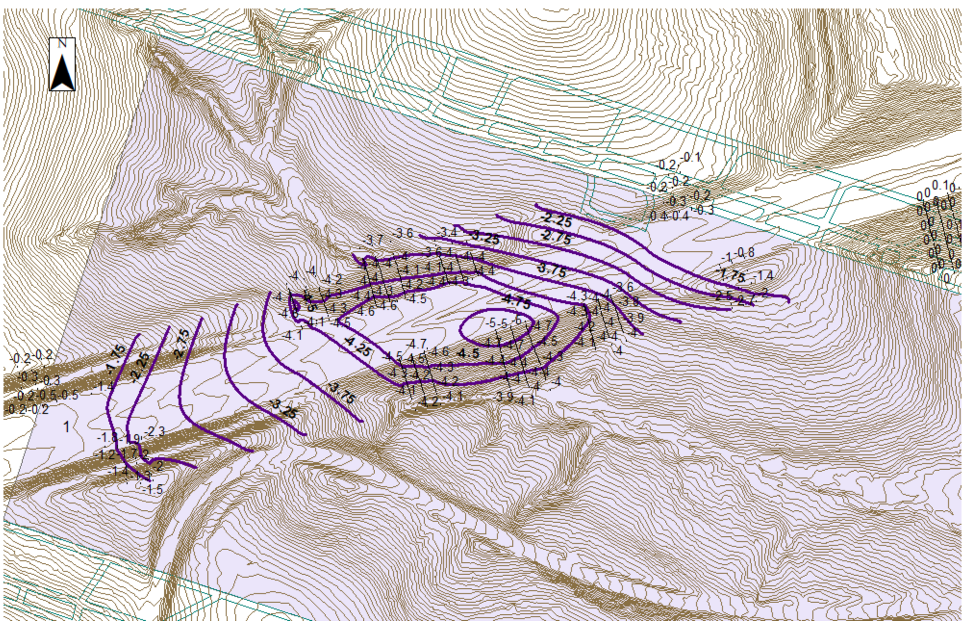

Figure IIb.19 - Vertical surface subsidence contours along the I-70 highway alignment in the study area (Figure Va.9, Task 2 Report)

A depiction of the outward spreading of Embankment #1 is shown in Figure IIb.20a, where four inclinometers are aligned along in one cross-section and on the same vertical plane. Figure IIb.20b shows a graph of magnitude and depth of horizontal movements at TB-4. The lateral deformations from slope surveys of Embankment #1 was previously show in Figure IIb.9. When this information is combined with the inclinometer measurements, between 1 and 2.5-ft of total horizontal movement along the north slope of Embankment #1 is confirmed. The movement was dominantly down slope. Inclinometer TB-4 reveals that much of the differential lateral movement in the embankment fill was concentrated ~10-ft above the fill-bedrock contact (Figure IIb.20b). This zone is referred to as a shear zone or band and became a focal point in modeling efforts, i.e. ‘embankment failure occurred when a shear band developed in the model in a manner similar to that reflected in TB-4’. These data not only confirm the lateral spreading within the embankment during subsidence, but demonstrate a likely development and progression of failure.

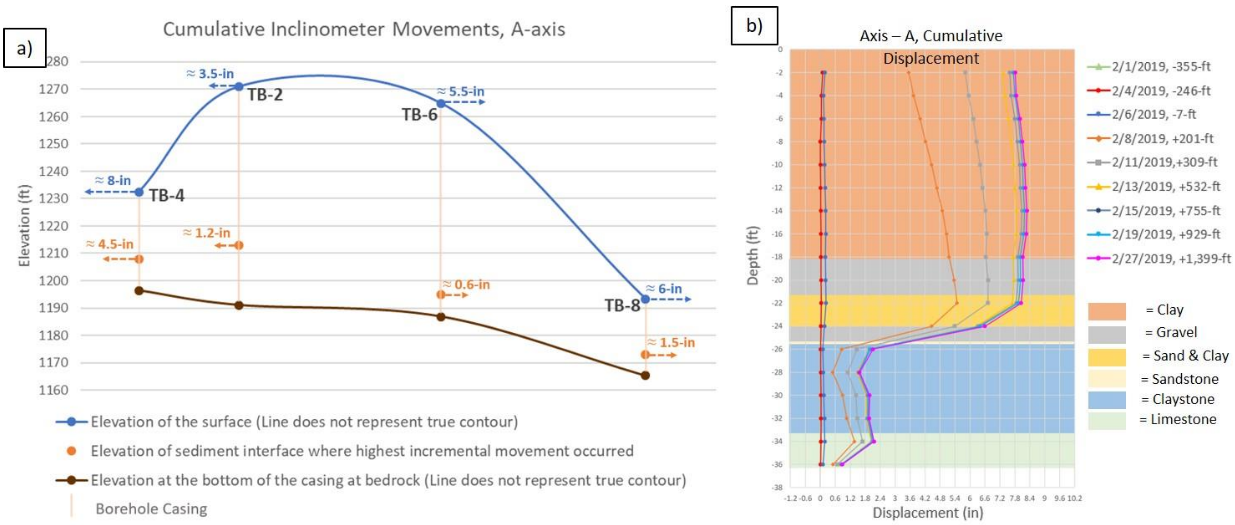

Figure IIb.20 – a) Lateral movement of the inclinometers as if they are on the same vertical plane (Figure IIId.4, Task 2 Report), and b) Lateral movements of fill and rock layers within borehole TB-4 in the north slope located at Station 720+00 (Appendix A-46, Task 2 Report)

Field observations were combined with piezometer readings to assess water conditions within the embankments. This data suggests that water enters the embankment along its slopes and the highway surface and moves generally downward. On the south slope of Embankment #1, a wet area was observed that extended, on occasion, to the elevation of 1,212-ft (Figure IIb.21a). The photograph in Figure IIb.21c shows the saturated condition of the fill where water was observed seeping from the slope. The piezometer in TB-7 was not functioning during this period. On the north slope, no water seepage was observed however, a small area near the culvert inlet showed minor slips (Figure IIb.21b&d). A phreatic surface was observed in TB-3 at ~1,212-ft. This piezometer is most likely within the original stream channel that is now partially occupied by the buried culvert. These data suggest the water moves downward into the lowest portion of the fill above the contact with the relatively impervious bedrock (Figure IIb.21a&b). Water within this zone exits the embankment along the bottom of the south slope in the area designated as the ‘wet zone’ in Figure IIb.21a. The saturated fill is relatively narrow in width along the north slope and widens significantly toward the south slope. The wet zone was estimated to extend as much as 50-ft along the slope above the base of the embankment.

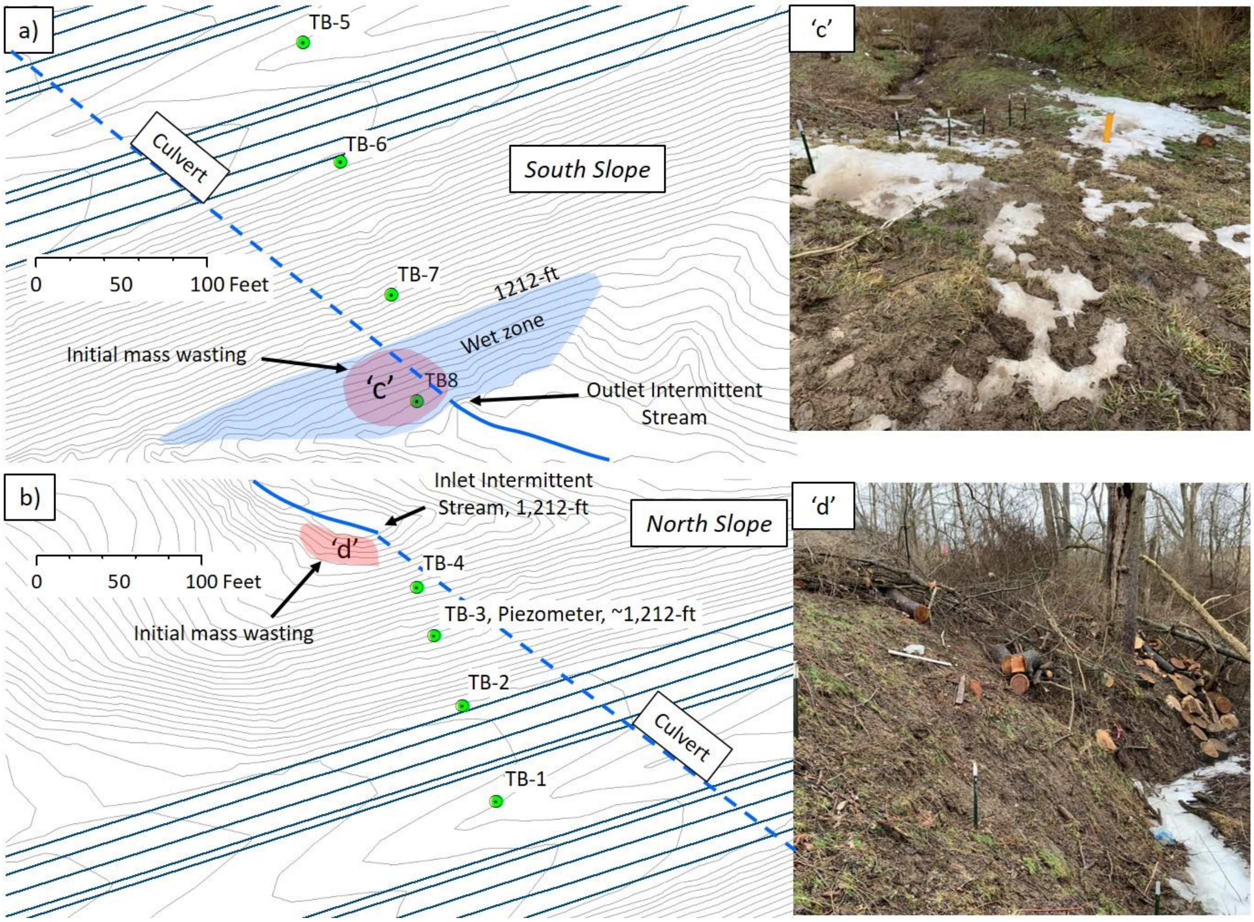

Figure IIb.21 – a) South slope showing the wet zone and the culvert trend with photo 'c' showing fill that is best described as saturated, and b) North slope showing the location of the initiation of mass wasting with a photo in 'd' providing a visual

As previously noted, PennDOT installed a tiltmeter between TB-7 and TB-8 within the area of highly saturated fill just prior to the passage of the longwall face underneath. Regardless, no serious slope instabilities developed along either the south or north slopes of Embankment #1. It is also worth mentioning that the differential movement of inclinometer TB-4 ~10-ft above the bedrock revealed the formation of a shear band within the fill. Fortunately the movement was arrested as the longwall face moved further away. It is also possible that the strain-hardening properties of some of the fill produced a material that gained strength under increasing deformation (Vallejo, 2020).

12.0 Modeling Slopes of Embankment #1

Numerous advancements to the University's finite element model of Embankment #1 were made, demonstrated, and assessed in the Task 2 Report. For example, a coupled analysis was implemented to allow for the development of positive pore pressure below the phreatic surface (Section Ve.4, Task 2 Report). Next various phreatic surfaces were selected to investigate potential rupture surfaces within the 720+50 cross-section. The shear strength reduction factor was used to determine the factor of safety, ranging from 2.1 to 2.3, for slopes with different water levels (Figure IIb.22).

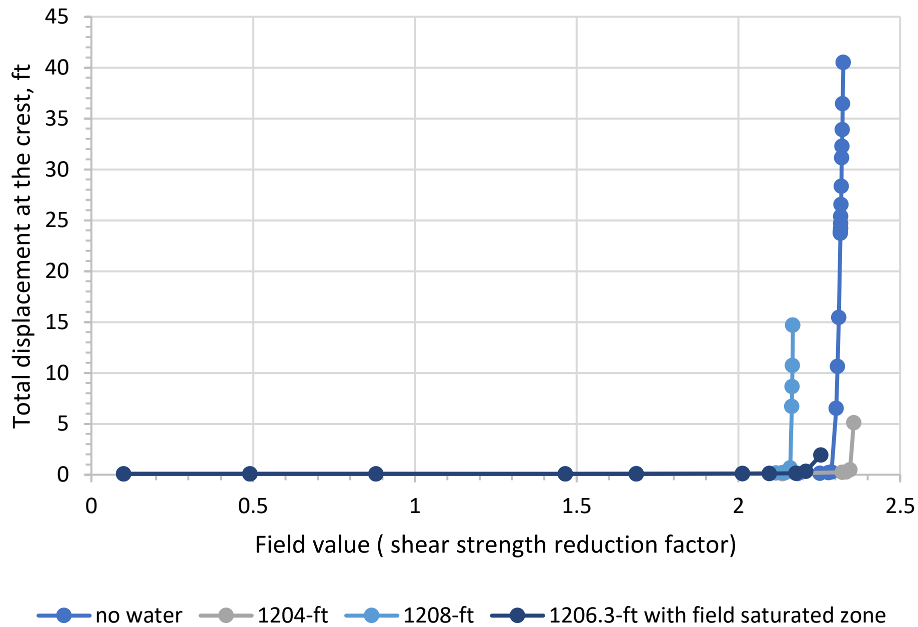

Figure IIb.22 – Determination of the factor of safety by plotting the total displacement at the crest versus the shear strength reduction factor (Figure Vd.10, Task 2 Report)

These simulations showed that the maximum plastic strain is predicted to develop on the bottom of the embankment slope near the toe area. When these areas are saturated, the plastic zone becomes more concentrated in the area near the toe. The majority of the plastic zone is found in the saturated lower part of the slope, while on the upper dry part of the slope, the magnitude of the plastic strain was much lower.

The next major effort was to develop a method to simulate the development of a subsidence basin below Embankment #1 using the existing finite element model. This method uses a numerical regression function of the vertical subsidence basin generated using SDPS analysis and then subject the 3D finite element model to a simulated developing subsidence basin. An example of the model output is shown in Figure IIb.23. The maximum 5.9-ft vertical downward movement for Embankment #1 developed when the longwall face was at Position #8. This is slightly higher than the 5.5-ft measured. More importantly, the location of greatest predicted subsidence matches that measured by the slope surveys (Figure IIb.19).

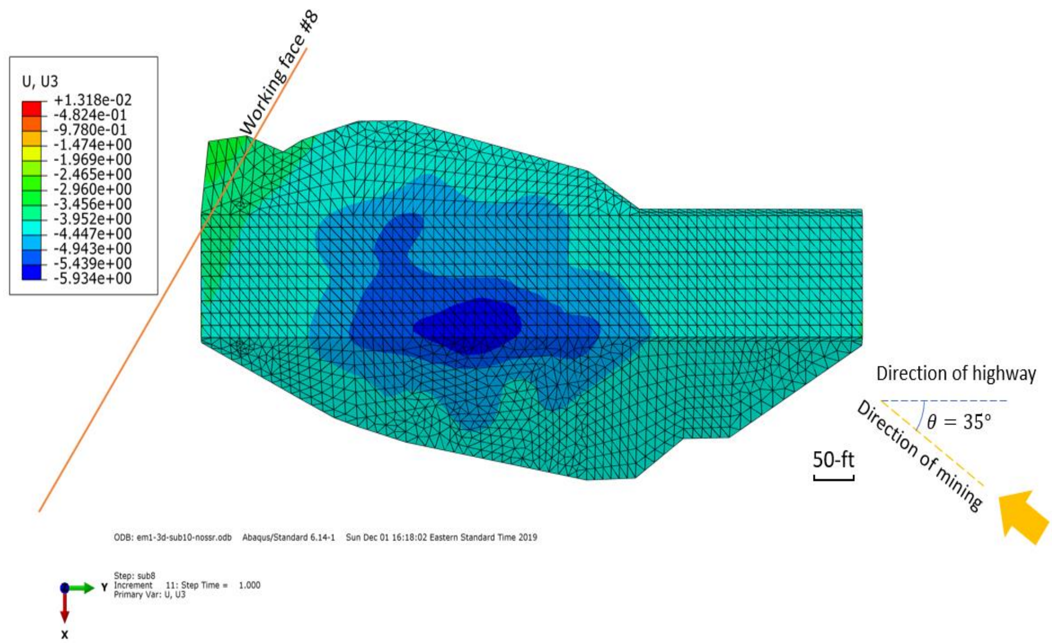

Figure IIb.23 - Vertical displacement on the surface of the Embankment # 1 subjected to successive subsidence when the working face is at Position #8 (Note the mining directions is at a 35-deg angle to the highway.) (Figure Ve.7i, Task 2 Report).

The obvious next step is to relate movements to a factor of safety for the embankment. As in previous discussions, the shear strength reduction method is used to determine when movements represented embankment failure. The analysis had two cases: the first was to determine the factor of safety for Embankment #1 prior to undermining; and the second was to determine the factor of safety during the development of the subsidence basin.

For the first case, slope failure is associated with zones of plastic strain (shear bands) causing a significant increase in movement, and producing a knee point in the factor of safety plot (Figure Ve.11, Task 2 Report). At this point the shear band reaches the top of the embankment and a complete ruptured face is formed. For this case, without subsidence, the upper bound and lower bound are close to each other. The embankment started to slide at a factor of safety of 2.5 and failed at 3.2.

In the second case, the total displacement at the crest of the embankment was measured during successive applications of the shear strength reduction method producing an overall factor of safety of 2.7 (Figure IIb.24a). The factor of safety of the embankment, when subjected to simulated subsidence, decreases and reached the lowest value at longwall face Position #6 where the working face is around the middle of the embankment (Figure IIb.24b). As the subsidence basin fully developed and the longwall face moved further away, the factor safety increased to the point that it became even higher than the factor of safety before subsidence. The position of working face at each step and the vertical displacement contour are shown in Figure Ve.9 (Task 2 Report).

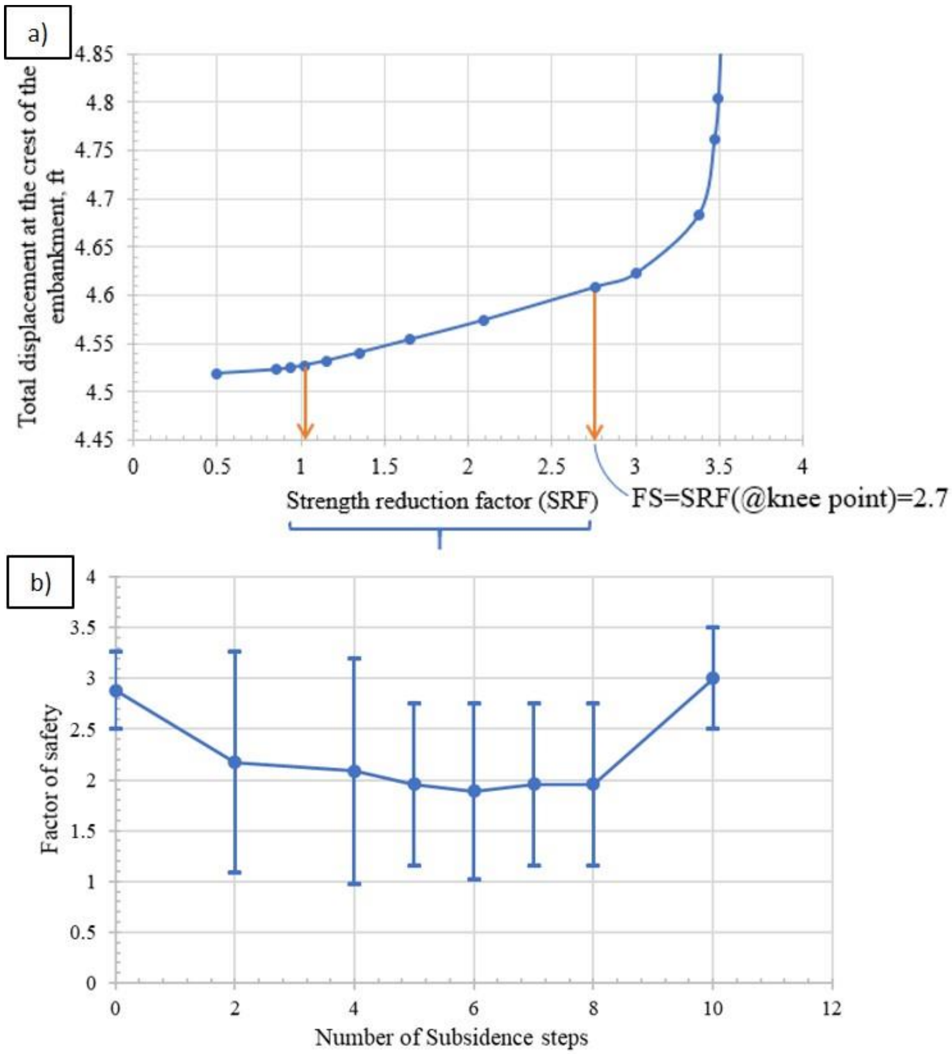

Figure IIb.24 – a) Total displacement at the crest of the critical cross section versus the shear strength reduction factor for the longwall face Position #6 (Figure Ve.13, Task 2 Report), and b) Plot of factor of safety versus the longwall face positions or subsidence steps ((Figure Ve.14, Task 2 Report)

Subsection IIc – Post-Undermining Activities

The Task 3 Report focuses on three topics:

- Additional analysis of data obtained during the mining of Panel 15 under I-70 in the winter of 2019 - In particular, the project team combined observations made by the University with those provided by PennDOT, to expand the inventory of identified subsidence impacts. The analysis of this data revealed the roadway pavement, especially after the longwall face passed under Embankment #1, behaved in an unanticipated manner. This lead to additional analyses aimed at characterizing the vertical subsidence, horizontal movement, and horizontal strain along the roadway at discrete time increments as the undermining was occurring. This more in-depth analysis helped to better identify the onset of highway impacts and the causes of the unexpected behavior. See Section II (Task 3 Report) for this discussion.
- Assessment of longwall subsidence risk to I-70 within the extended study area - The extended study area encompasses the Tunnel Ridge reserves of the Pittsburgh Coalbed in western Pennsylvania. A portion of these reserves has the potential to be mined beginning in 2024. Knowledge gained during the undermining of Panel 15 is used to evaluate potential longwall mining subsidence impacts within the extended study area along I-70. To accomplish this task, the University had to first propose a likely plan for longwall mining. Once that was accomplished, highway assets were located and characterized. Next, the SDPS model was used to predict potential surface subsidence along I-70 from the West Alexander to the Claysville interchange. After the completion of these steps the University was able to evaluate how the 28 significant assets identified within the extended study area might be impacted by the projected subsidence. See Section III (Task 3 Report) for this discussion.
- Analysis of the embankments supporting I-70 in the extended study area - The detailed finite element model of select embankments was subjected to a simulated, dynamically formed, subsidence basin. The shear strength reduction method (SRM) was used to evaluate the stability conditions of embankments under different material property values. This evaluation confirmed that the potential for instabilities along the highway surface increased with decreasing overburden. It was also found that excessive deformations increased as the orientation of the highway approached 90-deg to the direction of longwall panel advance. See Section IV (Task 3 Report) for this discussion.

1.0 Additional Analysis of Data Obtained During the Mining of Panel 15 under I-70 in the Winter of 2019

The Task 2 Report contained significant analysis of the events associated with the mining of Panel 15 under I-70. Further analyses were performed to build on the initial work completed under Task

2 so that the combination trends observed across the various datasets could be more deeply investigated.

1.1 Utilizing Topography Feature in SDPS

The Task 2 Report compared output from SDPS models with actual highway alignment surveys and predictions from a combination of empirical methods. These SDPS vertical subsidence profiles were adequate but a closer match was desired. The Task 2 Report SDPS models assumed the surface to be flat but the actual surface conditions are best described as hilly. The research question became "how much will topographic condition influence SDPS results?"

The University, with the guidance from Dr. Zack Agioutantis of the University of Kentucky, used a 3D rectangular grid model that interpolated topographic elevations from a triangulated network of elevation data points. The source of these elevation data points came the state's PAMAP elevation mapping program. The SDPS (with consideration of topography) predicted final vertical subsidence and this was compared to the measured highway alignment surveys recorded on 26 March 2019 (Figure IIc.1). A good match with measured values was found with the exception of areas over the embankment. The predicted maximum vertical subsidence is ~4.3-ft, ~1-ft less than vertical subsidence measured on the surface of Embankment #1 where the fill is the thickest (~75-ft). The additional subsidence, as discussed in the Task 2 Report, is caused by the settlement and lateral spreading of the fill comprising Embankment #1. Features like embankments have a large variation in material properties, especially when compared with the underlying strata. This cannot be accounted for by the SDPS model. Hence the lower predicted values than measured. It is also important to note the occurrence of minor surface heave over the gate road entries as measured along the highway shoulders in both the eastbound and westbound lanes. The SDPS model does not predict surface heave.

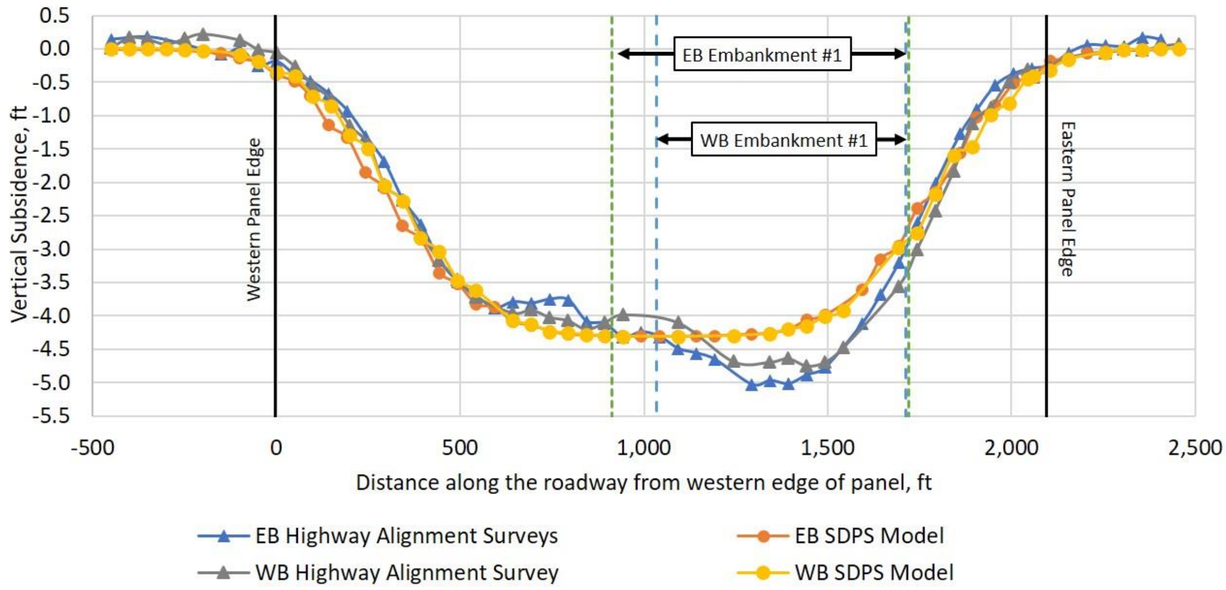

Figure IIc.1 – Final vertical subsidence associated with the extraction of Panel 15 along I-70 showing both highway alignment surveys and SDPS model results for both the westbound (WB) and eastbound (EB) travel lanes (Figure IIa.2, Task 3 Report)

1.2 Comparisons between Lateral Movements Predicted using SDPS and Highway Alignment Survey Measurements

The key operation in this analysis was to transform the movements so they conform with the orientation of the highway, i.e. parallel or perpendicular. As can be seen in Figure IIc.2, the horizontal movements parallel to the roadway experienced some deviations from the SDPS prediction, especially near the asphalt relief sections and within the western portion of the study area. Please note that the asphalt relief sections are located within the travel lanes and highway alignment surveys are made on the adjacent shoulder.

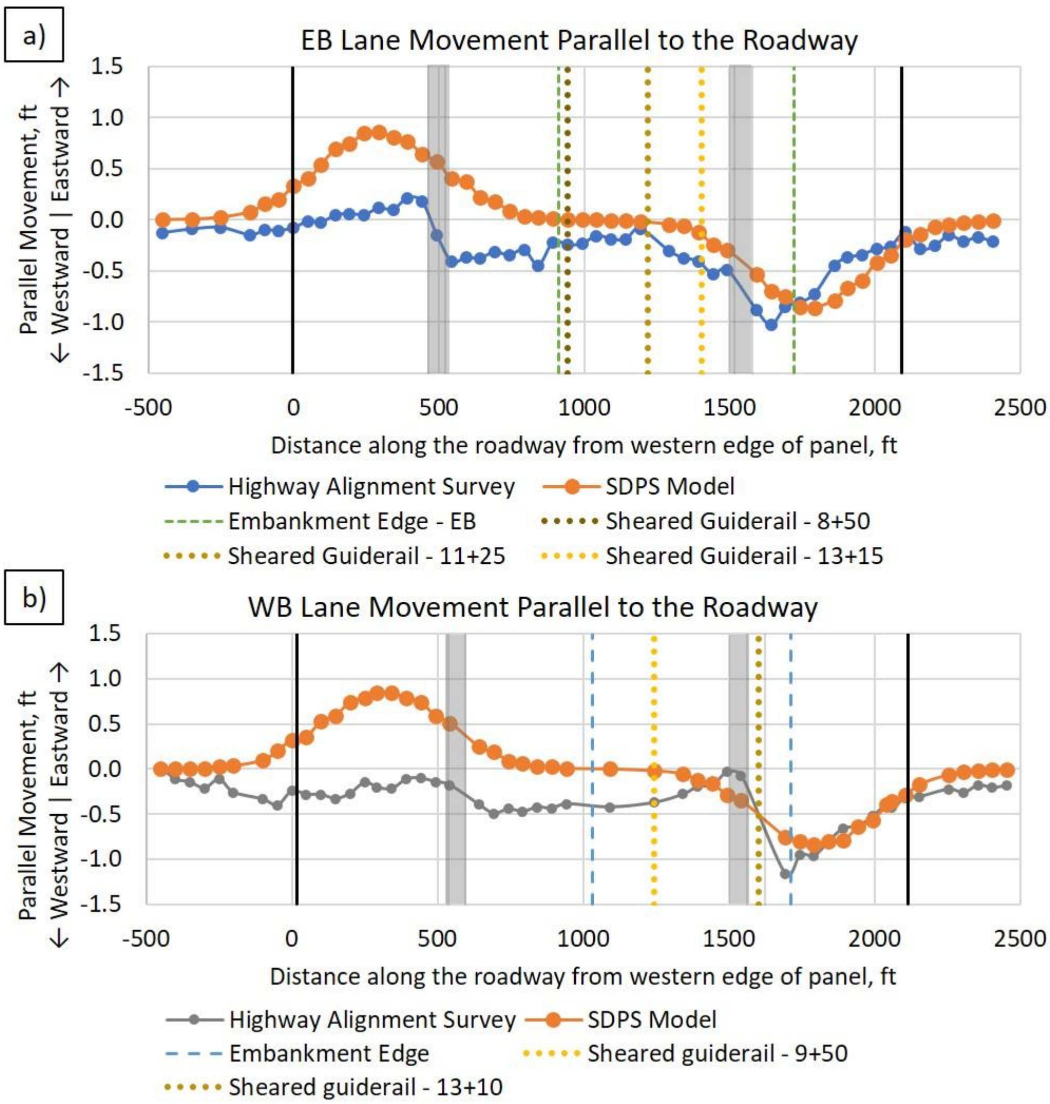

Figure IIc.2 - Comparison of horizontal movement parallel to the highway a) eastbound lanes (Figure IIa.3, Task 3 Report) and b) westbound lanes (Figure IIa.4, Task 3 Report). The gray stripes indicate the location of the eastern and western asphalt relief sections

Comparisons between the predicted and actual movements provides an opportunity to understand why differences, like the ones described above, occur. This is a powerful analysis technique that helps to explain:

- The influence of local conditions, i.e. bedrock verses fill
- The conditions / factors causing distress, i.e. expansion verse compression,
- The impact of a long, relatively narrow structure draped across a developing subsidence basin, i.e. evidence of roadway twisting, and
- The complex interactions between different segments of the pavement.

Through this kind of analysis, the influence of the asphalt relief sections, expansion joints, etc. on the highway alignment deformations and distress features was determined (Section IIc, Task 3 Report). Some of these factors/features are able to absorb some of the compressive forces in a manner that cannot be accommodated through the more rigid Portland cement concrete, causing different horizontal movements to occur between the traveling lanes and the shoulder (Section IIb, Task 3 Report).

1.3 Dynamic Subsidence

Perhaps the most striking comparison is obtained by examining both cumulative and incremental changes in predicted verses actual movement at different longwall face positions. The following dates represented periods where predictions, measurements, and observations were available: 15 January to 5 February 2019; 5 to 14 February 2019; 14 to 19 February 2019; and 19 February to 7 March 2019. Unlike the final predictions in the previous analysis, these cumulative and incremental analyses are made assuming that only the area of coal behind the longwall face on a given date had been extracted. These predictions are compared with the survey measurements and visual observations recorded on the respective dates.

On 5 February 2019, the longwall face was under Embankment #1. Cumulative horizontal movements showed only minor variations between the SDPS predictions and the measured survey data (Figure IIc.3a). The expansion of the surface parallel to the roadway directly followed the passage of the longwall face. This was then followed by surface compression ~300-ft behind the longwall face. On 14 February 2019 (Figure IIc.3b), the longwall face was beneath the western cut slopes in the study area. Both the predicted and measured horizontal movements parallel to the roadway showed a reasonably good comparison in the eastern portion of the study area. The overall surface movement is into / towards the center of the developing basin. On the western side of the study area, the measured values were consistently less than that predicted. On 19 February 2019 the longwall face had completely passed under the highway. In the eastern portion of the study area, the eastbound lanes showed reasonably good agreement between the predicted and measured horizontal movement parallel to the roadway with the exception of the western asphalt relief section (Figure IIc.3c). Section IIa.2 (Task 3 Report) also contains a detailed assessment of horizontal movements in the directions both parallel and perpendicular to the highway for the eastbound and westbound lanes.

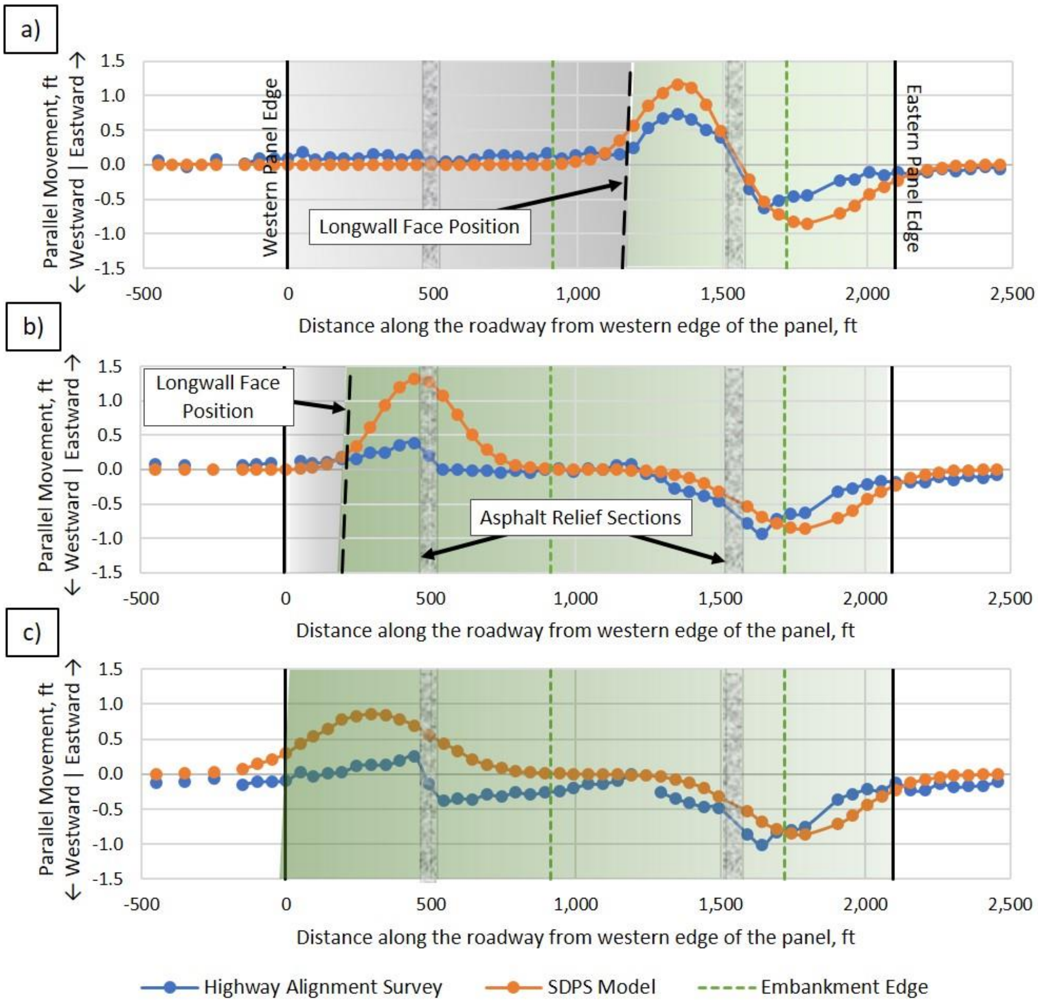

Figure IIc.3 – Comparison between predicted SDPS and measured highway alignment surveys cumulative movement in the eastbound lanes parallel to the highway as of: a) 5 February 2019; b) 19 February 2019; and c) 7 March 2019

The plots above depict cumulative vertical subsidence and horizontal movement both parallel and perpendicular to the roadway. Analyzing cumulative movements facilitates the investigation of the general development of the subsidence basin at different points in time. However, a cumulative subsidence analysis can mask the characteristics of the dynamic subsidence wave. It is important to recognize that many of the most significant impacts occur during discrete time periods through the duration of the undermining. When subsidence conditions are analyzed within smaller segments of time throughout the undermining, the relationship between subsidence characteristics and roadway impacts is more obvious. For example, when comparing measured movement parallel to the roadway during three different segments of time to the predicted values (Figure IIc.4), the dynamic nature of the wave is revealed, sometimes strongly revealed (eastern portion of the study area) or weakly (western portion of the study area).

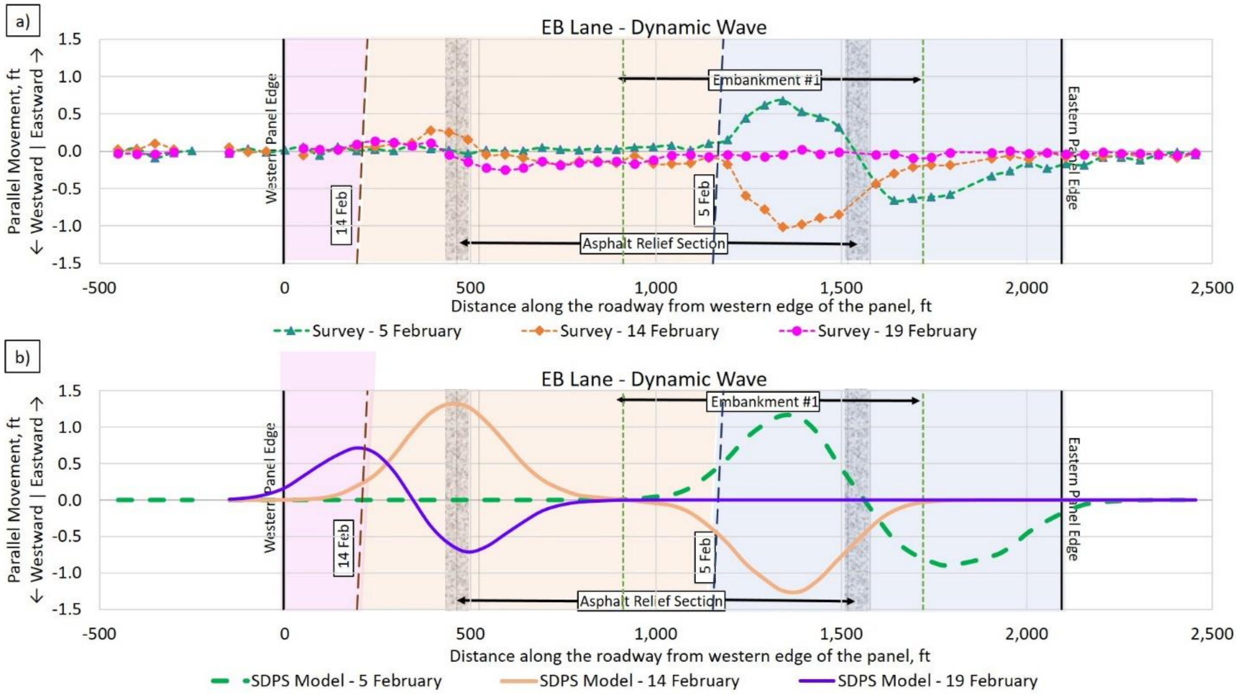

Figure IIc.4 – The dynamic nature of the developing subsidence basin is illustrated by superimposing the incremental horizontal movement of the eastbound lanes at three dates; a) measured values along the highway shoulder, and b) predicted values along the surface (modified from Figure IIa.15, Task 3 Report)

1.4 Twisting of the Pavement

Analysis of the horizontal movements parallel and perpendicular to I-70 in the study area show that the highway, defined by the continuous characteristics of the pavement structure, begin to behave differently than predicted after 5 February 2019. This is the approximate time when the longwall face moves under and away from Embankment #1. At this point, the ground surface begins to be pulled into the developing subsidence basin (Figure IIc.5a). At the same time, the measured survey points along the highway shoulder show the highway is being dragged toward the area of greatest vertical subsidence (Figure IIc.5b). In some areas close to the longwall face, the highway is moving in a different direction than the predicted ground movement directly below the pavement. It is thought that the highway began to twist at this point; thereby affecting how its western portion responded to the developing subsidence basin. It can be seen in Figure IIc.6a and b that the pavement rotated (or twisted) back in the opposite direction at the longwall mining progressed. The distress that developed in the pavement surface supports this theory, and will be discussed further in Section IIb. It is possible that this twisting is associated with a critical angle between the highway and the direction of longwall mining. The 35-deg angle found in the initial study area, as demonstrated above, can influence the potential for twisting. It is also likely that angles closer to zero or 90-deg are less likely to induce highway twisting.

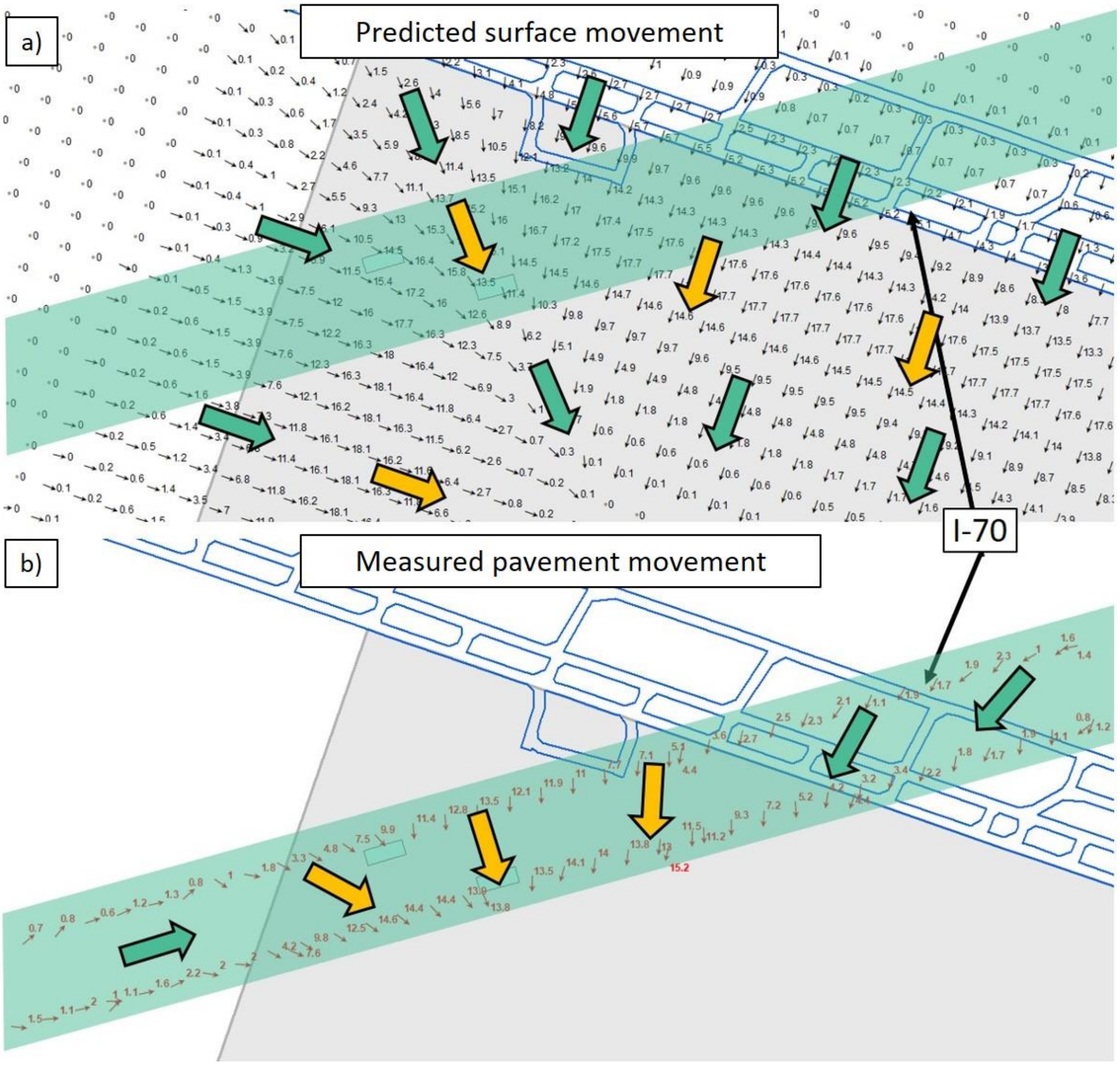

Figure IIc.5 – a) horizontal deformation as predicted using the SDPS model showing the movement of the surface into the developing subsidence basin on 5 February 2019; b) measured pavement movement along the highway shoulder on 5 February 2019 (modified version of Figure IIa.17, Task 3 Report)

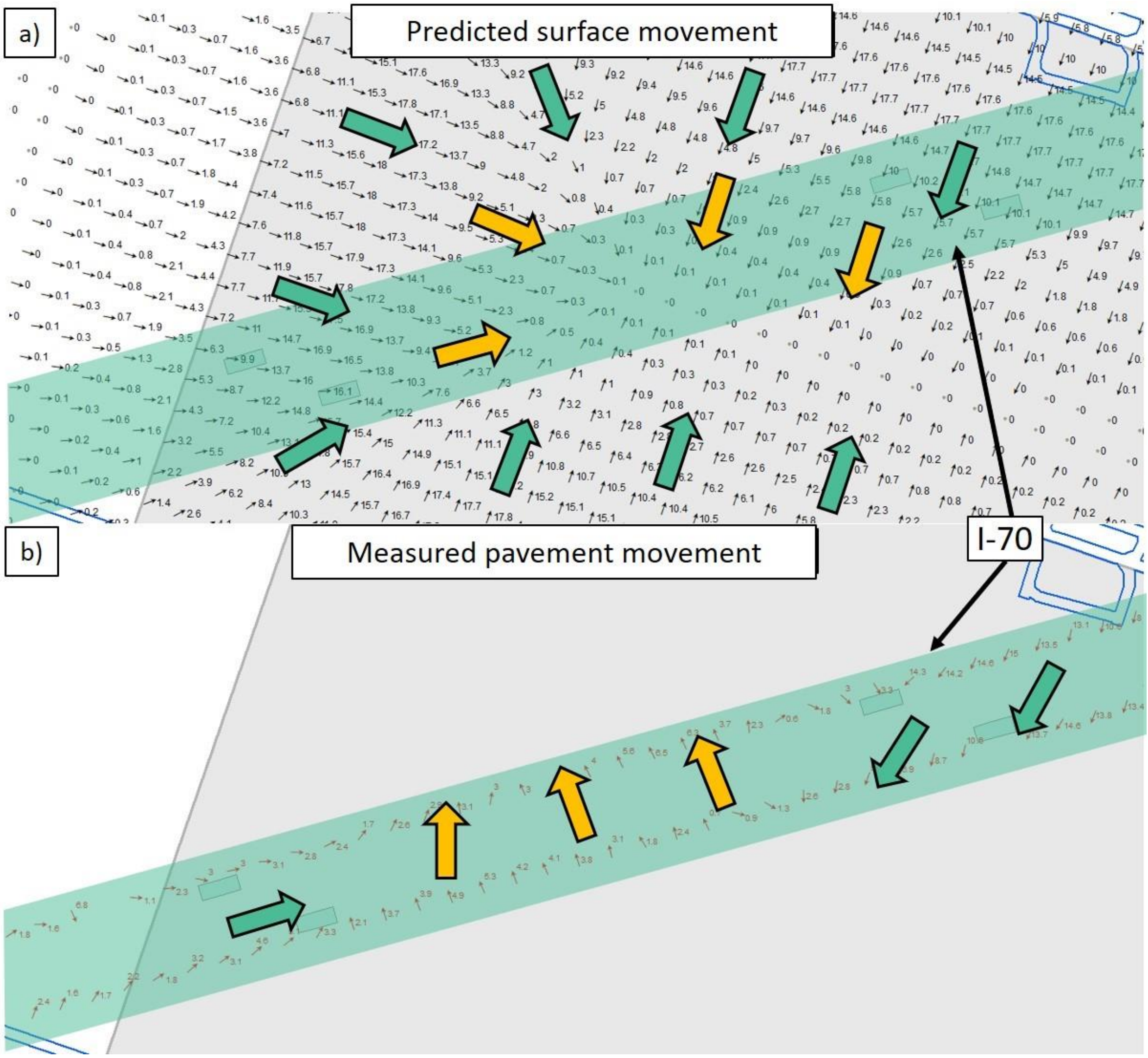

Figure IIc.6 – a) horizontal deformation as predicted using the SDPS model showing the movement of the surface into the developing subsidence basin on 14 February 2019; b) measured pavement movement along the highway shoulder on 14 February 2019

1.5 Pavement Characteristics

Section IIb in the Task 3 Report provides the design features of the pavement that spans across Panel 15. A portion of this discussion is included below:

> *This section of I-70 was reconstructed in 1989 (Figure IIc.7). A 13-in jointed concreate pavement lies over an open graded subbase. The skewed (1:6) transverse joints are 20-ft apart and contain 1.5–in diameter dowels that are 18-in long. The pavement has 4-ft inside and a 10-ft outside tied concrete shoulders that are 8-in thick adjacent to the lanes and tapered down 6-in at the outside edge. The tied shoulders contain #5 bars spaced 30-in on*

center and the transverse joints has 1.5-in diameter dowel bars. This section of roadway was eventually overlaid with 4 to 5-in of asphalt (Section IIb.1, Task 3 Report)). The travel lanes were constructed with a typical 2-pct cross slope, which sloped towards the outside shoulder. Both shoulders were constructed with a typical 4-pct cross slope, which sloped towards the outside shoulder. The westbound and eastbound travel lanes are separated with a grass median that varies between 30 and 70-ft in width.

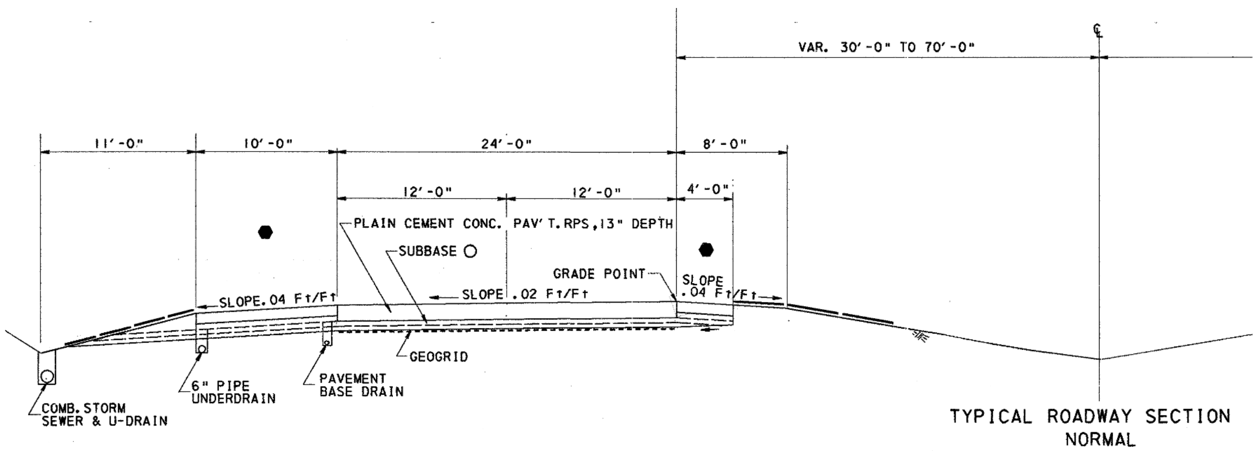

Figure IIc.7 – Typical cross section of I-70 from plans of 1980s highway reconstruction (Figure IIb.1, Task 3 Report)

The influence of the above characteristics on the pavement behavior during the undermining is highlighted with the following key points:

- Pavement connectivity – Smooth dowel bars located along the transverse joints serve as shear transfer devices to assist in transferring load across the joints between adjacent slabs. These dowel bars restrict vertical movements at the joints as well as horizontal movement perpendicular to the roadway and help to keep the slabs from shifting out of alignment. Movement of the slab parallel to the direction of traffic is not restrained by the smooth dowels.
- Tied shoulders – The shoulders are tied into the mainline, keeping the travel lanes from migrating out of alignment.
- Transverse contraction joints – Joints were observed to widen and close due to the extension and compressive forces generated during subsidence. The functioning dowels were able to accommodate this movement. PennDOT cut transverse joints into the asphalt overlay directly above the joints in the underlying JPCP to prevent transverse cracks from reflecting up into the overlay above each of the transverse joints when the joints opened.
- Asphalt relief sections – Excessive compressive stress that developed as a result of both dynamic and final subsidence were effectively absorbed in the asphalt relief sections. Six different compression bumps were documented during the undermining. All were quickly

milled with minimal disturbance to the traveling public. In addition, longitudinal shear cracks developed between the shoulder and the travel lane near these asphalt relief sections.

1.6 Strain and Distress Development

Previous sections have discussed the how horizontal deformation have affected the behavior of embankment slopes and pavement during undermining. The next logical step is to examine how excessive strains in the roadway can result in pavement distress. To begin this analysis lets identify the characteristics of the pavement and then outline how strains were determine and interpreted.

The visual distress observed was next compared to the horizontal strain (strain along the direction of travel). Two methods are used to define the horizontal strain. The first method uses the survey measurements taken along the highway. Strain is defined based on the differential movement between adjacent survey pins as the longwall face progresses from one position to another. The strain is derived by dividing the change in length, ΔL by the initial length, L_o, as shown in Figure IIc.8. Strains determined using survey measurements represent deformations in the shoulder and, in some cases, can be different from that in the travel lanes.

The second method consists of using the SDPS software to quantify the horizontal movements predicted from a scattered grid of points that surrounded the highway alignment. The predicted horizontal movements from this grid were then interpolated, creating a continuous surface of predictive horizontal movements along the highway alignment. Those predicted movement values from the surface were then extracted to the highway alignment pins, hereby creating a table that included both the movements recorded by the surveys and the predicted movements from SDPS. In both methods, the same formula is used. The first method calculated strains based on the surveyed movements, while the second method calculated strain based on the predicted movements from SDPS. It should be noted that the first method of using the alignment pins provides an estimate of the strain in the pavement surface, while the SDPS software provides the horizontal movement of the surface below the pavement and neglects the presence of the highway above it.

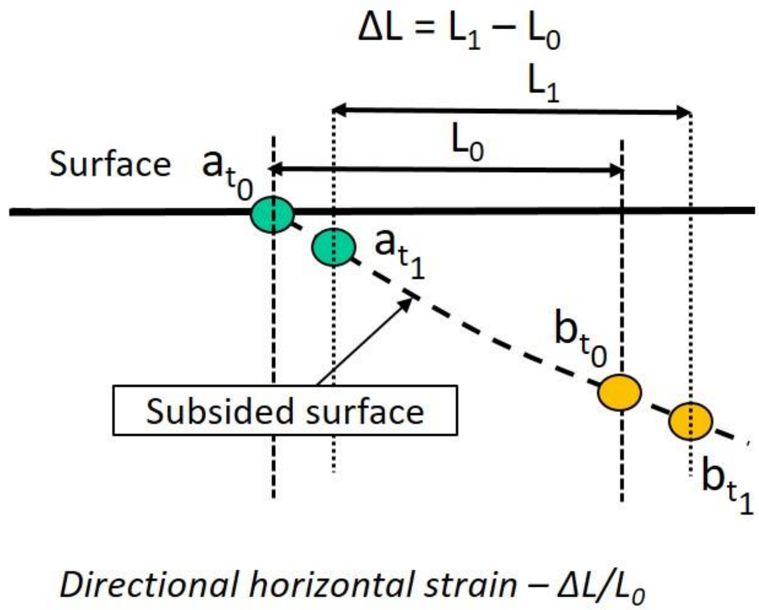

Figure IIc.8 – Components of directional horizontal strain defined using the highway alignment surveys (Figure IIIb.11, Task 3 Report)

Numerous strain profiles are provided for dates associated with when the mining of Panel 15 progressed below the interstate. This is an effective means for comparing the development of distress with pavement strain conditions. For example, eight different types of distress were observed in the eastbound lanes during the 5 February site visit (Figure IIc.9). When distress locations are added to horizontal strain profiles, important relationships are revealed. The wave shaped profile, for both predicted and measured strains, shows good agreement. Close to the longwall face position, surface strains are tensile. In this area, transverse cracks and widened transverse joints are common. The region directly behind the longwall face is in tension. Here transverse joints were observed to open (or widen), as shown in Figure IIc.9 Photo #1. Further away from the longwall face and near the asphalt relief section, the surface strains are compressive. Here the pavement experienced both compressive bumps and blowups as shown Photo #4 and #5, respectively (Figure IIc.9).

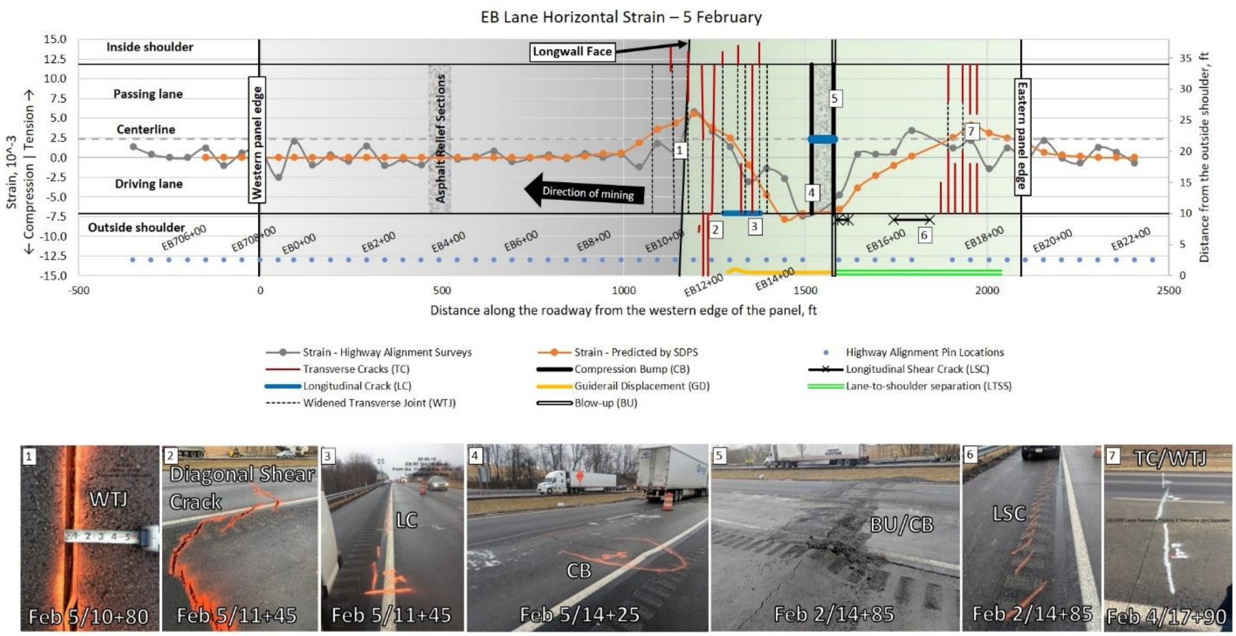

Figure IIc.9 - Horizontal strain and observed distress for EB lanes on 5 February 2019 (Figure IIb.16, Task 3 Report)

Strain profiles are useful in understanding how an engineering control like an asphalt relief section effects strains induced by longwall mining. On 5 February, both the predicted and measured horizontal strain profiles from the westbound lanes show good agreement except in the area of the asphalt relief section (Figure IIc.10). The predicted horizontal strain was just developing in this area, yet the measured horizontal strain was abnormally high (~12 x 10^{-3}). The horizontal strain is concentrated in the full-depth asphalt section because of the increased compressibility of the asphalt as compared to the adjacent, more rigid, concrete shoulder. This resulted in the development of longitudinal shear cracks along the lane/shoulder joint, which divides these two regions (shown in Photo #6 in Figure IIc.9), and longitudinal cracking (shown in Photo #3 in Figure IIc.10).

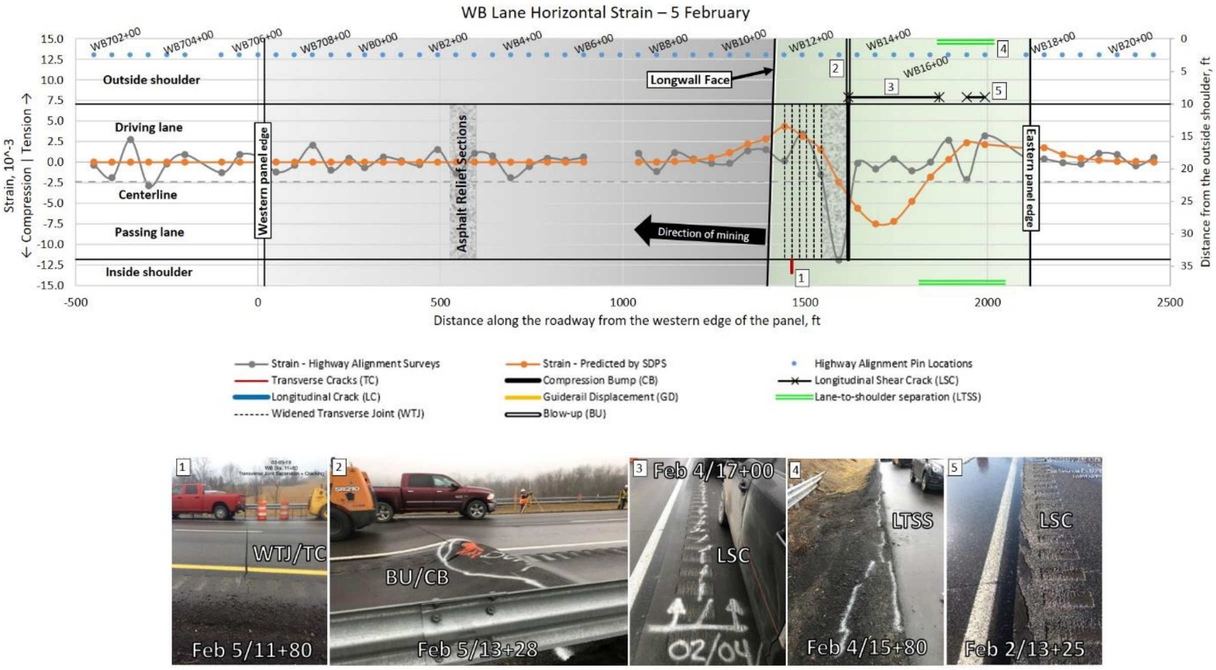

Figure IIc.10 - Horizontal strain and observed distress for WB lanes on 5 February 2019 (Figure IIb.17, Task 3 Report)

Section IIb of the Task 3 Report ended with a detailed discussion of other notable distress observed during undermining. In some cases, the distress is identified with a distinct strain condition. In others cases, the difference between the predicted and measured strain conditions is significant, especially close to when the longwall face was approaching the western end of the longwall panel under the highway.

2.0 Assessment Longwall Subsidence Risk to I-70 within the Extended Study Area

2.1 <u>Predicting Longwall Panel Locations, Orientation and Width within the Extended Study Area</u>

In the absence of an approved longwall mining plan for the area of unmined Pittsburgh Coalbed between the West Alexander and Claysville interchange, the University used knowledge about past longwall mining in this area to determine a likely layouts of the longwall panels (Figure IIc.11). Ten panels were identified and are placed based on the following considerations:

- Panel width will be ~1,200-ft since this is the dimension used by the current panels at the mine (it is possible the width could increase for the panels within the extended study area),
- Panel length is determined by how fast the adjacent gate road entries can be mined, ventilation and methane control requirements, property and coal ownership, and the occurrence of limiting geologic anomalies. Under expected current conditions, panels are

design to be from 14,000 to 20,000-ft in length. If panels are considerable less in length, operation can be effected by additional cost and risk associated with setting up and recovering longwall face equipment. The more the longwall face has to move (setup and recover), the less profitable the operation and potentially more hazardous the work environment.

- Panel orientation is closely tied to optimizing entry stability. There are certain orientations that can produce adverse ground conditions in the head gate entries. This is the area with the highest concentration of workers and where all the supplies enter the work area. It is also where the coal begins its transport to the surface. As a result, all current longwall panels in the Pittsburgh Coalbed (five total mines) are oriented between N 67° W and N 71° W to help mitigate the damaging effects of excessive lateral stress (Mark and Mucho, 1994).
- The current gate road entries are ~180-ft wide. The size of the pillars and the width of the entries are designed to meet ventilation and ground control safety regulations. They are not expected to change in the near future.

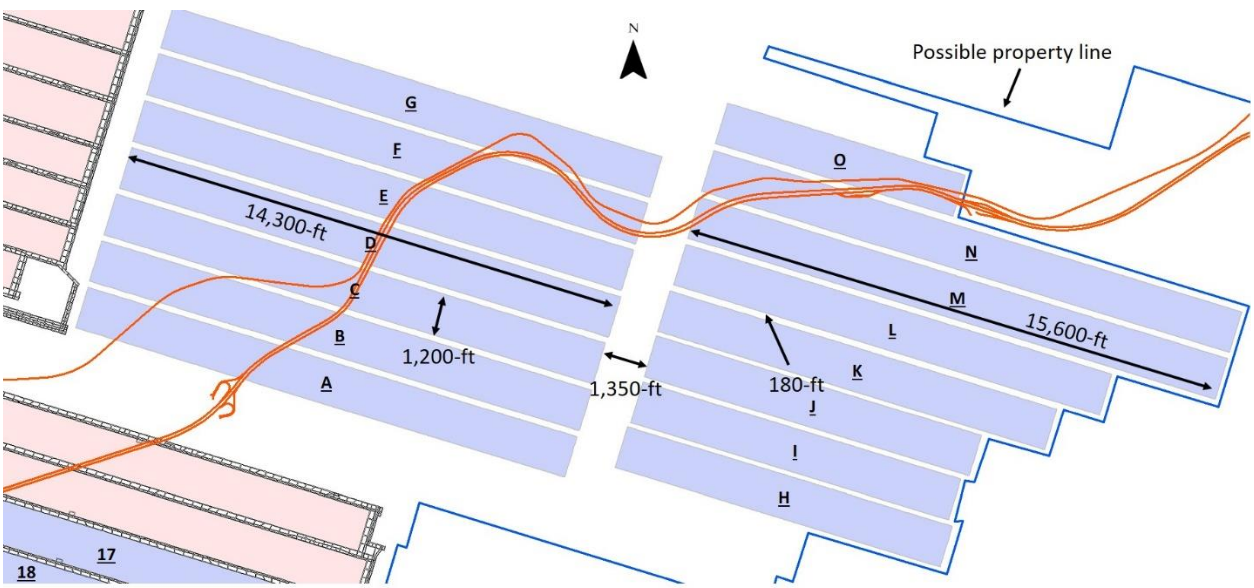

Figure IIc.11 – Projected location of longwall panels within the extended study area (Figure IIIa.4, Task 3 Report)

2.2 Subsidence Basin Characteristics

A longwall mining subsidence basin can be thought of as containing three characteristics parts that are based on geometric properties (Figure IIc.12). The flat bottom of the basin is called the mid-panel area. The surface above the mid-panel experiences the full dynamic subsidence wave but should not experience a permanent surface slope change. The quarter-panel area comprises most of the subsidence basin's sides. Here the surface slope can be permanently altered while the dynamic subsidence wave is lessened as the edge of the basin is approached. The surface above the gate road entry experiences much less vertical or horizontal movements and horizontal strains than the adjacent quarter-panel area. But, that is not to say impacts are not possible. Heave, or uplift, has been observed in these areas as well as tensile cracks that form along the boundary of the subsidence basin.

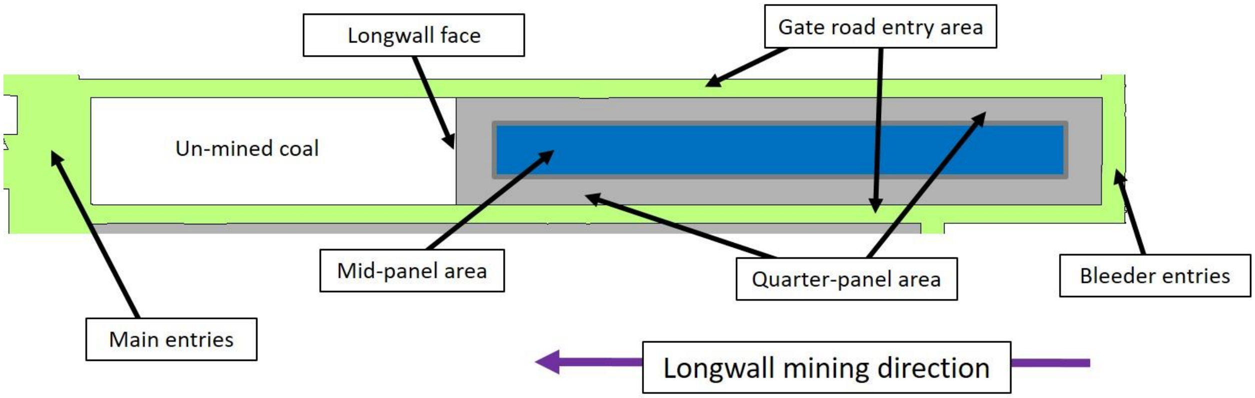

Figure IIc.12 - Conceptual drawing shows the two geometric components of a longwall panel (mid- and quarter-panels) and the three functional components of the room-and-pillar (main, bleeder, and gate road entries) mining methods (Figure IIIa.8, Task 3 Report)

The intricacies of these three characteristics can be further examined by studying profiles across the developing subsidence basin. The University used a combination of empirical relationships between overburden and vertical subsidence, the profile function method, and the SDPS model to define the size of the quarter-panel area. This analysis approach has been referred to in all three Task Reports. For example, the relationship between vertical subsidence and surface slope changes are dependent on the location of the Inflection Point (Figure IIc.13). For conditions representative of Panel 15, the width of the quarter-panel is shown to be based on the Inflection Point and the offset distance ‘d’. In this case, the width of the quarter-panel area is, by inference, 2 x d (165-ft) or 230-ft. The use of profile functions to model the general shape of a subsidence basin has been discussed by Hood et al., 1981; Karmis et al., 1984; Peng and Cheng, 1981.

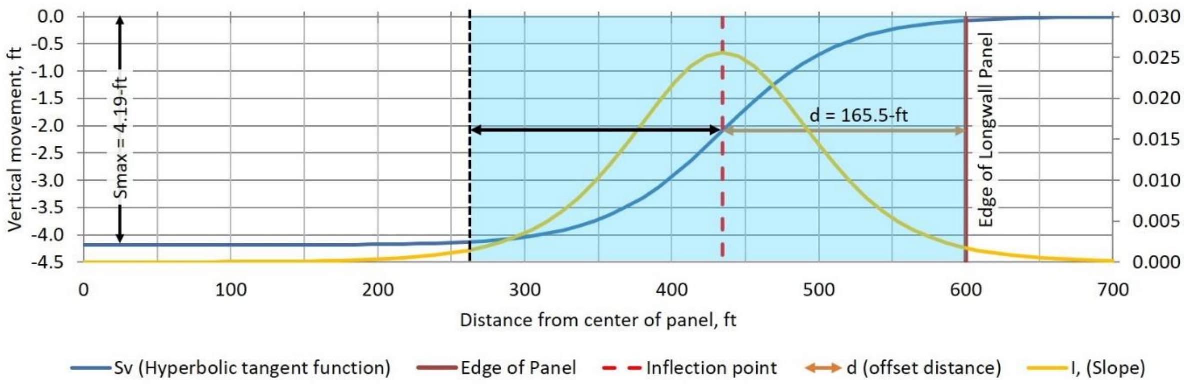

Figure IIc.13 – Vertical subsidence and surface slope profiles and the location of Inflection Point (Ip) and the corresponding width of the quarter-panel area (2 x d)

These analysis also show how the overburden influences the shape and intensity of the subsidence basin. With a low overburden, 400-ft, the Inflection Point is located 126-ft from the solid coal producing a quarter-panel width of 252-ft (Figure IIc.14). At higher overburdens, 800-ft, the Inflection Point is 175-ft from solid coal and the quarter-panel width is 350-ft. The majority of I-70 in the extended study area has an overburden of between 400 and 800-ft, producing a quarter-panel width of between 252 and 350-ft (Figure IIc.14).

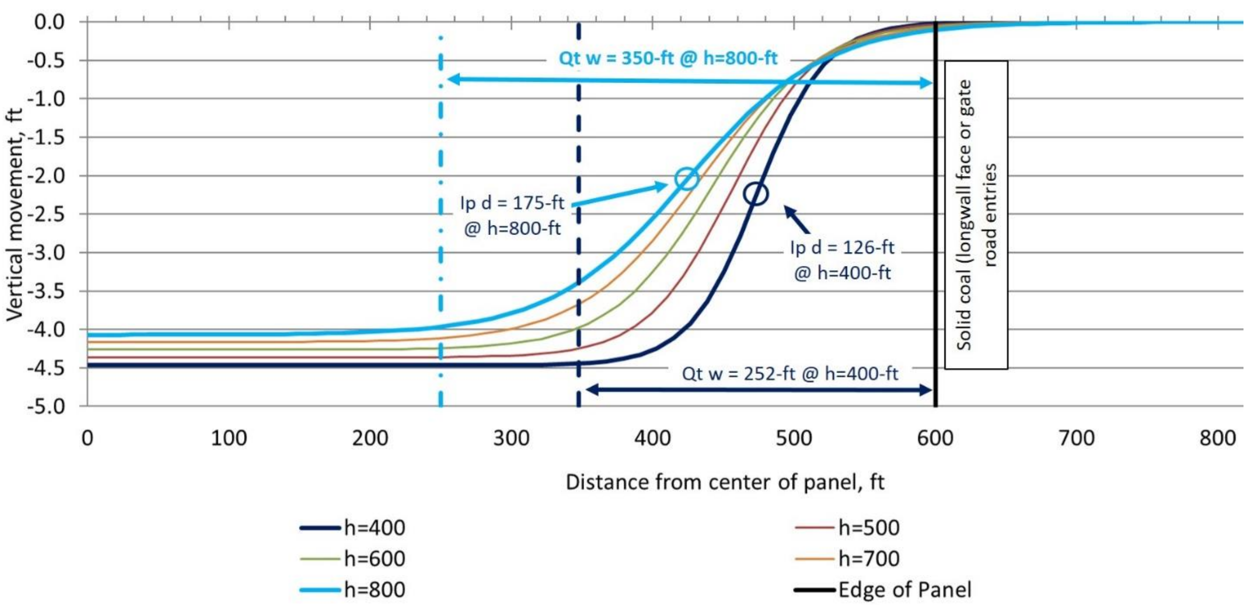

Figure IIc.14 – Vertical subsidence profiles at overburdens ranging from 400 to 800-ft with resulting changes to the shape of the subsidence basin and the width of the quarter-panel area (Figure IIIa.10, Task 3 Report)

2.3 Tolerances for Overpasses, Retaining Walls, and Culverts

Recommended tolerances for overpasses, conventional retaining walls, and culverts are established by both PennDOT, Design Manual Part 4 (Anon, 2019) and AASHTO (AASHTO; Anon, 2004a & b).

2.3.1 *Overpasses*

A key in maintaining stability is avoiding significant differential settlement between the foundations on each end of the overpass span. PennDOT and AASHTO design standards for both single and continuous span overpasses allows a maximum net foundation settlement up to 1-in (Table IIIa.5, Task 3 Report). In addition, the maximum allowable settlement shall be limited to 0.0025 and 0.0015.

Allowable settlement = δ'/l [Eq.IIIa.3, Task 3 Report]

Where: δ' = differential settlement, in

l = span between foundations, in

For example, for a 35-ft simple span, the allowable settlement is 0.0025. This yields a permissible differential settlement of 1.05-in.

2.3.2 *Conventional Retaining Walls*

The allowable settlement for conventional retaining walls is from 0.002 to 0.001 (Table IIIa.5, Task 2 Report). For a 35-ft long wall, the allowable settlement will be between 0.42 and 0.84-in.

2.3.3 *Culverts*

Reinforced concrete culverts are cast-in-place and are present either at the base of embankments or along a stream channel. In all cases, they are covered with fill ranging in thickness from 15 to 70-ft. AASHTO describes the Service Limit State (12.5.2) influenced by cracks, shear, thrust, and radial tension in reinforced concrete structures. Differential settlement along a culvert slope angle can cause cracks in the footing and between existing construction joints and thereby negatively affect the flow of water within the culvert.

2.4 Highway Assets within the Extended Study Area

Twenty-eight assets are identified within the extended study area and can be grouped into one of four categories: embankments, overpasses, conventional retaining walls, and culvert. Table IIIa.5 (Task 3 Report) list the assets as they are encountered when traveling from west (West Alexander

Interchange) to east (Claysville Interchange). The location of each of the 28 assets is shown in Figure IIc.15.

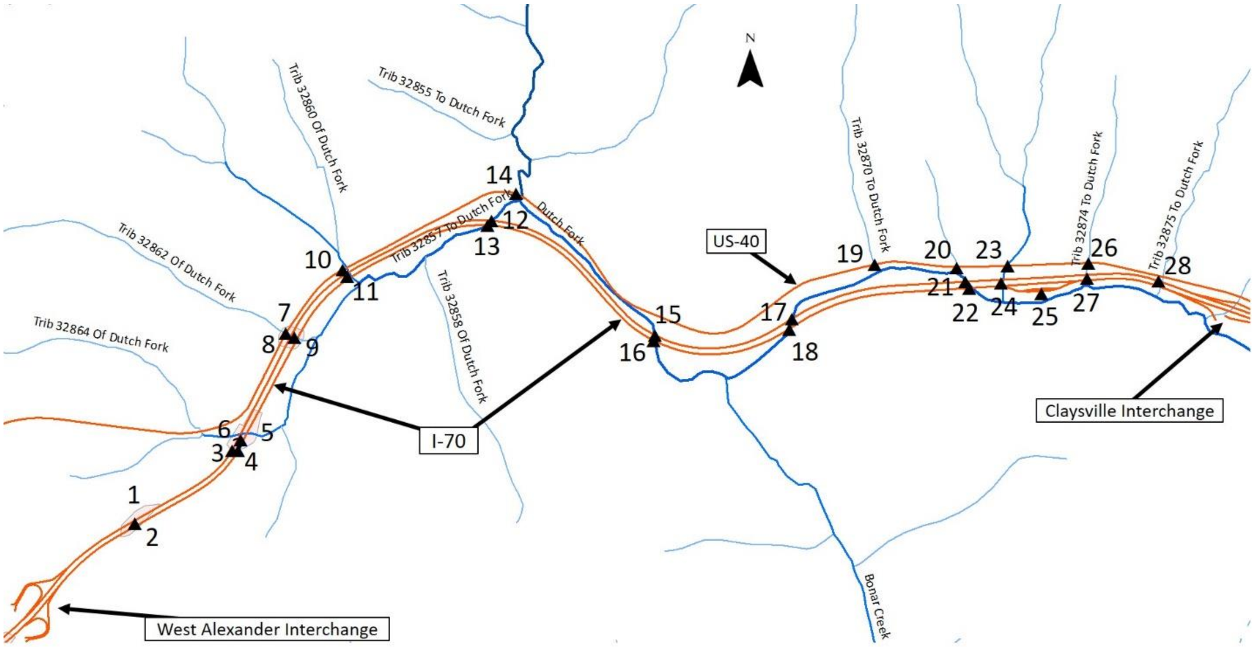

Figure IIc.15 – Location of the 28 identified embankment, overpass, and culvert highway assets in the extended study area (Figure IIIa.13, Task 3 Report)

2.4.1 *Embankments*

Nine of the assets shown in Figure IIc.15 (2, 3, 4, 6, 8 and 9) are contained within one of three embankments (#4, #5, and #6). The general characteristics of these three embankments is provided in Table IIc.1. Embankment #5 is assessed as the structure that presents the most risk during the undermining. A stability assessment of this embankment is provided in this section.

Table IIc.1 – General characteristics of the three embankments within the extended study area (Table IIIa.7, Task 3 Report)

Embankment	Panel ID & Panel Area	Avg. Overburden, ft	Max. Length of Highway Carried by Embankment, ft	Orientation of Highway to Mining Direction, deg	Max. Fill Thickness, ft
#4	A-Qt & Gate, B-Qt	598	~685	42	52
#5	**C-Mid & Qt**	**514**	**~785**	**79**	**70**
#6	D-Qt & Gate	492	~380	79	54

Panel area: Mid = Middle-panel area, Qt = Quarter-panel area, Gate = Gate road entries area

2.4.2 *Overpasses*

The undermining would represent a significant risk to the eleven overpasses. Nine of the 11 overpasses have a simple span layout, varying mainly in length and ranging from 30 to 52-ft (Table IIIa.8, Task 3 Report). Each structure has been assigned a structural conditions rating, which ranges from fair (5) to very good (8). Two of the overpasses with multiple spans have a structural condition rating of fair (5).

2.4.3 *Reinforced Concrete Retaining Walls*

Three pairs of overpasses are connected with conventional retaining walls (Figure IIc.16). The nature of the connection could not be determined. The retaining walls help to provide lateral support for the overpass stem walls, prevent highway fill from entering the stream channel, and help to maintain stream flow under a wide range of conditions. When considering the stem and retaining walls together, the total length averages 163-ft.

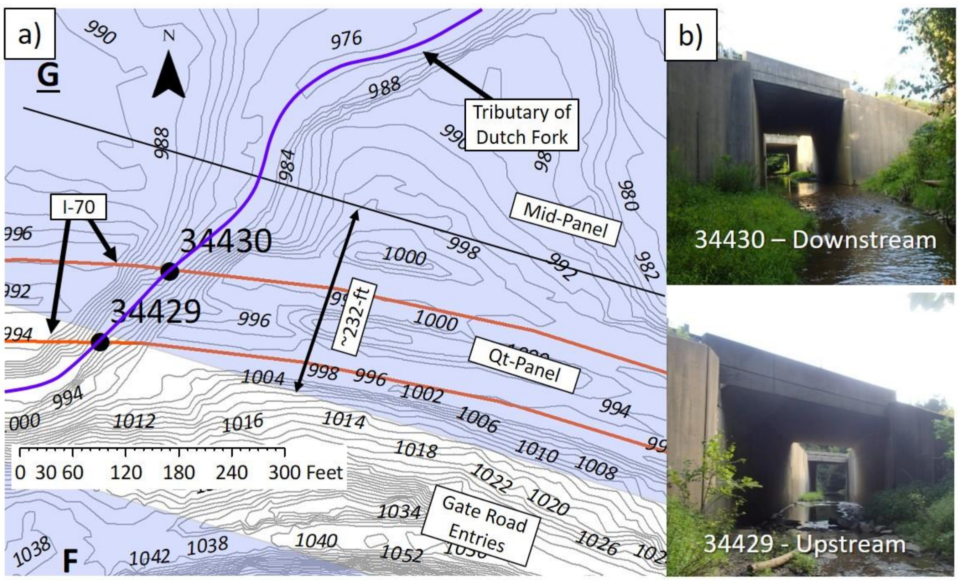

Figure IIc.16 – Overpasses 34429 and 34430 with connecting conventional retaining wall (Figure IIIa.22, Task 3 Report)

2.4.4 *Culverts*

Nine concrete culverts are identified within the extended study area (Figure IIc.17). One relative measure of the culvert flow capacity is to examine its stream order. The nine reinforced culverts found within the extended study area carry 3rd order streams. This is an indication of the relatively significant potential flow these culverts are expected to carry. The tenth culvert in the study area is a smaller diameter corrugated metal structure that carries a 1st order stream.

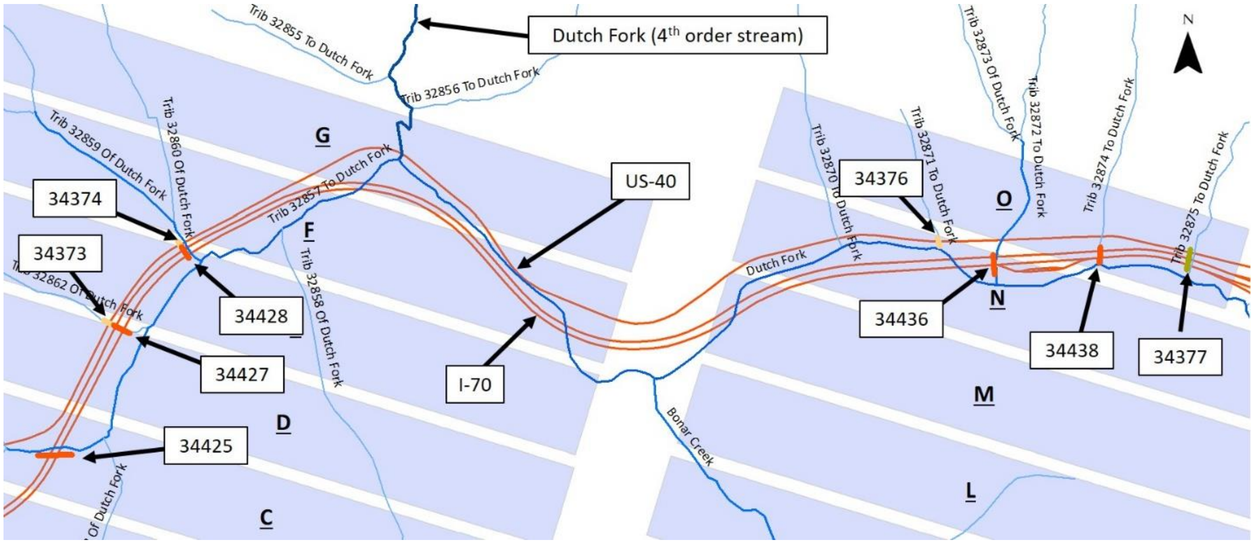

Figure IIc17. – Reinforced concrete culverts within the extended study area. Dutch Fork and portions of Tributary 32857 to Dutch Fork are 3rd order streams (Figure IIIa.24, Task 3 Report)

2.5 SDPS Prediction of Movements within the Extended Study Area

Previously (Section IIc.2), predictions of subsidence basin characteristics were established by combining empirical trends with the Profile Function Method. This provides a quick assessment but many simplifying assumption are required. For the extended study area, the SDPS model considered topographic influences, displayed in three dimensions, and determined movements / strains in a full range of orientations. Using SDPS, the final vertical subsidence caused by the longwall panels throughout the extended study area was predicted in Figure IIc.18.

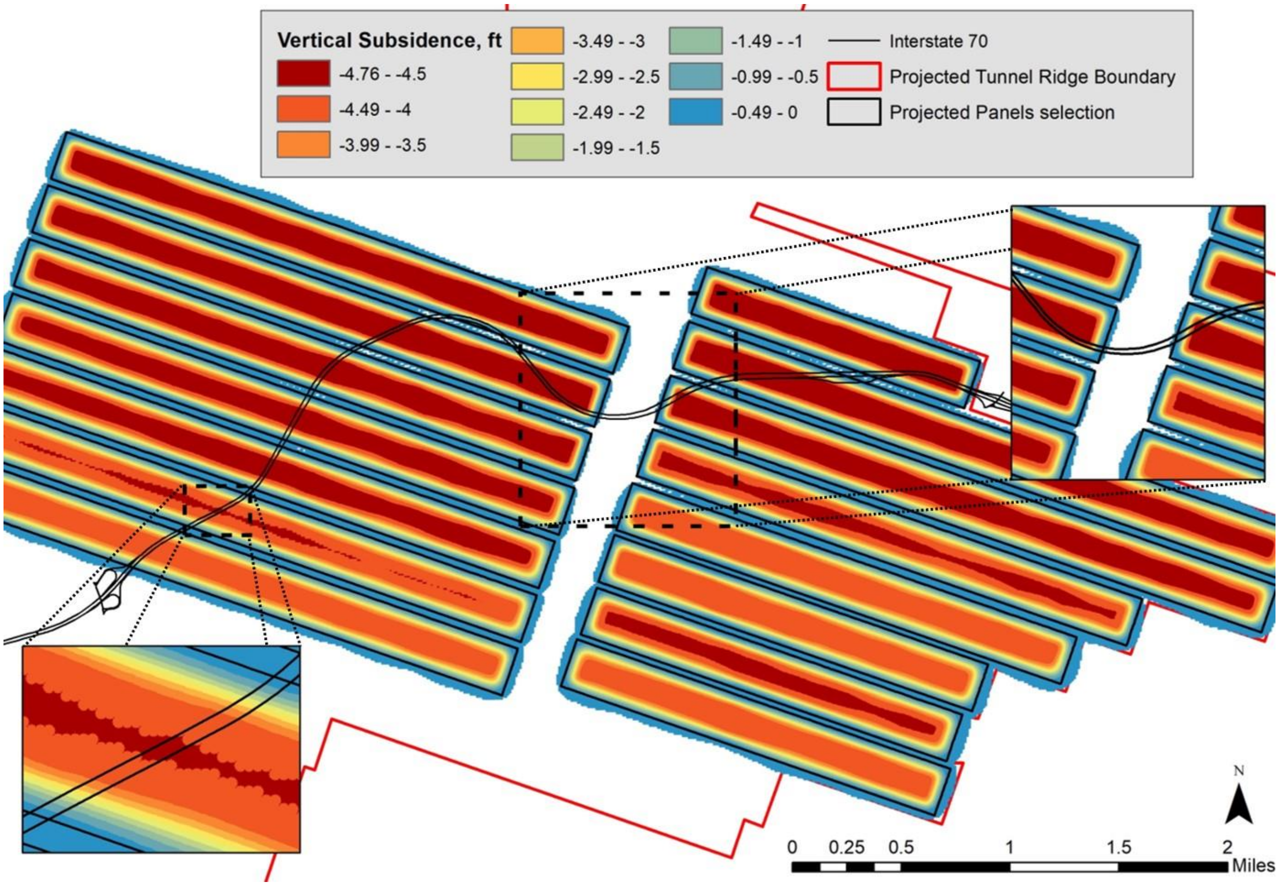

Figure IIc.18 – Vertical subsidence caused by longwall mining throughout extended study area (Figure IIIb.1, Task 3 Report)

In addition to vertical subsidence, predictions of the total horizontal deformation along cross-sectional profiles in the extended study area are possible. For example, a profile from Panel A to G is shown in Figure IIc.19, indicating a maximum horizontal deformation of ~1.67-ft. Note that the amount of maximum total horizontal deformation increases slightly as overburden decreases and develops within the quarter-panel area, where the vertical subsidence profile has the greatest slope. Lastly, the width of the quarter-panel areas (blue area, Figure IIc.19b) produced from empirical relationships is slightly less than the width displayed by the SDPS curves (purple line, Figure IIc.19b)

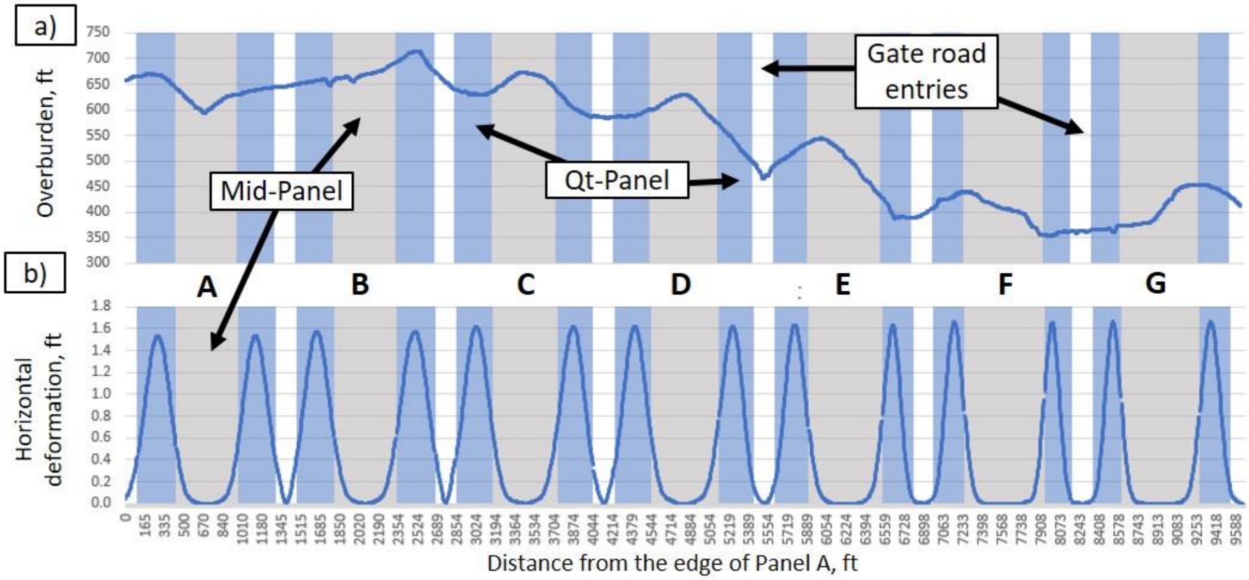

Figure IIc.19 – Profile of a) overburden and b) predicted total horizontal deformation for Panels A to G (Figure IIIb.7, Task 3 Report)

SDPS predictions of maximum horizontal strain for a profile from Panels A to G is shown in Figure IIc.20. The maximum horizontal tensile and compressive strain predicted for these panels varies from ~9 to 16 (10^{-3})-ft/ft depending on the overburden in that area. The lower values are associated with Panel A and B, while the higher values were associated with Panels F and G. For this area, a decrease in the average overburden from ~700 to 400-ft could produce a 50 to 60-pct increase in the maximum horizontal strain values. These calculations match well with the predicted and measured horizontal strain for the Panel 15 study area (Section IIc.1.6).

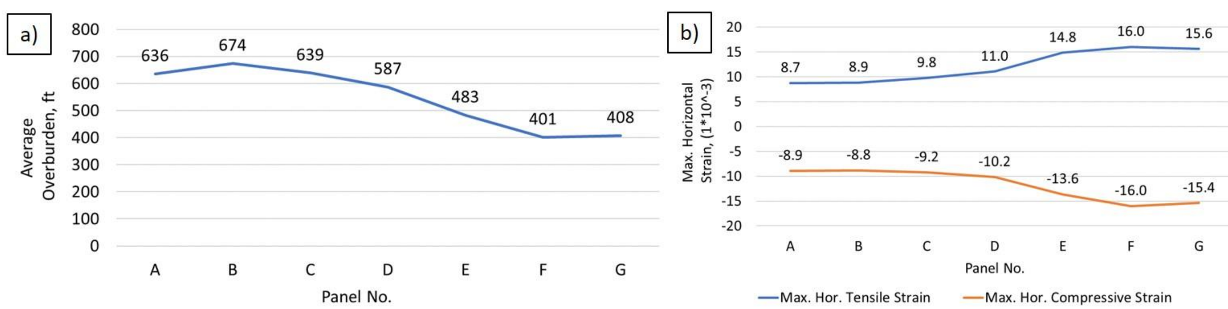

Figure IIc.20 – Graphs of a) average overburden and b) predicted horizontal strain for Panels A to G (Figure IIIb.9, Task 3 Report)

2.6 Selected Detailed Asset Analysis

The University selected a subset of the 28 identified significant assets for further study. The aim was to illustrate how different assets, located at dissimilar positions within a subsidence basin, could react to these potential subsidence events. The impact of both permanent as well as dynamic subsidence conditions are presented. In some cases, assets would see more potential impacts from permanent subsidence, i.e. culverts crossing a quarter-panel area. In other cases assets would experience impacts only during dynamic subsidence, i.e. differential settlement of overpass foundations. The SDPS model provided an opportunity to predict vertical subsidence and horizontal movements along the profile of assets. Understanding how structures deform helps to assess potential performance issues and implement the most effective engineering interventions to mitigate impact.

2.6.1 *Culvert 34425*

Culvert 34425 is the longest culvert identified in the extended study area; is under the most fill; and has the lowest (5) condition rating (Table IIIa.10, Task 3 Report). As the culvert is located in the center of where longwall Panel C could potentially be located, it is expected to experience a similar amount of total or permanent vertical subsidence and horizontal deformation. However, during the dynamic subsidence event associated with the passage of the longwall face, this culvert is predicted to experience significantly different deformations in both the vertical and horizontal planes. Figure IIc.21a shows eight face positions (Face A through H) associated with the undermining of this asset. The initial face position is located just under the western end of the culvert. Eight face positions later, the longwall is over 300-ft past the eastern end of the culvert. Figure IIc.21b shows how the surface profile above the culvert subsides. It also shows that there is no permanent change in the slope of the culvert. Figure IIc.21c displays the change in vertical subsidence along the length of the culvert during the eight face positions. At face position D, more than 200-ft of culvert is predicted to subside at a rate of ~10-in every 50-ft. There are no design guidelines or severity indices that provide some indication as to how this structure will respond to this magnitude of differential movement. What complicates this assessment is the role of the surrounding fill in absorbing predicted settlement rates. It should be mentioned that for a short time during the development of the subsidence basin, the inlet of the culvert has the potential to settle as much as 55-in more than the culvert near the outlet. Temporary ponding could result.

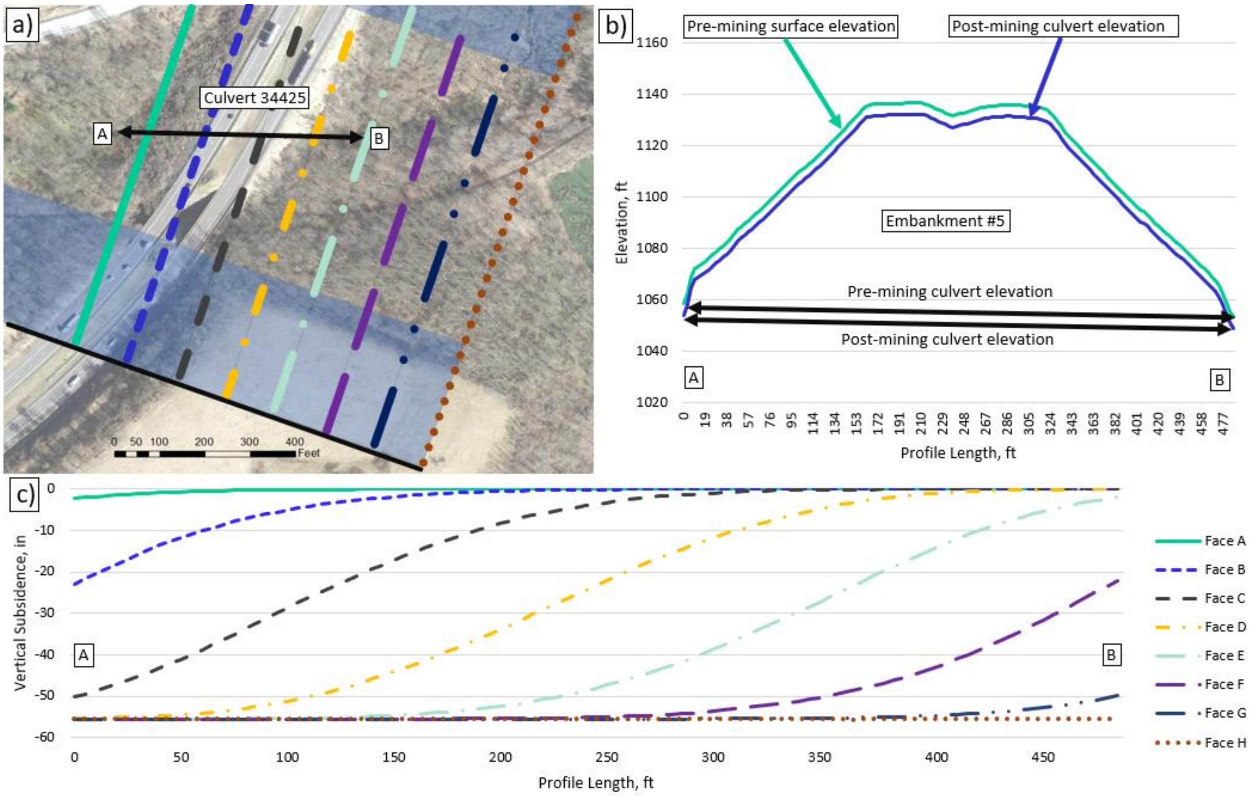

Figure IIc.21 - Summary of predicted vertical subsidence of Culvert 34425; a) longwall face position of potential Panel C, b) pre- and post-mining surface and culvert elevations, and c) vertical subsidence at eight face positions (Figure IIIb.16, Task 3 Report)

2.6.2 *Overpasses 34435 and 34437*

As shown in the previous sections, Overpasses 34435 and 34437, which lie above potential Panel N will deform gradually over a several day period as the longwall face approaches and subsequently passes beneath them. Conversely, because the overpasses are located within the mid-panel area of potential longwall Panel N, they are expected to experience only minor amounts of permanent differential settlement. This can be seen by comparing the vertical subsidence profiles between the foundation for Points A and B (Figure IIc.22b) as well as Points C and D (Figure IIc.22c). The differential settlements between these abutments at Faces F and K are predicted to be at most a few inches. A bigger risk to the structural integrity of the overpasses is the dynamic differential settlement during undermining, especially when the longwall face is 200 to 300-ft past the overpasses. At Face I (Figure IIc.22b) and Face H (Figure IIc.22c) the foundation for the overpasses (Points A, B, C, and D) is predicted to experience as much as 10-in of differential settlement.

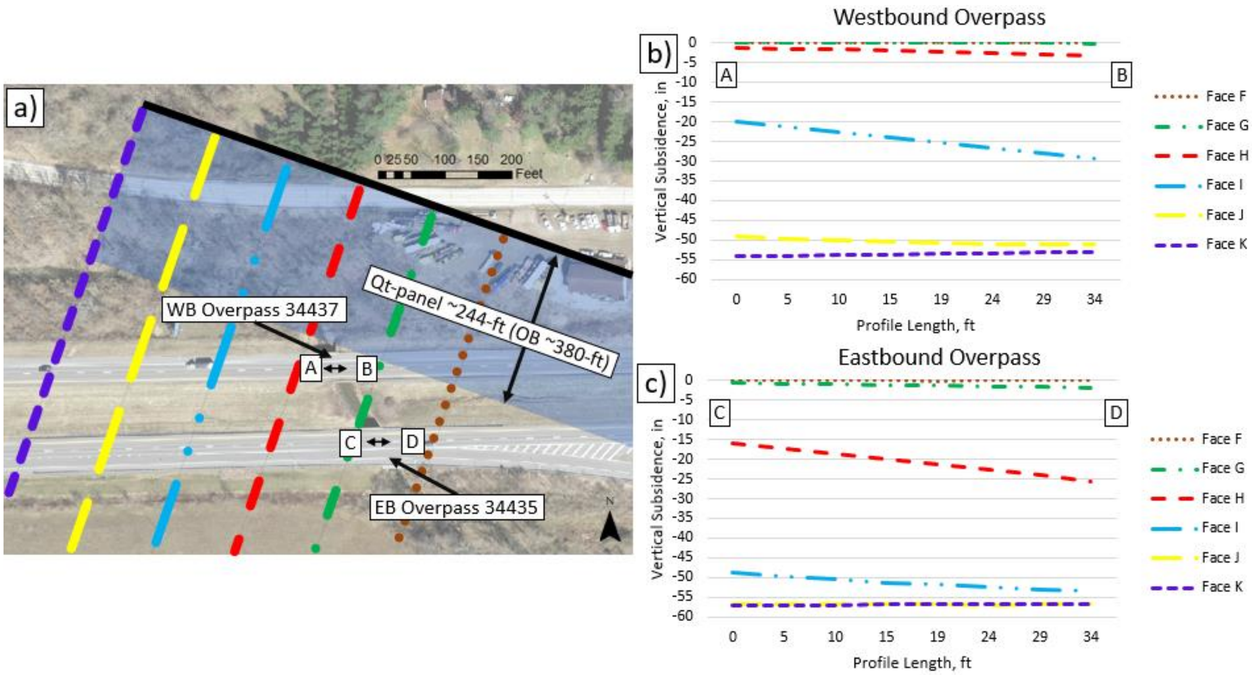

Figure IIc.22 – Summary of predicted vertical subsidence conditions for Overpasses 34437 and 34435 during undermining by Panel N; a) longwall face positions, b) westbound overpass (A-B) vertical subsidence, and c) eastbound overpass (C-D) vertical subsidence at six face positions (Figure IIIb.25, Task 3 Report)

The next question to consider is how predicted horizontal deformations might impact Overpasses 34435 and 34437. Differential horizontal deformations of a few inches are seen when the longwall face is underneath the overpasses (Face H, Figure IIc.23b; and Face G, Figure IIc.23c). Peak horizontal movement approaching 20-in are predicted when the longwall face is 200 to 300-ft past the overpass (Face I, Figure IIc.23b; and Face H, Figure IIc.23c). In this analysis the differential horizontal deformation is rarely more than 5-in. One exception is Face I (Figure IIc.23b).

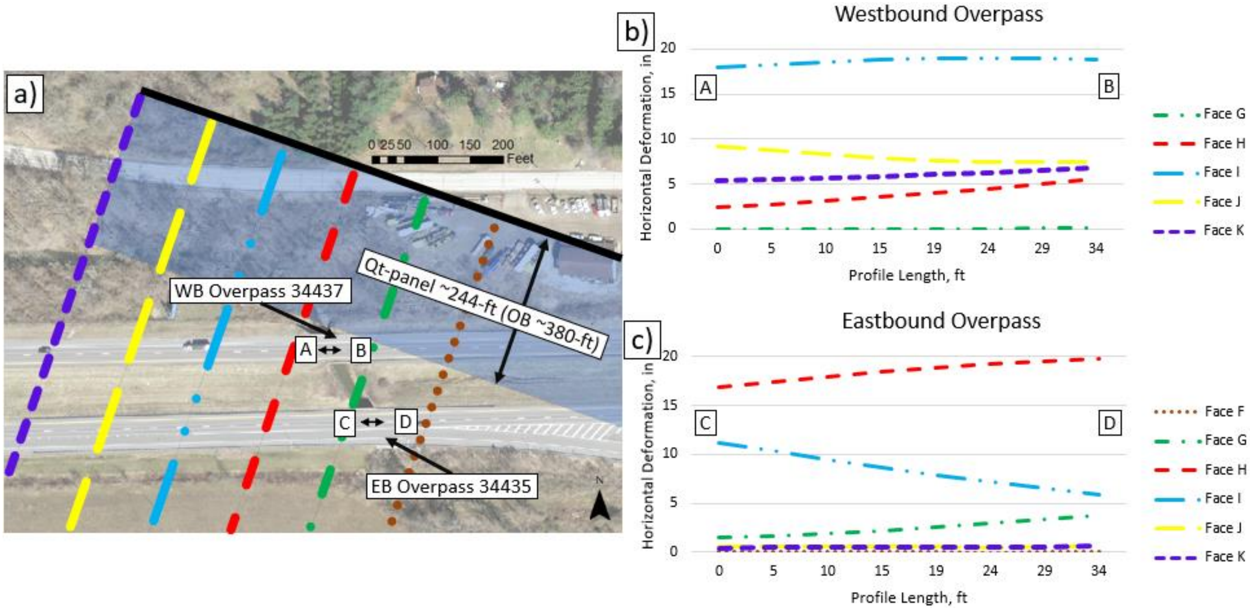

Figure IIc.23 - Summary of predicted horizontal deformation conditions for Overpasses 34437 and 34435 during undermining by Panel N; a) longwall face positions, b) westbound overpass (A-B) horizontal deformation, and c) eastbound overpass (C-D) horizontal deformation at six face positions (Figure IIIb.26, Task 3 Report)

2.6.3 *Other Assets Analyzed*

Six other assets are subjected to dynamic subsidence and analyzed within Section IIIb.3 (Task 3 Report). Two are three-span overpasses (34424 and 34426), located almost entirely within the mid-panel area of potential Panel C. The three other assets are found within projected Panel N. One of these assets is a culvert (34436) located almost entirely in the quarter-panel area with the potential for significant permanent changes to the elevation / slope of this structure. The two overpasses (34435 and 34437) discussed above also contain two retaining walls. These retaining walls present a special challenge for predicting potential subsidence impacts.

3.0 Perform an Analysis of the Embankments Carrying I-70 within the Extended Study Area

The University performed an analysis using the finite element method to examine the influence of highway orientation and depth of the longwall panel on embankments subjected to subsidence. For comparative purposes, modeled panels were placed within the center of a developing subsidence basin. Initially, the characteristics of Embankment #1 were used, i.e. shape, size, and material properties. The use of the shear strength reduction method and the incremental distributed reduction of the embankment base are unique characteristics of these numerical simulations. These models were first applied to Embankment #1 to quantify the influence of longwall panel orientation and overburden on the factor of safety. The three different highway orientations analyzed are 0, 35, and 90-deg with respect to the direction of longwall mining. Then for each of these cases four overburdens, 400, 500, 600, and 675-ft were considered. Elevated deformations developed within the slopes of the modeled embankment when the direction of longwall mining approached 90-deg and overburdens decreased. Of the six embankments analyzed in this study, Embankment #5 was identified as the one with the highest potential for slope instabilities and with the most significant assets. Finally, this same approach discussed earlier is used to model the undermining of Embankment #5 by Panel C.

3.1 Influence of Highway and Longwall Panel Orientation

A finite element model of Embankment #1 is subjected to a simulated mining subsidence basin at three angles, 0, 35, and 90-deg (Figure IIc.24). Slope deformation, plastic shear band development, and factor of safety were analyzed for Embankment #1 in all three cases. Plastic strain, which represents the formation of a failure surface, is plotted for each case showing dramatically different responses (Figure IIc.24). The shear strength reduction factors were set to be equal to one. Higher plastic strains develop on the top of the embankment, when the direction of the longwall mining is 0-deg. When the direction of mining is 90-deg, large plastic strains occur within the embankment, contributing to the local deformations and failure in the embankment.

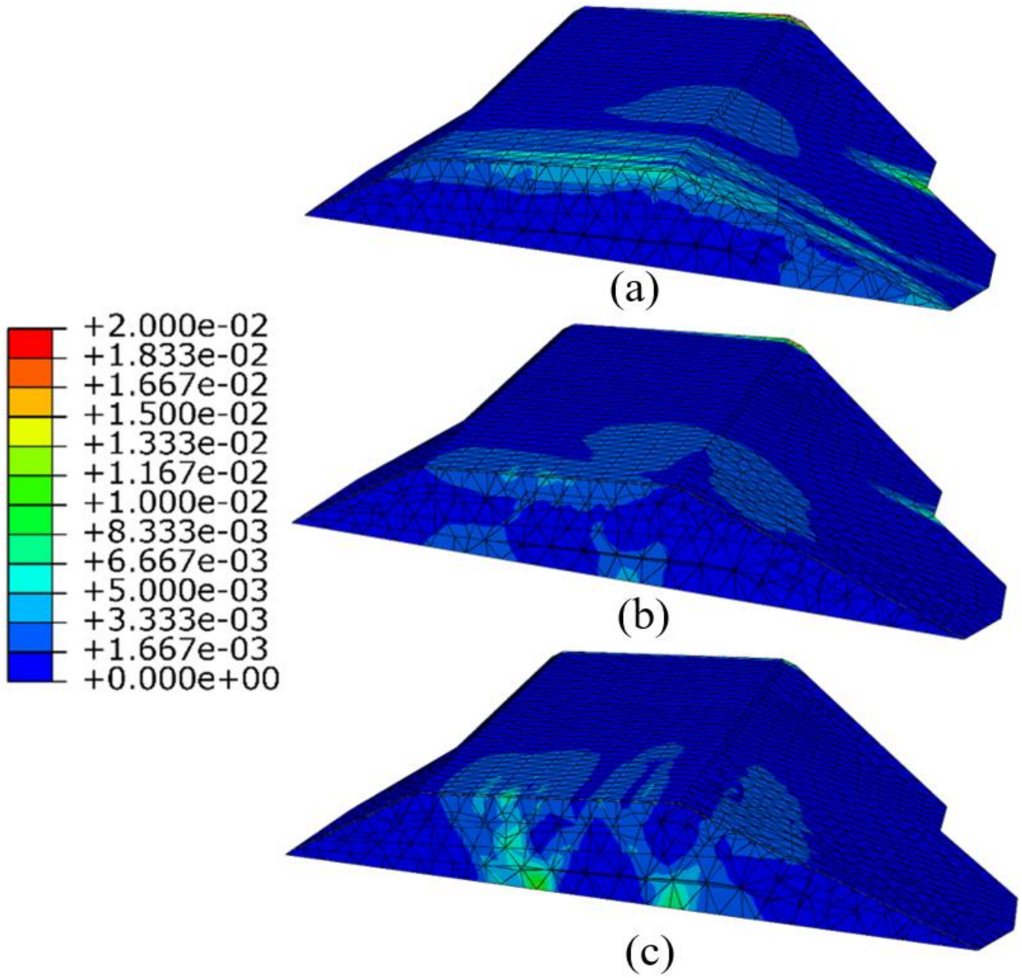

Figure 24 – Plastic strain at the critical cross section of Embankment #1 when the angle between the orientation of the highway and mining is (a) 0-deg; (b) 35-deg; and (c) 90-deg with a SRF equal to one (Figure IVa.13, Task 3 Report)

The shear strength reduction method is used to obtain the factor of safety for each orientation (Figure IIc.25). The factor of safety decreases as the direction of mining with respect to the embankment increases. For the 90-deg case, the lower bound of the factor of safety is just below one, which is consistent with the large amount of plastic strain observed within critical sections of Embankment #1.

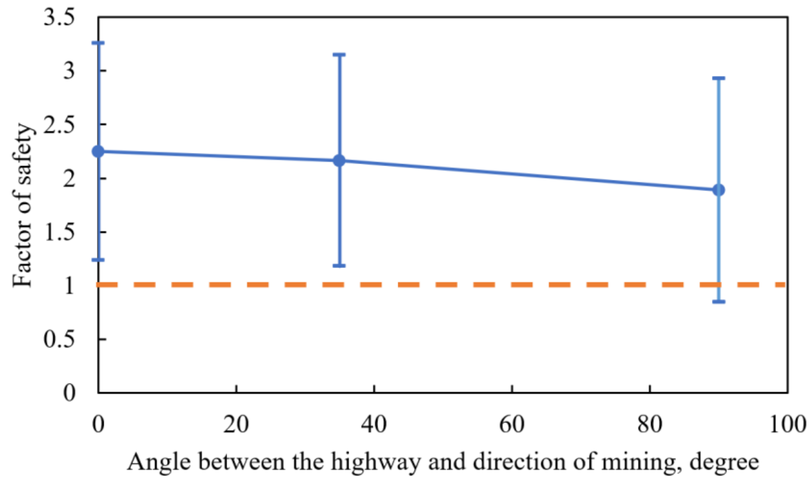

Figure IIc.25 – Factor of safety for Embankment #1 at different angles with respect to the mining direction (Figure IVa.14, Task 3 Report)

3.2 Influence of Overburden

For each orientation discussed above, Embankment #1 was subjected to longwall mining subsidence at overburdens of 400, 500, 600, and 675-ft. Not surprising, the model produced an increase in vertical subsidence with a decrease in overburden, responding directly to the greater amounts of downward movement applied to the base of the embankment. The lower bound (conservative) factor of safety for each of the twelve cases analyzed are shown in Table IIc.2. This table shows that the lowest factor of safety occurs when the direction of mining is 90-deg and the overburden is 400-ft.

Table IIc.2 – Critical factor of safety for Embankment #1 subjected to longwall mining with different overburdens and orientations (Table IVa.4, Task 3 Report)

	Highway orientation with respect to mining direction		
Overburden, ft	**0-deg**	**35-deg**	**90-deg**
400	0.98	0.94	0.68
500	1.06	1.04	0.72
600	1.16	1.12	0.85
675	1.24	1.18	0.85

3.3 Analysis of Embankment #5

The model used in the finite element analysis performed on Embankment #5 was based on information from multiple borings and laboratory test results. Shear parameters established during the evaluation of Embankment #1 were enhanced by a factor of 1.3 to take into account the greater amounts of gravel observed in the borehole samples. In addition, the original slope of the embankment was assumed to be equal to 1:2 (26-deg). Embankment #5 is modeled to be within the mid-panel area of projected Panel C. The average overburden in this area is 500-ft. The orientation between the highway and the direction of future mining is 79-deg (Figure IIc.26). Embankment #5 is expected to be impacted more by the formation of the subsidence basin than Embankment #1. Both embankments are similar in shape and thickness and are located mostly within the mid-panel area. However, projected Panel C is 175-ft closer to I-70 and the highway is more closely aligned with the advancing longwall face.

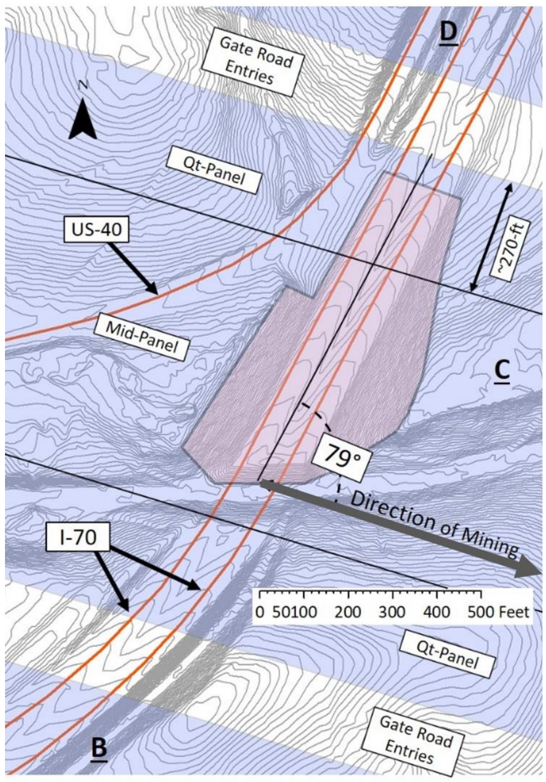

Figure IIc.26 – Location of Embankment #5 within the mid-panel area of projected Panel C (Figure IVb.1, Task 3 Report)

3.3.1 *Excessive Deformation*

The vertical displacement contours were plotted for Embankment #5 for selected working face positions (Figure IIc.27). The displacement is small at working face position #0. When the working face is at the middle of the embankment, the soil at the crest of the south slope spreads apart perpendicular to the highway direction. The local depression in the form of a sinking region is shown in a light blue color in Figure IIc.27c. When the working face passes the embankment, the top of the embankment experiences a settlement of about 7.6-ft at two different regions shown in Figure IIc.27d. Such deformations can be considered significant and can produce damage 1) along the crest of the slopes, where the fill is the thickest, and 2) along the foundation of the pavement between these two points.

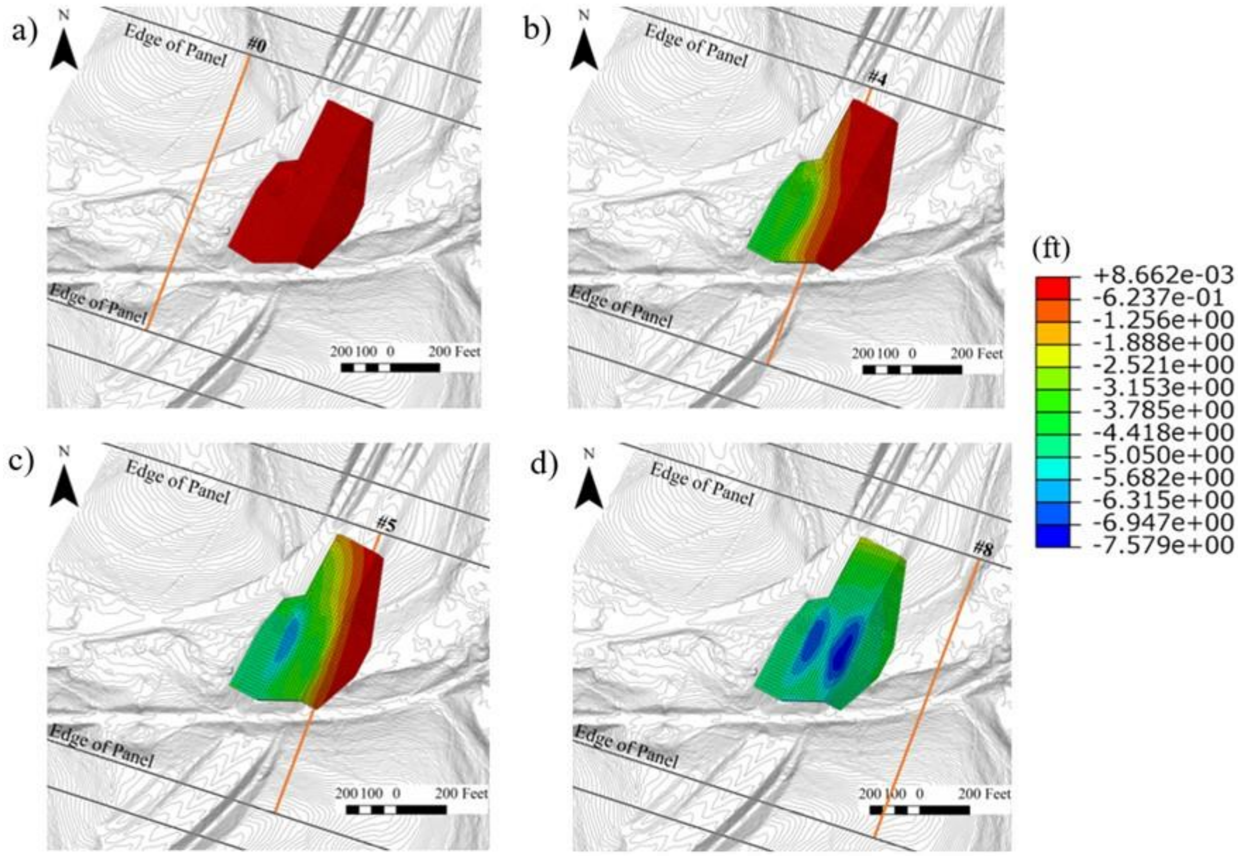

Figure IIc.27 – Vertical displacement on Embankment #5 with working face positions a) #0, b) #4, c) #5, and d) #8 (Figure IVb.6, Task 3 Report)

The ability to use realistic material properties in the model, replicate the shape of the subsidence basin applied to the base of the model, and the application of the shear strength reduction method all helped to estimate the factor of safety for Embankment #5 during different longwall face positions. The effect of the substantial deformations discussed above is that a factor of safety less than one is possible under certain material properties, highway orientation, and overburden conditions. For the potential conditions outlined in this research study, significant settlement can occur on the crest of Embankment #5 with the potential to form longitudinal depressions in the highway alignment.

3.3.2 *Factor or Safety*

The factor of safety is obtained using the shear strength reduction factor to reduce the cohesion and $tan\phi$ until the embankment failed. Total displacement is plotted against the shear strength reduction factor to estimate the factor of safety. Embankment #5 is estimated to have a pre-undermining factor of safety of ~2.8. In the model, failure along the embankment's critical cross section occurs when a shear band reaches the top of the embankment and a complete rupture surface is formed (knee point). The critical factor of safety occurs when the longwall working face is located under the middle of the embankment (working face #4, Figure IIc.27). Figure IIc.28 indicates that the lower bound factor of safety is ~0.8. Before this point, the displacement increased at a relatively low rate. After this point, the displacement rate increases. The different shear strength reduction factors demonstrate the potential impact of shear parameters higher or lower than the initial conditions.

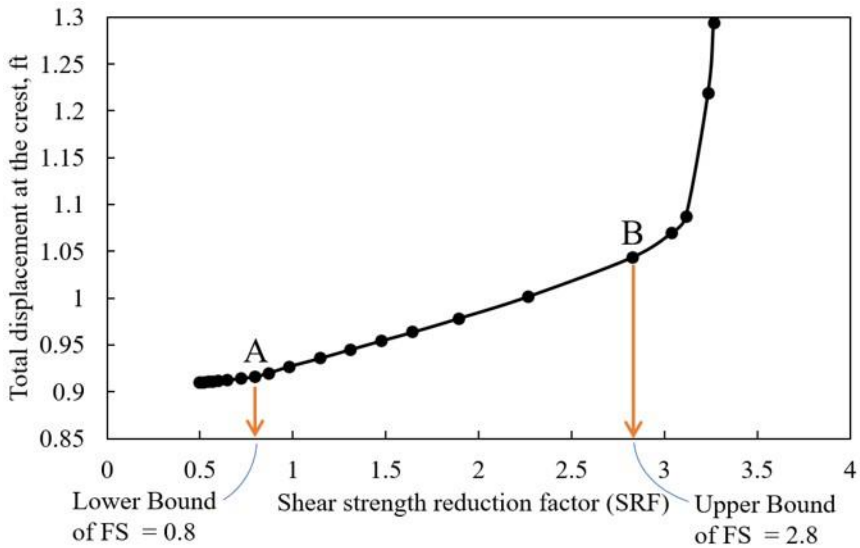

Figure IIc.28 - Total displacement at the crest of the critical cross section in Embankment #5 versus the shear strength reduction factor for the case with working face position # 4 (Figure IVb.12, Task 3 Report)

When using the method outlined in this research study for predicting stability conditions, the lower bound factor of safety represents when the embankment initially experiences limited deformations. At large deformation levels in the embankment, when a shear band completely develops, the upper bound factor of safety is in effect. The upper bound of the factor of safety indicates if the embankment will develop large deformations. All the upper bounds of the factor of safety are much higher than lower bounds of the factor of safety. The lower bounds factor of safety indicates that plastic strains were small and of limited extent inside the embankment. However, it does not mean the embankment is stable. For example, some limited deformations were observed in Embankment #1 and inclinometer measurements and field observations validated its occurrence (Task 2 Report). In addition, the highway alignment and slope surveys documented settlement at the regions of the model experiencing high but limited plastic strain. Consequently, the lower bound factor of safety was utilized to identify whether the embankment is stable.

3.3.3 *Proposed Framework for Estimating Embankment Stability during Undermining*

The lower bound factor of safety was used when developing a framework for assessing embankment behavior under longwall mining-induced subsidence. This research study has demonstrated the influence of the angle between the highway and the direction of mining and overburden on slope stability. These factors are shown in Figure IIc.29. This chart allows for a first approximation of the risk posed by the unique orientation and overburden associated with individual embankments. For example, Embankment #1 overburden is estimated to be 675-ft and the highway is at a 35-deg angle with the direction of longwall mining. The lower limit estimated factor of safety is ~1.2. This value is also plotted on Figure IIc.29 and is in the zone of potential small deformations. Whereas, Embankment #5 overburden is estimated to be 500-ft and the highway is at a 79-deg angle with the direction of longwall mining. The lower limit estimated factor of safety is 0.8. These two values are plotted on Figure IIc.29 and is in the zone of potential large deformations. It should be noted that this analysis subjected Embankment #5 to a mid-panel subsidence conditions. If the embankment were subject to a portion of the full subsidence basin, this analysis would not apply.

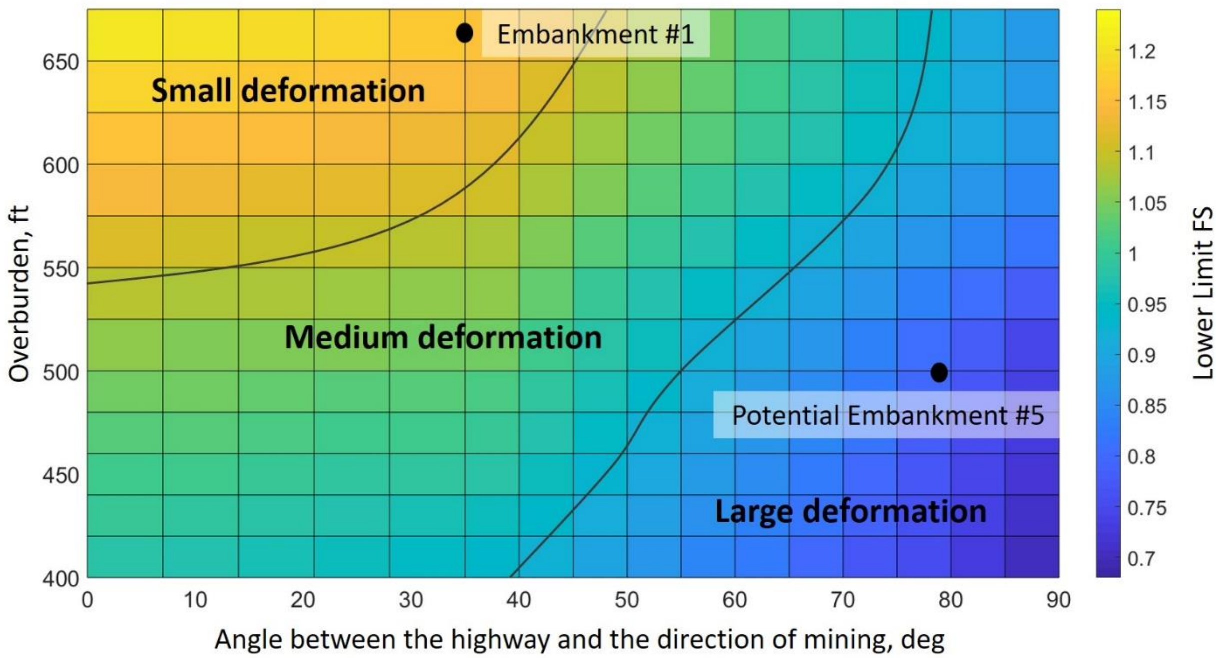

Figure IIc.29 – Chart showing the proposed method for estimating orientation and overburden influences on embankments found within the study area. All conditions apply to a fully developed subsidence basin. The lower limit factor of safety for Embankments #1 and #5 are provided (Figure IVb.18, Task 3 Report)

SECTION III – CONSIDERATIONS FOR FUTURE UNDERMINING OF I-70

The final reporting tasks associated with this project is to provide PennDOT with a list of considerations while planning for the future undermining of I-70 between the West Alexander and Claysville Interchanges. Some of these considerations may be easy to implement. Others might require long lead-times and could be considered research topics. Lastly, a few considerations will require that the location of the longwall panel and adjacent gate road entries be precisely known.

Subsection IIIa – Monitoring Strategies

1.0 Pavement Monitoring

Monitoring of the pavement is essential to achieve the following two objectives:

1. Ensure the safety of the traveling public during the undermining, and
2. Assess the long-term impact longwall mining subsidence will have on the remainder of the pavement's performance life.

Under this study, pavement monitoring efforts primarily focused on a continuous visual inspection of the roadway to insure a prompt response in performing any interventions, such as milling compression bumps, necessary to keep the traveling public safe as the subsidence occurred. Additional monitoring activities can be deployed to assist with these two objectives as described below.

1.1 Instrumentation Installation

For the duration of the undermining of I-70 in 2019, visual inspection was used as the primary means of assessing the need for an intervention. The timely identification of these distresses during the undermining event is essential so that repairs can be made before becoming hazardous to passing traffic. Sensors, such as static strain gages, can also be installed into the pavement to alert the construction crew of a distress developing prior to it being visually observed so that a more timely response can be achieved. This provides the opportunity to be more proactive in diverting traffic into adjacent lanes or performing pre-emptive measures to mitigate the impact of the subsidence on the safety of the passing traffic. Sensors can also be used to help quantify the magnitude of the loads resulting from the subsidence so that the impact of these loads on the performance life of the pavement can be quantified.

1.2 Survey Locations along the Pavement

As, previously mentioned, visual observations were a key component in characterizing the impact of the dynamic and final subsidence. Monitoring the movement of the pavement using survey points in the asphalt shoulder was a key source of this observational data. The information was very informative in quantifying the impacts of the undermining on the surface deformation. This data was limited by the fact that the repeatability of the location where each survey coordinate was measured could vary between surveys because these survey point locations were not defined using survey pins. In the future, concrete anchors, such as those produced by companies like Hilti for anchoring dowel baskets prior to paving an unbonded overlay, can be installed into the concrete shoulder to serve as survey pins. This would greatly help increase the quality of the data generated by the survey measurements.

1.3 Pre and Post Undermining Falling Weight Deflectometer Testing

The falling weight deflectometer (FWD) is commonly used to nondestructively assess the structural integrity of a pavement as well as the support conditions beneath the paved surface layer. As previously stated, a major objective in monitoring the pavement is quantifying the effects of the undermining on the future performance life of the pavement. Two primary considerations for quantifying this effect is in capturing the impact the subsidence has on joint performance for a jointed plain concrete pavement and the support conditions beneath the slab. With the large opening and closing of the transverse joints that occurs during the subsidence, the dowels along the transverse joints can become misaligned, thereby restricting the ability of the joint to open and close freely. This will lead to blowups. The support conditions beneath the slab are also critical. Slab thickness is designed such that it can carry an anticipated level of traffic with the assumption that the slab is fully supported. As the soil and granular layers beneath the slab move and deform during the subsidence event, gaps, as well as areas of increased support, can develop beneath the slab. Both can lead to early cracking of the slab. FWD testing can be performed to assess the impact the subsidence has on both joint performance and the slab support conditions. Ideally FWD testing is performed both before the undermining occurs as well as after so that the pre-condition of the pavement structure can be established. This will reduce the possibility of attributing pre-existing performance issue to the subsidence.

2.0 LiDAR

2.1 Timing of LiDAR Scans

One of the most critical aspects of any dynamic change detection study is the temporal resolution, or the timing between surveys. Appropriate timing and number of surveys is dependent on the application and over what period of time the object or area of interest is expected to move. Ideally, many surveys are needed to completely characterize movement before, during, and after the area of interest has fully subsided.

To track movements to the surface of the interstate while the subsidence basin was in development, eleven LiDAR scans were conducted. Of these eleven, four were taken before undermining (29 April 2018, 7 January 2019, 15 January 2019, and 22 January 2019); four were taken while the subsidence basin was developing underneath the interstate (28 January 2019, 5 February 2019, 10 February 2019, and 18 February 2019); and three were taken after the basin was formed (25 February 2019, 9 March 2019, and 18 April 2019).

As mentioned above, four surveys were performed while the interstate was being undermined. These were done on a weekly basis, as was scheduled prior to the undermining event. The original schedule placed each scan a week apart from each other, but due to inclement weather, the 12 February 2019 was moved to 10 February 2019. More LiDAR surveys, specifically when the longwall face was under the highway, would have significantly enhanced the overall characterization of the developing subsidence basin. With five or more days of active mining between surveys, the longwall face was able to progress several hundred feet forward. This resulted in an absence of scans during certain critical portions of the roadway when dynamic subsidence was occurring. By increasing the numbers of surveys taken during the undermining event, a much better characterization of the developing subsidence basin could have been possible. With increased temporal resolution, it might be possible to answer important research questions, such as how varying topography impacts subsidence rates; or how the stoppage of mining over the weekend impacts the formation of the subsidence basin.

2.2 Methods of LiDAR scans (Statics versus Dynamic)

Terrestrial LiDAR, or LiDAR which is collected from the ground, can be performed with two different methods: static and mobile. Mobile LiDAR is the collection of points from a moving vehicle and static LiDAR is taken from a stationary position. Which method is used depends on the project need, as both static and mobile surveys have distinct advantages and disadvantages. These are listed below for both methods:

- Mobile
    - Advantages
        - High spatial resolution (point density)
        - High accuracy
        - Ability to cover large areas of ground quickly
    - Disadvantages
        - Limited to roadways and other access ways
- Static
    - Advantages
        - Higher spatial resolution (higher point density)
        - Higher accuracy
    - Disadvantages
        - Limited to one vantage point at a time

Dynamic LiDAR scans were utilized to model the interstate so that subsidence related movements could be tracked between surveys. This was seen as an appropriate method because of its ability to obtain high point densities over the entire span of interstate that was over Panel 15 in a timely fashion. The truck equipped with the LiDAR scanner was able to scan the entire study area with one pass on both the eastbound and westbound lanes.

It has been stated that mobile LiDAR is able to obtain high spatial resolutions, and this was true for the scans of I-70. The drawback in this method was the spacing between scan lines. A scan line is produced with each pulse sent out from the LiDAR scanner. Each pulse is able to collect millions of points (up to 2 million for the REIGL VMX-1HA unit). Between each pulse, or scan line, there could be up to 2.0 to 3.0-in of space (Figure IIIa.1). This spacing made it difficult to precisely record the locations of transverse joint. The University attempted to locate the joints where they intersected with the travel lane strips. The preciseness of this location was important because in order to accurately measure horizontal movement, exact points are needed. With this scan line spacing, it was more difficult to digitize the exact locations of the transverse joint and the intersection with the travel lanes.

In theory, static scans would help alleviate the issue created by the scan line spacing. Because static scans are stationary, they are able to repeatedly scan the same area multiple times. This would create a higher spatial resolution, hence eliminating the scan line spacing that made it difficult to locate the transverse joints. With denser point spacing, it would be easier to measure movements of these smaller features and could even make it possible to measure the widening of the transverse joints as they began to diverge.

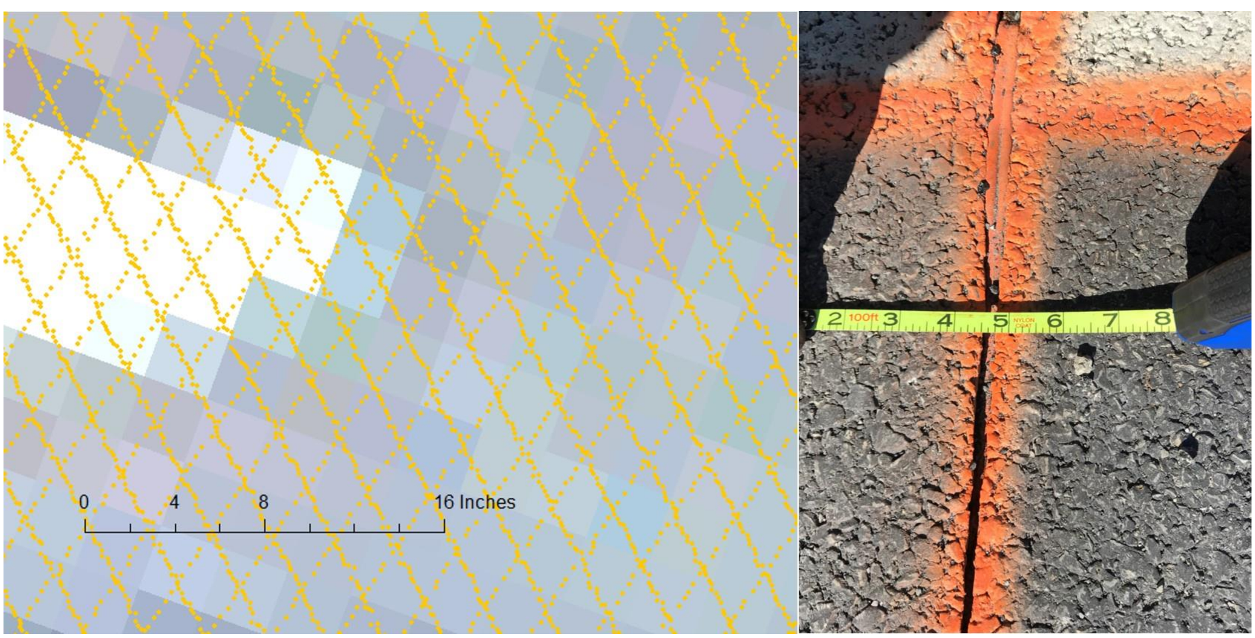

Figure IIIa.1 – Snapshot of the scan lines in the LiDAR point clouds (left) and the width of the transverse joints within the travel lanes (right)

Because both methods have inherent advantages and disadvantages, one possible solution that could alleviate these issues would be to use a combination of the two methods. Combining multiple scanning methods has the potential to make up for their disadvantages. For instance, it was essential to scan the entire study area in a timely fashion to get a holistic timestamp of dynamic subsidence, therefore the mobile method was suitable. But certain features, such as the transverse joints, did not have the appropriate spatial resolution in the point cloud to precisely identify their movements. While stationary scanners might not be able to capture the entire study area, certain areas that require higher detail could be identified and surveyed with a static scanner. Stationary scanners would also be effective for areas that could not be reached by car, such as the hillsides of the cut slopes and embankments.

2.3 Research the Capability of using Drone-Based LiDAR Capable of Real-Time Change Detection

Another method that could potentially improve spatial resolution across the study area would drone-based LiDAR. Using a drone has several benefits, including high spatial resolutions, quick collection times, and the ability to scan large areas. As added advantage to drone-based mobile LiDAR compared to car-based LiDAR is the layout in which the scanner can collect the data. For this study, the truck was limited to using the inside passing lane, which led to varying levels of spatial resolution across the scene. This could potentially be mitigated with a drone-based approach. When surveying a site with a drone, the flight path is typically set up so that there is considerable overlap between passes. This overlap is built into the flight plan so that targets that are detected in both flight passes can be used to tie together the entire scene. With that comes the added benefit of highly detailed and more consistent point clouds across the area of interest.
It is also possible to equip drones with more than one type of sensor. With an added camera attached, it is possible to gather orthographic images at the same time as the LiDAR capture.

Recent advances in 3D imaging and reconstructions allow for the contextual, quasi-real time construction of hybrid LiDAR-RGB point clouds, by gathering the LiDAR depth information (in the form of a point cloud) and establishing a correspondence map with the RGB information (in the form of RGB matrices) by means of polar-grid mapping representations or Structure from Motion (SfM) techniques. This enables the point cloud to retain RGB information. The ability to colorize a point cloud by its real color would make it easier to identify targets in a point cloud, which would increase the efficiency of the feature extraction process in the 3D point cloud. This would ultimately allow for clearer outputs that will enable a more accurate analysis of surface movements.

There are several drawbacks to drone based collection, however. Before every flight plan, permission must be granted to fly in that zone. The drone operator would need a Remote Pilot Certificate from the Federal Aviation Administration. Stable weather conditions are also a requirement for drone flights. It has already been mentioned that LiDAR cannot operate in inclement conditions. With drone-based LiDAR, it would be further limited by weather conditions because it could not operate in windy conditions. Most survey grade drones can operate resist speeds of 15 to 20-mph, but extra precautions would likely be necessary in order to maintain the accuracy standard required for these surveys.

3.0 Observational Data Frequency

As previously stated in this report, monitoring pavement for distresses is important for ensuring the safety of travelers on the interstate. In addition to the immediate safety reasons, monitoring the location and timing of damages enables for accurate assessment of types and characteristics of damage and their distance to the longwall face. This distance relationship between types of distresses and the longwall face in turn provides a good indicator as to how the dynamic subsidence wave creates different types of distresses to the roadway surface.

To better understand how the roadway responded to the undermining event, the University took weekly trips to the site. On these trips, team members utilized scroll maps of the highway alignment to document the location of the damages that were occurring (Figure IIIa.2). With each damage feature, information such as the size, length, and the date it formed were all documented. Probably the most important of this information was the timing of the failure. With an accurate timestamp of when the failure occurred, it is possible to better understand the relationship between the feature and the distance to the longwall face. This relationship is critical to understanding how the dynamic subsidence wave creates different types of roadway damage.

Figure IIIa.2 – Example Scroll Map used to locate and document distresses

A great example of when accurate timestamps helped in defining the relationship between damages and the distance the longwall face is depicted in Figure IIIa.3. Photo(s) #1 and #2 provide evidence of the widening of a joint and a transverse crack forming at the end of the joint on 7 February and early on 8 February. At that point in time, the longwall face was just beyond the location of these features. Photo #3 shows this same location ~24 hours later. At this point, the longwall face would be over one hundred feet further away. The crack now compresses to form a blowup. Relating these features to the position of the longwall face was possible because of the timestamps, as is shown in Photo(s) #2 and #3.

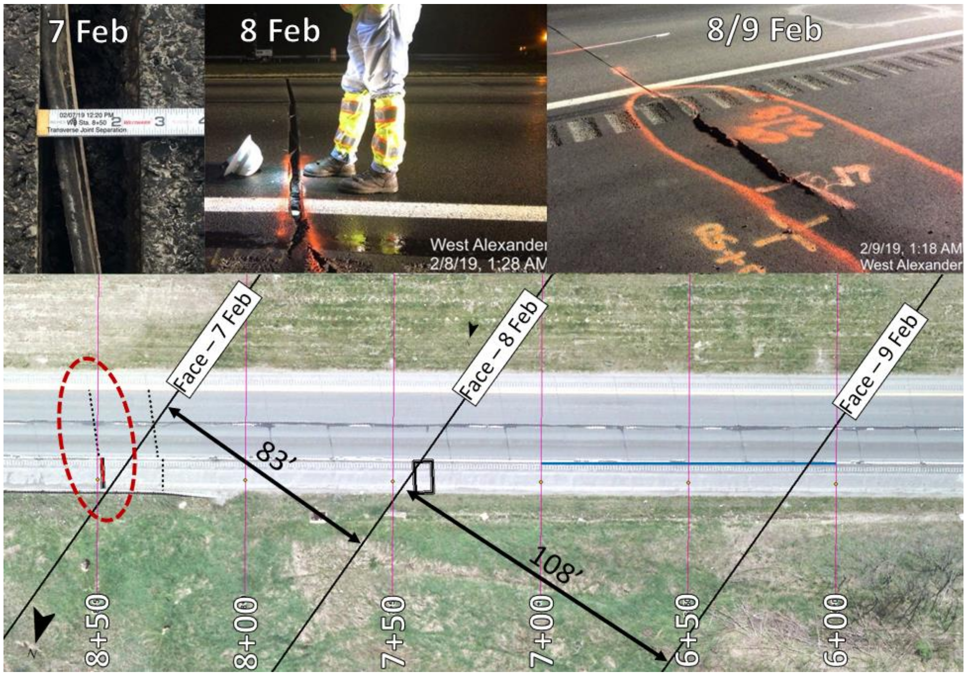

Figure IIIa.3 – Example of a documented feature as it was subjected to the dynamic subsidence wave

On the other hand, when failures are not documented, it is more difficult to establish a relationship with longwall face position. Figure IIIa.4 provides a few examples of compression features that are not dated, making it more difficult to relate the dynamic subsidence wave with longwall face position. Many of the unmarked features consisted of widened transverse joints but some did not open and close in a traditional manner, making it more difficult to assess how the roadway behaved during the dynamic subsidence.

Figure IIIa.4 – Examples of undated distresses and joints that widened and closed

In the future, the University recommends an observational approach that ensures the roadway is routinely checked for failures. This approach would include the following:

- Identify the type of failures to be documented, such as the list that is compiled in Subsection IIb.4.3 of the Task 3 Report.
- Record the earliest date and time on which the distress is observed. Certain features may benefit from status updates, i.e. compression features continuing to develop, or joints closing after initially opening up.
- Document the distresses. For example, draw distresses on scroll maps, collecting GPS data, record feature attributes is official field notes.
- Assure that there is adequate personnel to observe the greatest number of distress occurrences.

4.0 Climate Consideration

In Pennsylvania, the existence of four distinct seasons has a profound impact on how climate effects monitoring strategies. In the late winter / early spring snow thaw and increased precipitation produces elevated water saturation levels in soils, increased phreatic surfaces in embankments, and higher flow in steams of all sizes. The reverse is true in the late summer / early fall. The winter season can produce unexpected snow fall that negatively affects schedules. Perhaps the instrument that are most impacted by climate are the LiDAR / photogrammetric surveys. Water, snow, and ice make these monitoring strategies ineffective. Instrumentation performance can also be impacted by temperature in other ways. For example, in some cases, the calibration protocols for certain instruments can be altered. Additionally, the pavement is dramatically impacted by temperature. Expansion joints will open in the winter and close in the summer masking the effects of the developing subsidence basin.

Subsection IIIb – Effects of Multiple Panel Extraction

Detailed monitoring of Panel 15 occurred over a 50 day period from 14 January to 5 March 2019. During this period, the longwall face advanced ~4,063-ft over thirty-six (36) production days, averaging 113-ft/production day (Table IIb.1, Task 2 Report). Safety concerns and the need to return the highway to normal travel speeds, made further monitoring at the site impractical beyond Monday 5 March. In addition, much of the data collected and analyzed in the task reports indicated that deformations were approaching, or at, background levels. In other words, the subsidence basin appeared to be fully developed and that final or permanent conditions exist.

This section advises that in the future, some optimal level of monitoring needs to be continued until the adjacent longwall panel has mined by the highway asset of interest. Information is presented demonstrating that:

- Differential vertical movements over the gate road entries should be expected in most cases, and
- Horizontal movements at significant distances from panels, where coal extraction is currently occurring, is possible.

This is a concern because longwall subsidence does not always happen so quickly and completely as it did in Panel 15. There are examples both locally and internationally that demonstrate what might be called anomalous or deviating behavior from that which we would normally expect.

1.0 Gate Road Entry Influence

A study performed by Yancich (1986) at West Virginia University analyzed the subsidence characteristics of the first three longwall panels at the Gateway Mine that undermined I-79, i.e. 0-Butt, 1-Butt, and 2-Butt. This study included the regular monitoring of fixed survey monuments along the northbound lanes of I-79 and ultimately compiled a final subsidence profile for the three panels (Figure IIIb.1). The surveys clearly depict three separate subcritical subsidence basins, all of which come to a point around a maximum vertical subsidence of 2.5-ft. It is also noteworthy that, after the completion of all three panels, there is approximately one foot of additional vertical subsidence over the gate road entries between Panel 1-Butt and 2-Butt. One possible explanation for this vertical subsidence variation is associated with the yielding or failing of gate road pillars.

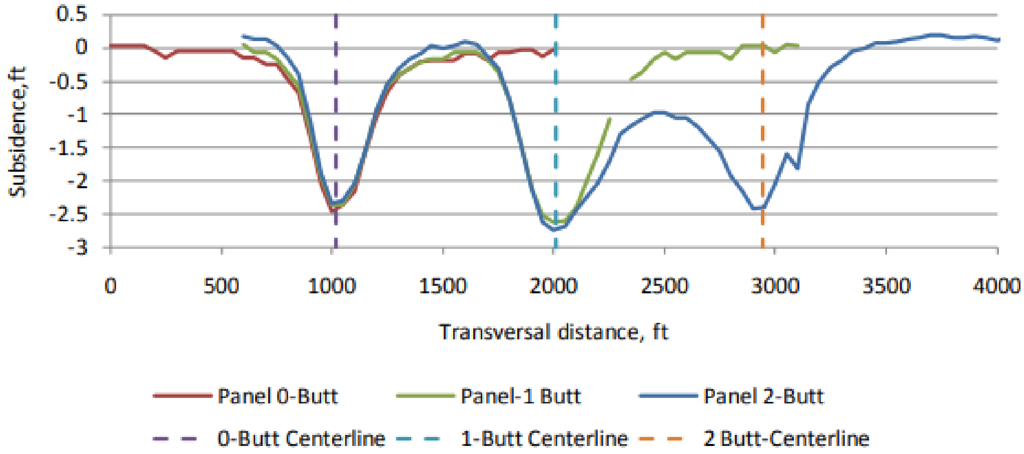

Figure IIIb.1 – Final subsidence profiles for three Gateway panels undermining I-79 (Yancich, 1986) (Figure IIa.2, Task 1 Report)

The potential for gate road entry stability, or more specifically pillar failure, was investigated using the Analysis of Coal Pillar Stability program (Mark and Agioutantis, 2019). An overall tailgate stability factor of ~1.4 is determined for the current Tunnel Ridge mine layout using the input parameters below:

- Assume 18-ft wide entries
- Extraction height of 7.25-ft
- Overburden of 675-ft
- Panel width of 1,200-ft
- Crosscut spacing for yield pillars (center to center) of 137.5-ft
- Crosscut angle for abutment pillars of 80-deg
- Crosscut spacing for abutment pillars of 275-ft
- Yield pillar width of 50-ft
- Abutment pillar width of 117-ft
- Gate road entry width of ~180-ft
- Coal Mine Roof Rating of 38 (suggested value for Northern Appalachian coal mines)

This analysis indicates that tailgate entries are likely to be stable. However, this gate road configuration uses two dramatically different pillar sizes (Figure IIIb.2). The larger abutment pillar has relatively high strength capable of resisting vertical deformation and, as a consequence, subsidence on the surface. The other smaller yield pillar has relatively low strengths, providing far less resistance to vertical deformation and increasing the potential for subsidence on the surface. A potential result would be differential subsidence on opposing sides of the gate road entries.

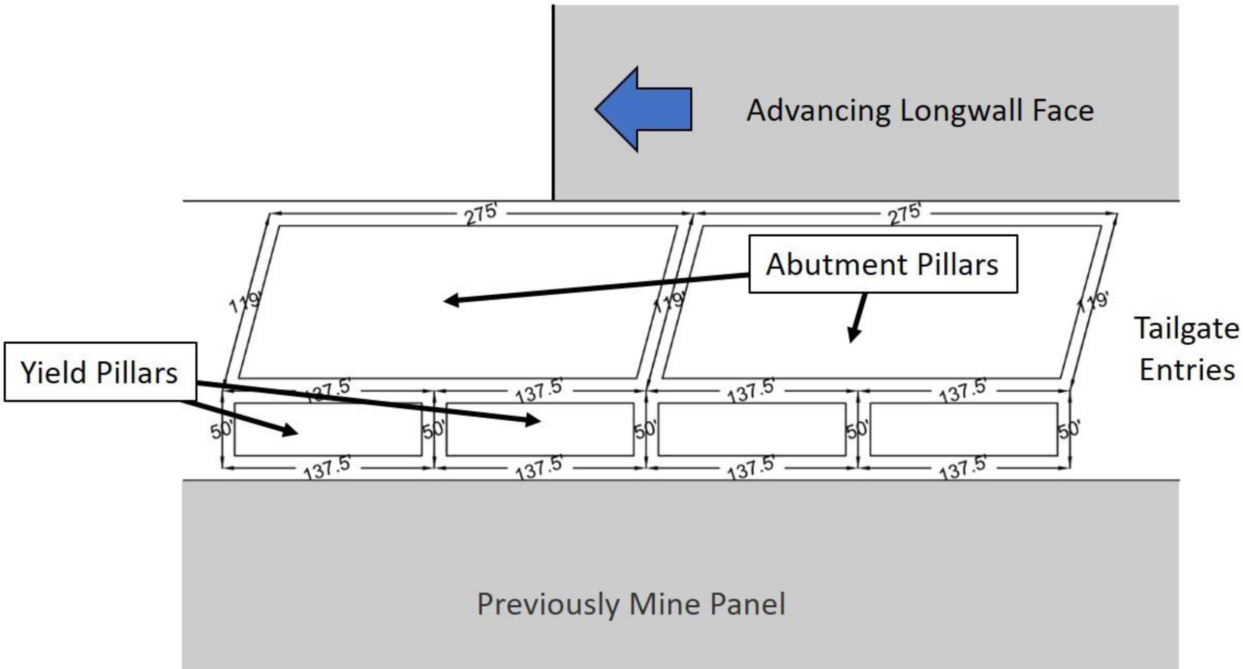

Figure IIIb.2 – Gate road entry layout used by Tunnel Ridge in the Panel 15 area

The occurrence of differential subsidence over gate road entries utilizing the abutment-yield pillar design can be found in another study completed by Gutierrez, et al., 2010. This PennDOT sponsored University of Pittsburgh study analyzed the subsidence characteristics associated with the mining of eight panels from the Emerald (2) and Cumberland Mines (6). Both of these operations are mining the Pittsburgh Coalbed some 30 miles from the study area. Like all current operating Pittsburgh Coalbed longwall mines in Pennsylvania, a similar three-entry abutment-yield pillar design was used. Figure IIIb.3 shows the final subsidence basin along the I-79 highway alignment for Cumberland Panels 51 and 52. In the current analysis, SDPS predicts a symmetrical vertical subsidence over the gate road entries between two extracted panels. However, both the actual survey results as well as the Gutierrez analytical model (based on these actual measurements) shows a non-symmetrical vertical subsidence profile. Significantly more vertical subsidence occurred over the gate road yield pillars than the adjacent abutment pillars. In this example, a difference of ~1-ft in the amount of surface subsidence over the opposite sides of the gate road entries is shown (Figure IIIb.3). If differential gate road entry subsidence occurs in the extended study area, the impact on roadway assets in these areas will need to be re-evaluated.

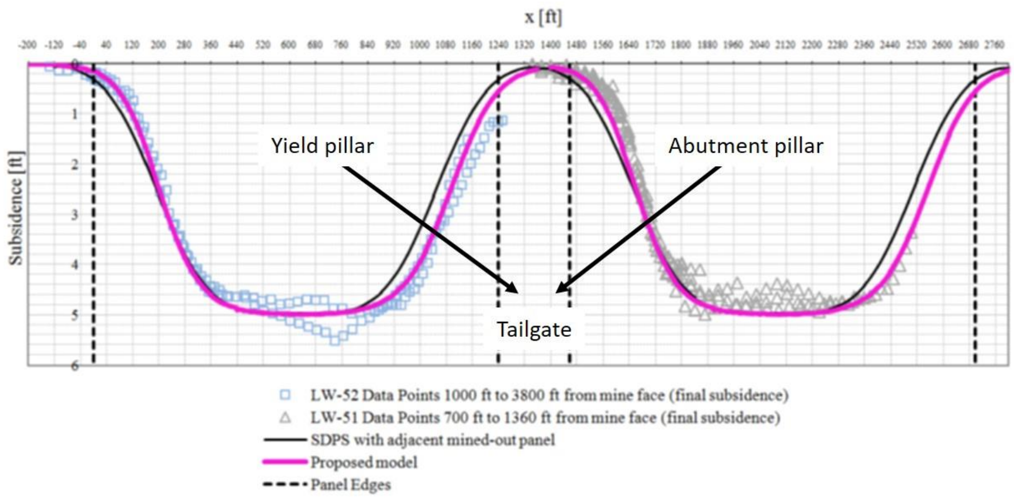

Figure IIIb.3 – Comparison of final subsidence data for longwall Panels 51 (left) and 52 (right), Cumberland Mine (Gutierrez, et.al, 2010)

2.0 Far-Field Lateral Movement

Another relevant issue for supporting longer term monitoring within the extended study area has to do with the potential for far-field lateral movement impacting roadway assets. The problem of far-field subsidence induced lateral movement is not new. It has been recognized and reported on in both the U.S. and Australia. The most famous U.S. example occurred in 2004 to 2007 some 20 miles to the south of the study area. Subsidence impacts associated with undermining Ryerson State Park are well documented in a report by Hebblewhite and Gray (2014). The significance of this occurrence and the impact it has had on industry, government, and research communities are far ranging. For example, the following is an extract from the Hebblewhite and Gray report:

> *The DCNR and the mining company were engaged in litigation over this matter from 2005 until April 2013, when settlement was reached following a mediation session. The mining company has consistently denied that the dam was damaged as a result of longwall mining, but as part of the terms of settlement, has agreed to pay US$36M to DNR for the reconstruction of the dam.*

This agreement is noteworthy since subsidence models based on the influence or profile function methods would not have predicted subsidence impacts this far from longwall mining. Figure IIIb.4 shows that the horizontal distance from the northeastern corner of the dam to a point closest longwall panel is ~900-ft. If the concept of ‘angle of draw’ is utilized, the subsidence basin is predicted to extend only ~276-ft from the edge of the panel. This determination is based on a 21-deg angle of draw at ~720-ft overburden.

The Hebblewhite and Gray report also provided data from survey stations 918 (Figure IIIb.4) showing ‘major movement’ as the Panel I7 passed 700-ft to the south in June of 2006. Some of this horizontal movement also resulted in minor amounts of surface heave. The horizontal movement from stations like 918, demonstrate that

> *“there was a consistent valley closure occurring at all locations along the southern edge of the reservoir, with movements occurring towards the centerline of the main reservoir valley, and away from the mined exaction goaf (gob) area.”*

Hebblewhite and Gray referred to this phenomena as valley closure. In the Ryerson Station area, valley closure was measured to be in excess of 3-in, ‘*even where the valley was particularly wide, remote from mining, and with relatively gently sloping sides.*’

Figure IIIb.4 – Longwall mining panels in the vicinity of Ryerson Station State Park

As has been discussed in the Task 3 Report, I-70 will enter the Dutch Fork valley within the extended study area and may then experience similar valley closure phenomena. It is therefore recommended that long-term monitoring be considered.

Subsection IIIc – Pavement

1.0 Introduction

The length of the pavement section affected by each panel varies substantially within the extended study area as the orientation of the panel to the highway alignment changes (Figure IIIc.1). The panels are projected to be mined at angles near 90-deg to the highway alignment to potentially running directly parallel along the highway alignment. This angle effects the magnitude and shape of the subsidence basin and therefore the type and severity of the distress that develops in the pavement. It also dictates the length of the roadway to be impacted. Figure IIIc.1 also clearly shows the roadway drop in elevation on entering a western tributary to Dutch Fork.

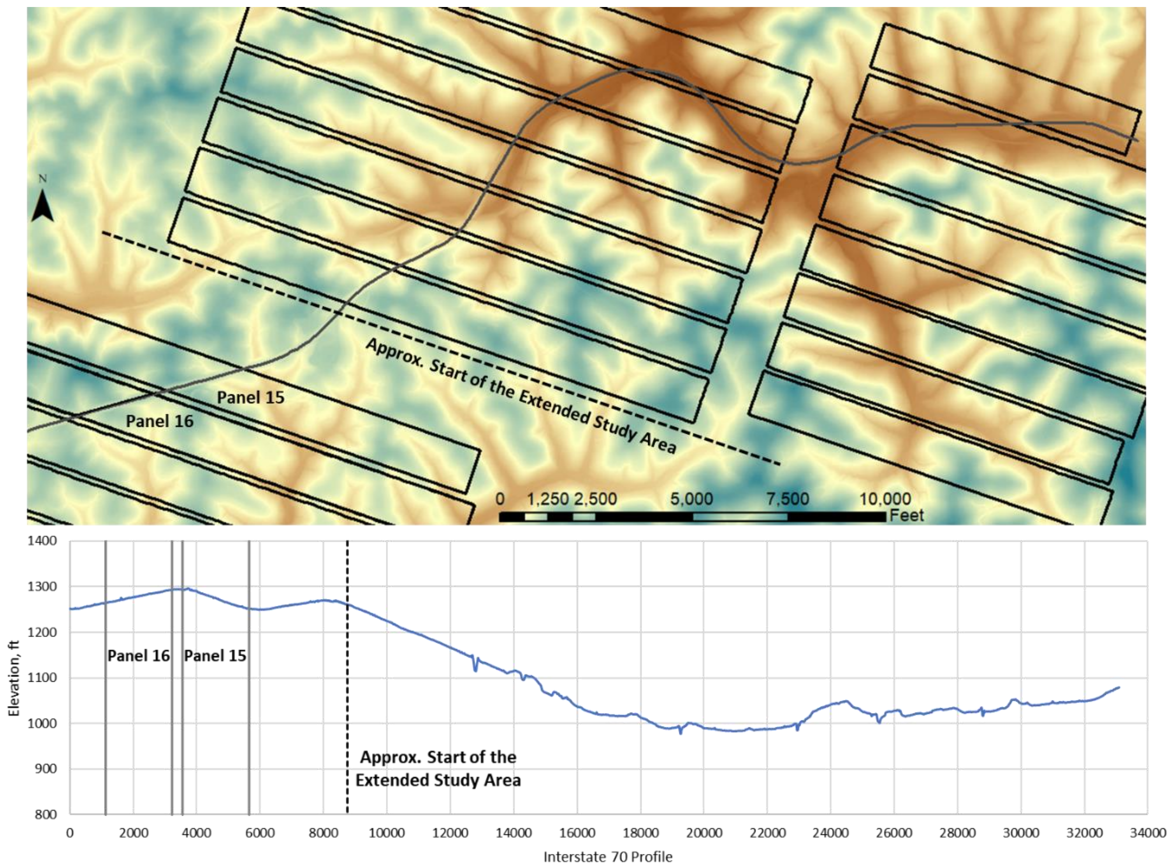

Figure IIIc.1 - Highway alignment with respect to panel orientation in extended study area. In addition, the elevation drop into the Dutch Fork valley is clearly shown

The general elevation moves from 1,250-ft to around 1,000-ft above sea level when traveling from the western to the eastern end of the section of interstate in the extended study area. This stretch of highway also consists of both cut and fill regions. The overburden, soil conditions (which will very between cut and fill areas), and topography effect the magnitude and shape of the subsidence basin and therefore the development of distress in the pavement. The influence of the surface topography on subsidence was investigated and presented in Section IIb.3 of the Task 3 Report. Figure IIIc.2

shows the influence of topography on the final length (compression and extension) of the roadway. This is impactful because the type and magnitude of distress that will develop is dictated by the stress state in the pavement (compressive or tensile). Section IIb.3 of the Task 3 Report provides a detailed summary of the pavement distress that develops as a result of compressive and tensile forces that develop during the subsidence. As can be seen in Figure IIIc.2a, a subsiding hill will result in a decrease in the pavement length (compression) and a subsiding valley of similar magnitude will result in an increase (tension) in length. Figure IIIc.2b shows the length of the pavement above Panel 15 remained approximately the same when comparing pre and post mining conditions. The elevation profile for this section of interstate was a slope with a concave shape prior to mining and a convex shape after mining. This would indicate that the length of the pavement shortens (compressing) during dynamic subsidence but the pavement extended back to its original length once final subsidence was allowed to develop. These temporal effects contribute to the development of distress in the pavement during the occurrence of the dynamic subsidence.

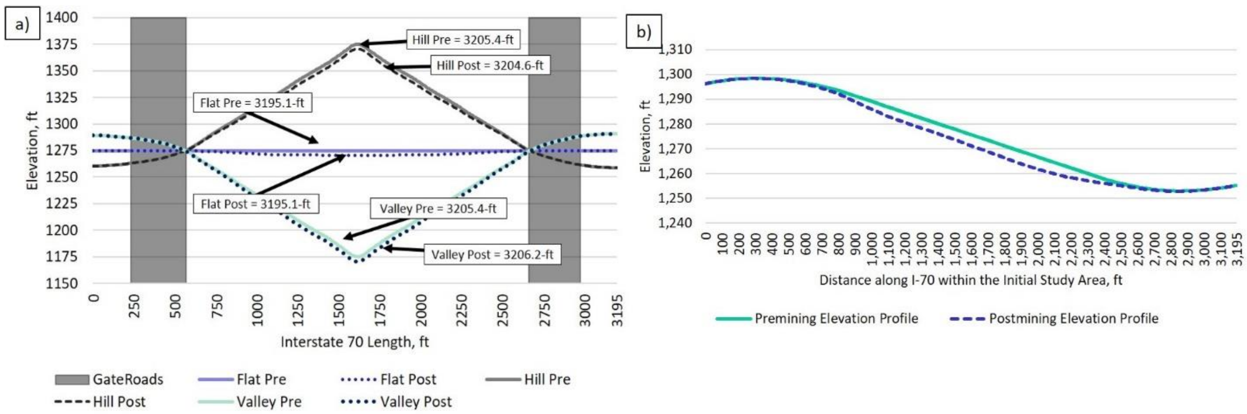

Figure IIIc.2 – a) Effects of three general surface topographic features on the extension/compression of the overlaying pavement and b) Highway profile before and after undermining Panel 15 (Figure IIb.6 and IIb.7, Task 3 Report)

The effect of the subsidence on a pavement can only be estimated after each of the factors discussed above have been quantified. These factors along with the rate at which the mining occurs (considering both projected production rates as well as down time) will contribute to the type, amount and severity of the distress that develops within the pavement. The production rates for Panel 15 are shown in Figure IIIc.3 below.

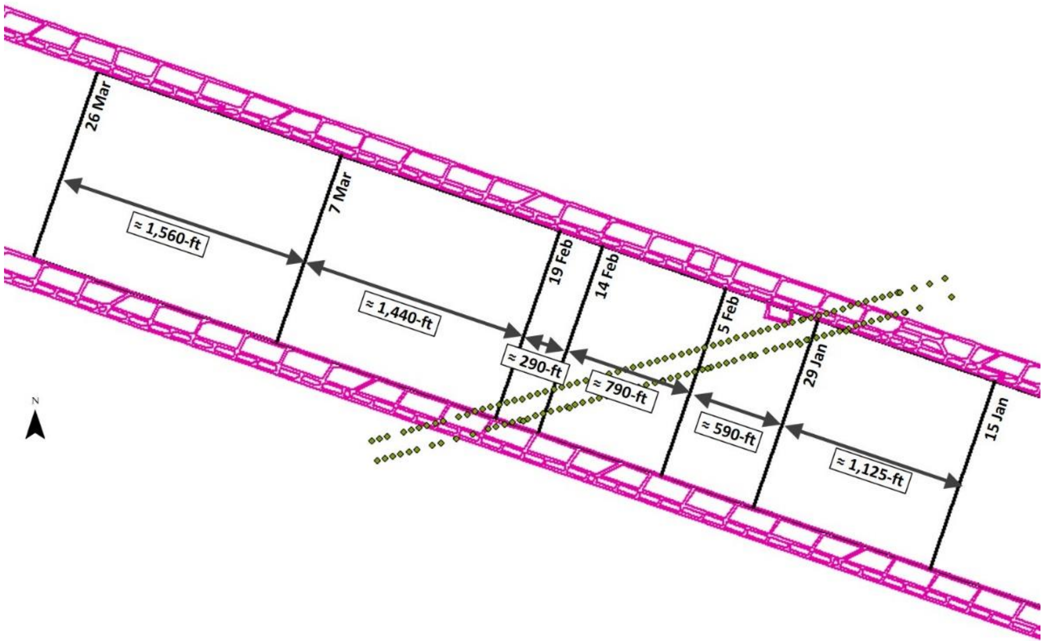

Figure IIIc.3 - Production rates when Panel 15 was mined

2.0 Structural Design

The design of the pavement and its condition prior to the undermining have a significant influence on the scale and characteristics of subsidence impacts. The roadway above Panel 15 and in the extended study area consists of a joint plain concrete pavement overlaid with an asphalt pavement. Design features of the pavement about Panel 15 that appear to be beneficial in mitigating the impact of the subsidence include:

1. Functioning dowels at the transverse joints that facilitated the large opening and closing of the joints without the development of blowups,
2. Very open graded underlying base layer that reduced friction between the slab and the underlying layers mobilized by the subsidence, and
3. Tied concrete shoulders that were maintained across that asphalt relief sections to reduce lateral displacement between the regions adjacent to these relief sections and thereby maintain highway alignment.

The pavement in the extended study area appears to have a similar design but, at least in a few areas, there is an asphalt shoulder instead of a tied concrete shoulder. This is similar to the highway design for the portion of highway above Panel 15 in West Virginia. It was not reported that this lack of lateral confinement resulted in major misalignments of the highway near the asphalt relief sections in West Virginia. Regardless, it is possible that what was observed for the highway above Panel 15 is not representative of how the highway will respond to the subsidence in the extended study area. It does appear that the pavement in the extended study area is constructed on an open graded subbase material and the transverse joints are doweled. The open graded granular subbase can act as a slip plane, allowing the ground below the pavement to move laterally without dragging the pavement with it, while the dowels also help restrict displacement of the highway in the direction perpendicular to the direction of travel. A detailed analysis of all of these factors would be needed to better understand the effect the subsidence will have on the pavement structure within the extended study area.

3.0 Asphalt Relief Sections

The installation of asphalt relief sections proved to be beneficial in limiting the development of distress to these localized areas by absorbing the deformation caused by the subsidence. The distress causing the primary concern to traffic during subsidence are compressive bumps and blowups. The asphalt relief sections facilitate the development of compression bumps, which most likely do not develop instantaneously, like the blow-ups, but can be quickly milled so that the disruption to traffic is minimized. These asphalt relief sections have traditional been installed at the estimated location of the highest deformation with span lengths of ~60-ft in Pennsylvania upwards of 100-ft in West Virginia. It is unclear how this length is established. A shorter length could potentially be adequate for absorbing the necessary strain based on the observations during the mining of Panel 15. This should be further evaluated based on the future undermining conditions, including the pavement structure and predicted subsidence. The length of the asphalt relief section should be established based on the level of confidence with the following factors:

- The exact location of the point of highest deformation (increasing the length of the section with increases in uncertainty), and
- The estimated magnitude and area of high deformation.

Other aspects of the asphalt relief section design that could be evaluated would include types of fill material (alternatives to asphalt concrete), the depth at which the fill material should be placed, and a determination if the relief section should be constructed across both the traveling lanes and the shoulders or limited to just the traveling lanes. The type of existing shoulder would be a consideration in this decision. For example, can it be shown that a tied concrete shoulder maintained across the asphalt relief section provides connectivity that effectively dissipates the effects of subsidence and the resulting damage to the highway by preventing translational displacements? Or, does this additional rigidity result in higher damage?

A detailed analysis of the how each of these factors will affect subsidence impacts can be performed once the plans for the orientation and location of the undermining in the extended study area has been finalized. Only then will a better understanding of the impact of the subsidence on the development of distress in the pavement be obtainable.

Subsection IIId – Guiderail Analysis

1.0 Movement of the Guiderail in the LiDAR

When I-70 was undermined several guiderails experienced buckling and bended over the travel lane outside shoulder. To better understand these occurrences the University analyzed movement characteristics to both the ground and the guiderail support columns. Figure IIId.1 includes an example of one of these displacements. As can be seen in this image, the guiderail was separated from the support columns by a maximum distance of ~4-ft.

Figure IIId.1 – Example guiderail displacement

The images in Figure IIId.2 display the guiderail as it appears in the point clouds produced by the LiDAR scan surveyed on 5 February 2019 and 10 February 2019. At this point in time the longwall face was ~290-ft beyond the center portion of the displaced guiderail; although it began to bend outward in the morning on 8 February 2019 when the longwall face was ~190-ft beyond the displaced guiderail. This is the approximate time this area was expected to transition from tension to compression. Figure IIId.2 is separated into two images of the displaced guiderail. Figure IIId.2a represents the eastern portion of the guiderail, while Figure IIId.2b represents the western portion of the guiderail. On the eastern side, the guiderail support columns tilt inward toward the longwall face and into the portion of the guiderail that bent. On the western side, there does not appear to be as much tilt, but the base of the guiderail column are observed to move toward the displaced portion.

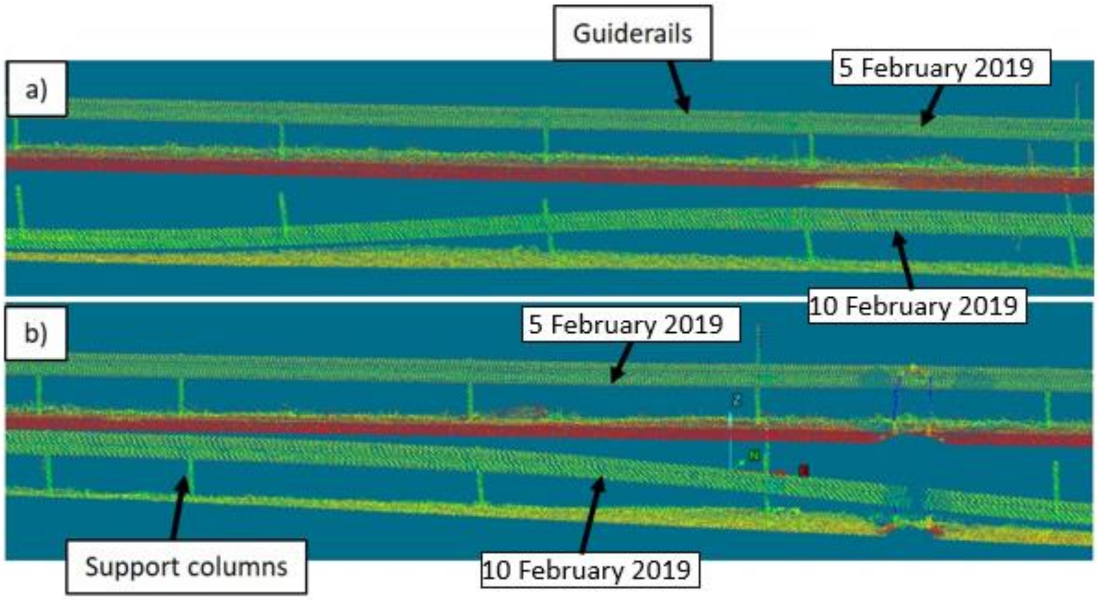

Figure IIId.2 – Guiderail and the columns as they appear in the LiDAR point clouds. a) Represents the eastern portion of the guiderail, and b) represents the western portion of the guiderail.

2.0 Observation of Vertical Post (angles) and Horizontal Deformations of the Guiderail Columns

The University utilized I-Site Point Studio to digitize the support columns to analyze their tilt and ground movements (Figure IIId.3). The digitized columns can be seen as they appear in the point clouds. Again, in the 5 February scan the support columns appear to be mostly upright, while in the 10 February scan are pointed inward. This would be in the direction of the longwall face, and also toward the area of extreme buckling.

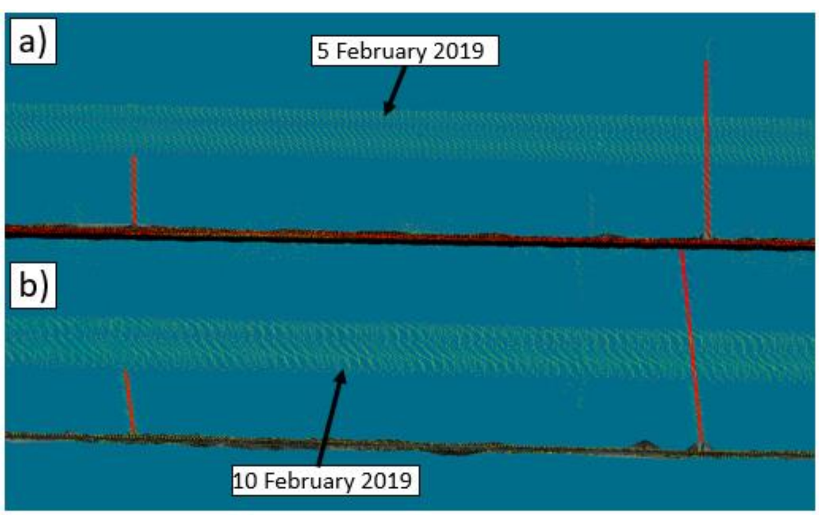

Figure IIId.3 – Example of the digitized columns in Maptek's I-Site Point Studio; a) 5 February, and b) 10 February 2019

The digitized columns were transferred from I-Site program into ArcGIS where locations and angles could be calculated and analyzed. Because these columns are digitized in three dimensions, the locations of the tops and bottoms of the columns could be tracked, allowing the tilt to be calculated. The resulting movement and tilt changes can be found in Figure IIId.4. Similar to the analysis that was described in Subsection IIa of the Task 3 Report, the northing and easting positions were transformed to match the orientation of the highway. By doing so, the movement is analyzed parallel and perpendicular to the direction of travel. The movements of the support columns were then compared to that of the expansion joints located in the travel lanes.

The combined movement displayed in Figure IIId.4a and IIId.4b indicate that support columns and expansion joints moved predominantly towards the northern face of Embankment #1. Figure IIId.4a seems to also indicate that there was some compression just east of the displaced guiderail, as the points that represent these features converged. Also of note is the differential movement that occurred between the guiderail columns and the travel lanes. The base of the guiderail columns consistently experienced higher magnitudes of movement than the travel lane joints. This is seen in both the parallel (Figure IIId.4a) and perpendicular (Figure IIId.4b) direction. In the parallel direction, the travel lanes show movements in the range of 0.3 to 2.6-in of movement while the support column bases indicate a range from 1.5 to 7.6-in. In the perpendicular direction, the travel lanes show a maximum value of 5.0-in, while the guiderail columns experienced up to 6.2-in. This differential movement most probably occurs because the travel lanes are connected with rebar, while the guiderails columns have bolted connections. The fact that the support columns are placed on the side of the highway and are anchored several feet into the ground also may have contributed to the differential movements, as they are likely more heavily influenced by subsurface movements.

Another result of the movements forced upon the guiderails was the change in the angular tilt and direction of the support columns (Figure IIId.4c). This figure shows that the columns began to tilt westward toward the longwall face. When compared their movements shown in Figure IIId.4a and IIId.4b, it can be seen that the high level of angular tilt corresponds to the high levels of horizontal movement. Once the horizontal movement began to taper off, so too did the change in angular tilt. As is depicted in Figure IIId.4a and IIId.4b, the base of the guiderail columns moved out toward the north facing slope of Embankment #1. Movement in this direction caused the guiderail columns to tilt in the opposite direction, as the tops of the columns did not move at the same rate as their bases.

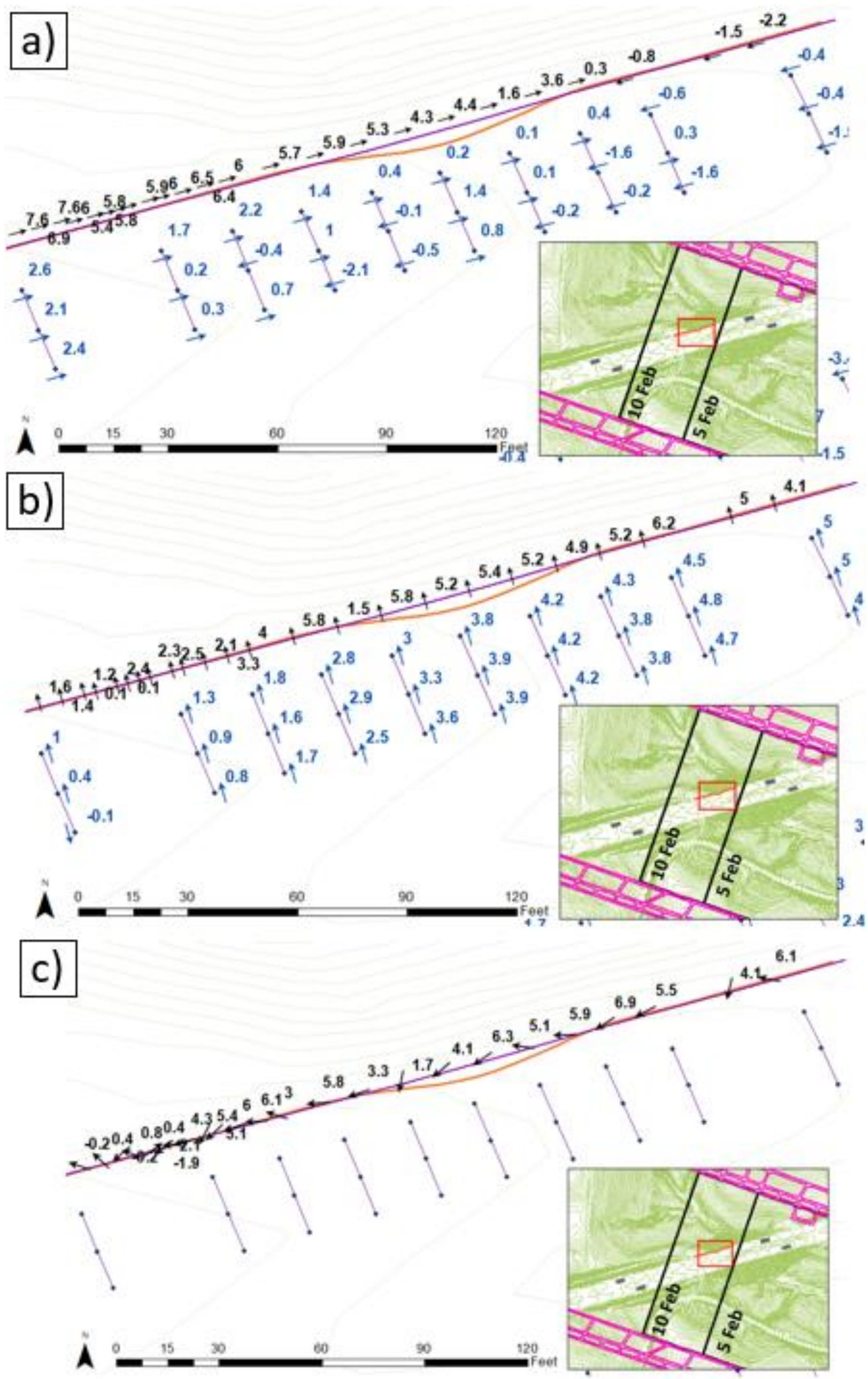

Figure IIId.4 – a) Movement values (in) for guiderail columns, b) transverse joints parallel and perpendicular to the interstate's orientation, and c) change in angular tilt and direction for guiderail columns near the guiderail displacement in the westbound lane

3.0 Accuracy of Measurements

When digitizing features within a point cloud, the accuracy and precision of any specific feature should be questioned. Depending on a feature's distance from the scanner, it is subject to varying levels of point density and line-of-sight issues. The guiderail and its support columns are located further from the scanner on the passing lanes of the interstate. As is shown in Figure IIId.5, point densities are highest in the passing lane and decreased toward the outside shoulder. In this image, the lighter points in the passing lane indicate higher point densities, while the darker areas in the outside shoulder show lower point densities. This distinction is important because the accuracy of a feature is dependent on the point density. Because points are sparser on the support columns, the precision and accuracy of these digitized features are more variable. Regardless, the University believes a high enough level of accuracy was obtained to produce meaningful movement results.

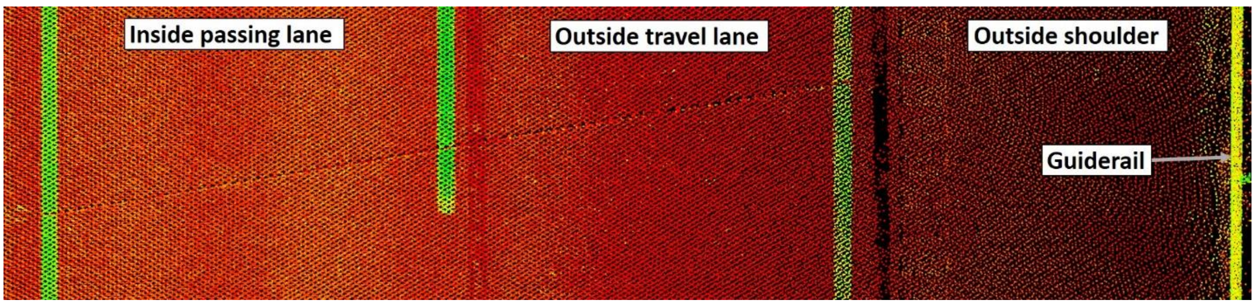

Figure IIId.5 – Example snapshot of the travel lanes as they appear in the point cloud and the varying level of point density associated with distance from the passing lane

4.0 Guiderail Deformation Associated with Surface Extension and Compression

During dynamic subsidence, the portion of the surface immediately behind the longwall face becomes subject to tensile strains. As the longwall face progresses, the tensile strains will transition to compression. When guiderails are positioned inside the tensile portion of the dynamic wave, the support columns will extend further apart, which should in theory cause instability in the guiderail beam as its support columns begin to diverge. As the portions of the I-70 subsided, the roadway seem to get pulled into the developing basin. In this case the guiderail appeared to be extending. When the University visited the study area on 5 February 2019, it observed a section of guiderail ~190-ft long that started to deviate away from the columns it was supported on. At this point in time, the displaced guiderail was already completely within the zone of compression (Figure IIId.6). It is possible that the displacement took place prior to the University's visit on 5 February when the guiderail was in the zone of tension, but no evidence of this is documented.

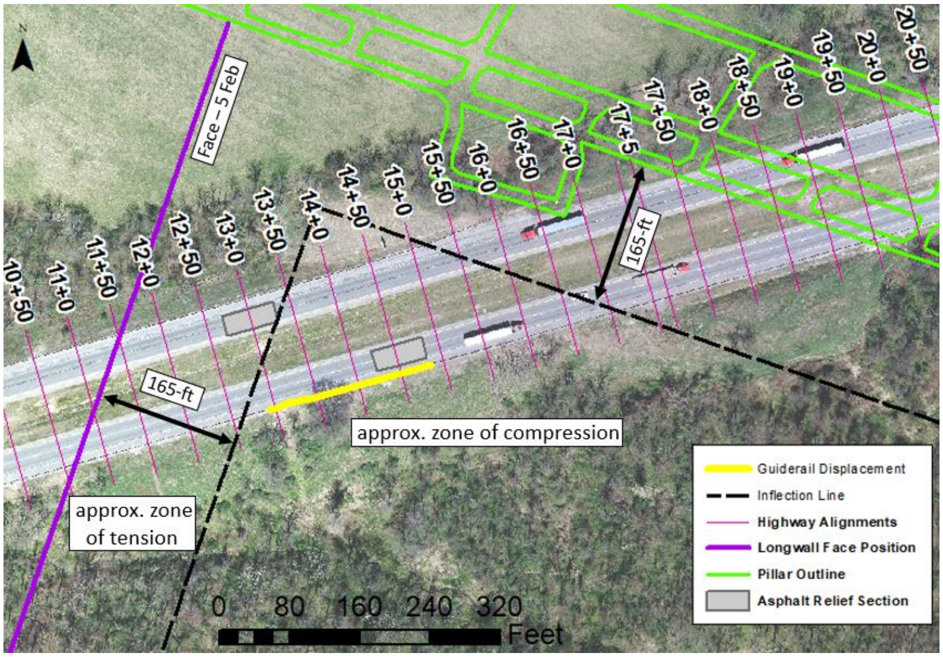

Figure IIId.6 – The portion of displaced guiderail observed by the University's team members on 5 February 2019

5.0 Safety Considerations

There were five occurrences of guiderail displacements over panel 15 (Figure IIId.7). Each displacement occurred when the guiderail transitioned from tension from tension to compression. Figure IIId.7 shows each guiderail displacement, along with the date they occurred and the approximate distance to the longwall face on that date. Each displacement occurred within 190 to 310-ft of the longwall face, or within 2-3 days of the being undermined. Most were similar in form, as they were bent outward into the outside shoulder of the travel lanes. The only exception is the displacement that was located near the westbound asphalt relief section. This displacement formed a zig-zag shape, with a portion of it forced out over the embankment. It is important to note that the displacements shown in Figure IIId.7 only depict the locations where displacement are obvious. Some other portions of the guiderails experienced less severe displacement. While each displacement occurred within the boundary of the embankment, it is not possible to determine if the embankment contributed to these displacements.

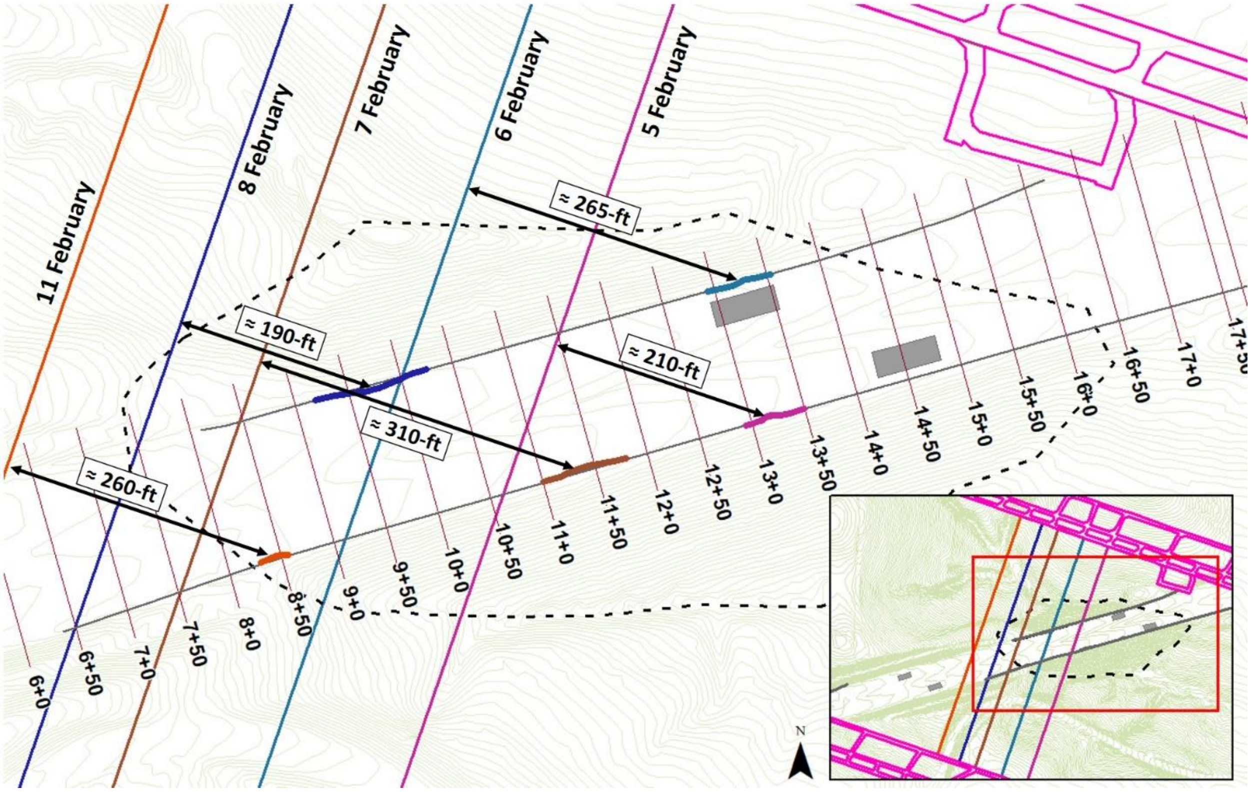

Figure IIId.7 – Map that depicts each guiderail displacement along with the face position on that date and the approximate distance

Subsection IIIe – Potential for Stream Pooling

1.0 Historical Trends in Pooling Impact Associated with Subsidence Basin Formation (Act 54)

Subsidence induced stream pooling has been documented in a series of Pennsylvania Department of Environmental Protection's Act 54 Five Year Assessment Reports (Iannacchione, et. al, 2011; Tonsor, et. al, 2014; and Bain, et. al, 2019). Pooling can occur when a stream has a new gradient below 2-pct and is subjected to greater than 1-ft of subsidence. Conditions along the Dutch Fork flood plain within the extended study area are locally conducive to the formation of subsidence caused stream pooling.

One dramatic example of this occurred a decade ago along Templeton Fork in the area of the East Finley Township Park (Figure IIIe.1). Here subsidence induced pooling occurred along a section of the stream and resulted in a significant intervention by the responsible mine operator as required by Pennsylvania's Act 54.

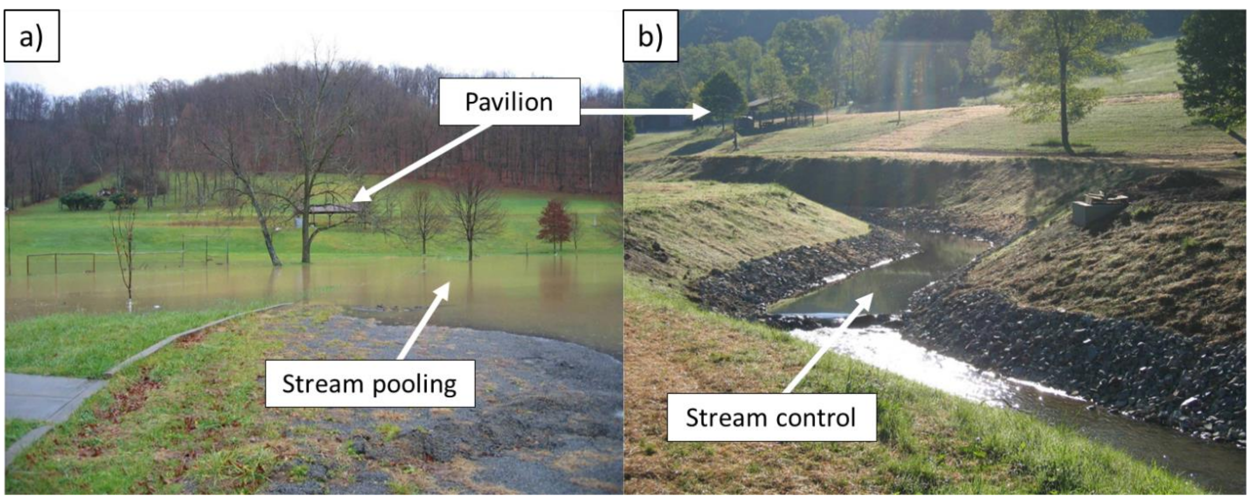

Figure IIIe.1 – a) Flooding of Templeton Fork as a result of longwall mining subsidence, and b) Post stream restoration activities as required by Act 54 and payed for by the responsible mining operation (Iannacchione, et. al, 2011)

This potential for pooling and the consequential construction activity needs to be understood since Dutch Fork will potentially cross over a future longwall panel. Through much of this area, Dutch Fork is a 3rd order stream. Many of the highway overpasses and associated concrete retaining walls, discussed in the Task 3 Report, could be undermined in the future. The problem arises when undermining causes existing stream gradient to be altered, increasing the potential for pooling. One example is provided over potential Panel F where Dutch Fork and the westbound lanes of I-70 are less than 50-ft apart (Figure IIIe.2).

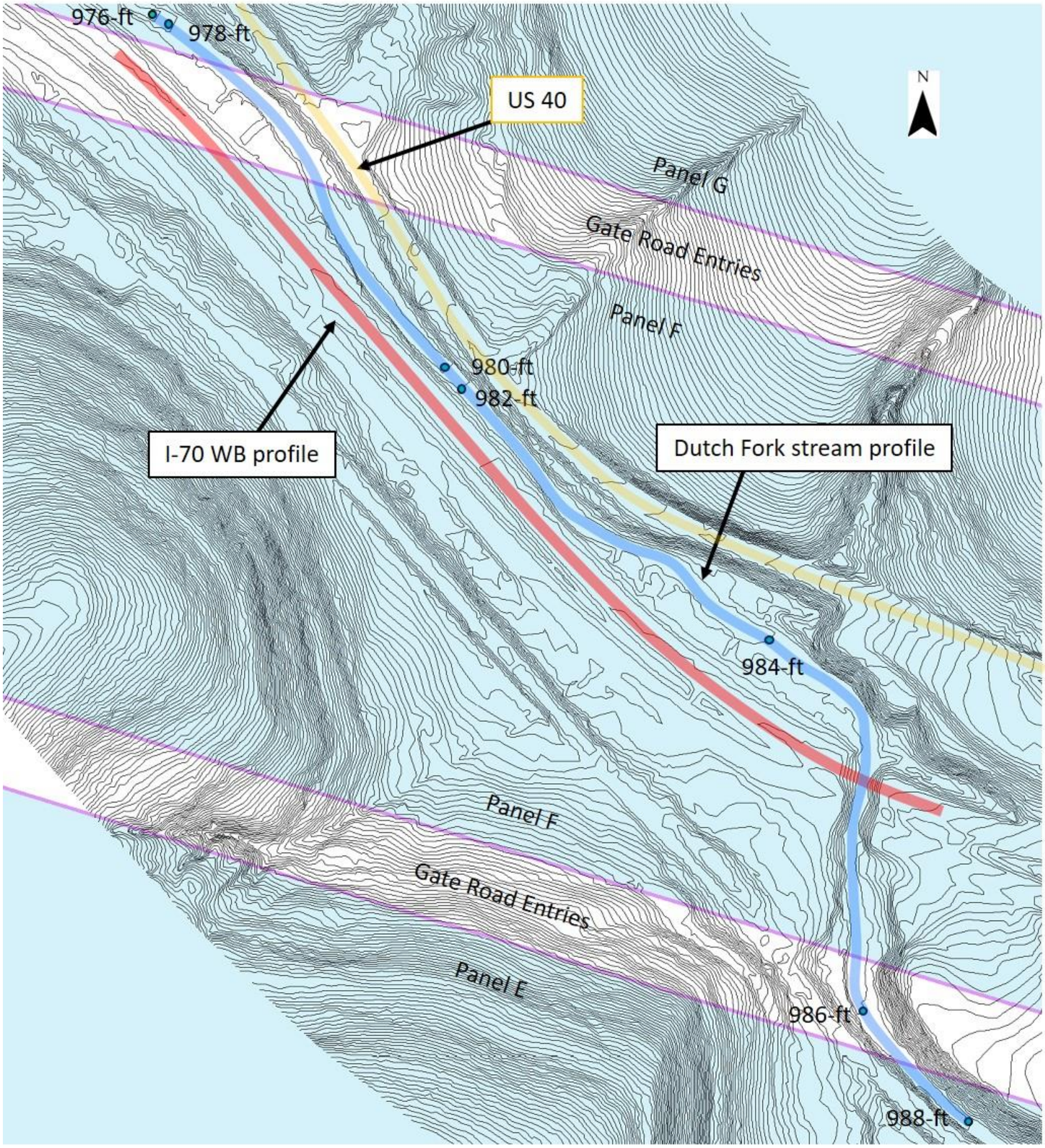

Figure IIIe.2 – Two elevation profiles, one along I-70 and the other along Dutch Fork over Panel F and its gate road entries, are plotted in Figure IIIe.3

Three profiles are developed over the gate road entries and Panel F to its south (Figure IIIe.3). One profile is along the westbound lanes of I-70 the other two along Dutch Fork. The elevations along profiles are estimated from existing surface contours and plotted in Figure IIIe.3. One profile is of the pre-subsidence westbound lanes of I-70 and the other two are stream gradients along a similar cross-section. Vertical subsidence over the gate road entries is minimal so elevations remain virtually the same. The stream elevation profiles over the Panel F are modified based on the distance from the measured stream elevation to the edge of the adjacent gate road entries. Panel F is ~400-ft below the surface in this area so the maximum vertical subsidence is estimated to be ~4.5-ft. Conversely, the influence point is ~126-ft from the edge of the panel and by definition will have a vertical subsidence of 2.75-ft (1/2 max. vertical subsidence). Using these values, a post-subsidence stream gradient is constructed. In this example, the surface above the gate road entries acts as a dam, causing water to pool for ~1,500-ft from that point. It should be noted that the pre-subsidence pavement of I-70 is about 10-ft above the current Dutch Fork stream channel. After subsidence this difference is potentially lessened since a pool several feet deep is possible. But even here the distance between the pool surface and the westbound lanes of I-70 would be 6 or 7-ft.

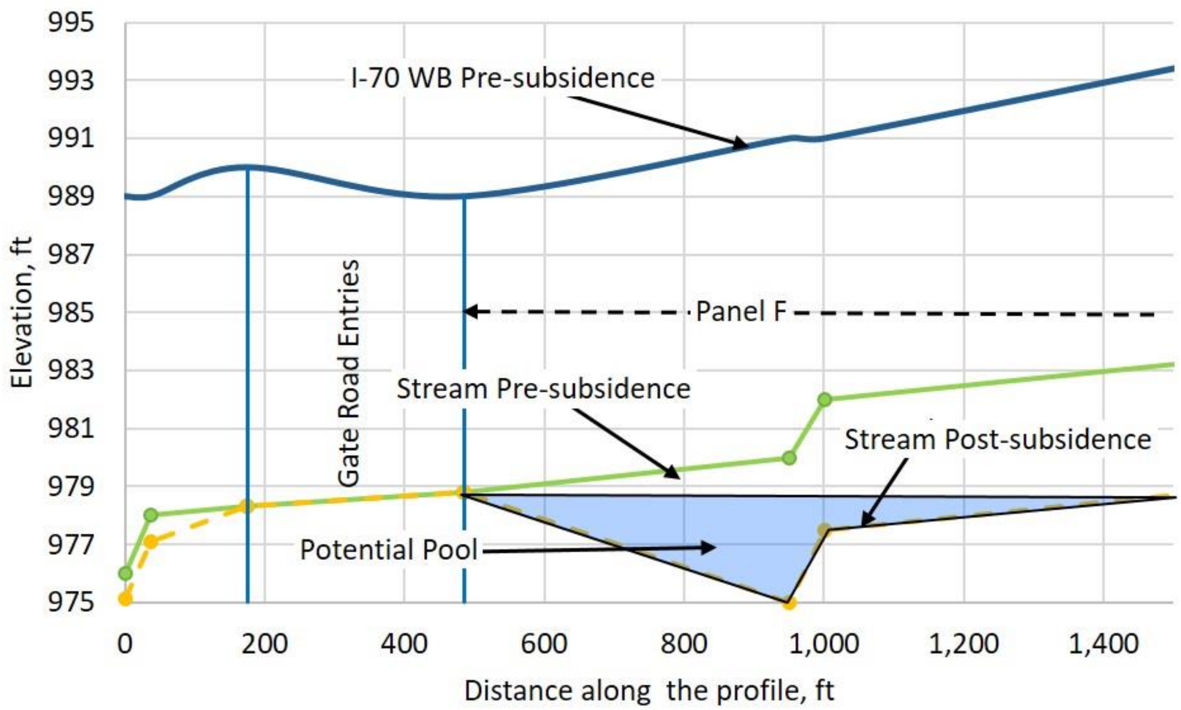

Figure IIIe.3 – I-70 and Dutch Fork stream profiles over Panel F showing the location of a potential pooling impact

The more likely problem will not be the potential for ponding on the roadway but for the significant construction activity that will be require to repair the stream to its approximate original gradient. This construction activity is called gate cutting and consist of reducing the elevation of the stream over the gate road entries concordant with the areas of greatest subsidence in the adjacent panel. Gate cutting consist of three distinct steps. In the first step the flow is diverted around the stream channel. This requires large capacity pumps with equally large diameter flexible water conduits, possibly discharging the flow into a protected rip-rap (Figure IIIe.4a). The second step alters the stream gradient by clearing debris from the stream channel, ripping and breaking stream bedrock, and re-grading the stream channel (Figure IIIe.4b). The third step establishes habitats with in-stream structures, adding bank stabilization to reduce erosion, and returning the stream to standards capable of sustaining future use (Figure IIIe.4c). All of these activities will need to take place in the very narrow corridor between the westbound lanes of I-70 and US 40.

Figure IIIe.4 – Gate cutting consist of three steps: a) diverting stream flow; b) altering the stream gradient; and c) restoring ecology and stabilizing stream banks

Subsection IIIf – Research Ideas

1.0 Advanced Lidar-based monitoring of undermining operations: challenges and perspectives

LiDAR-based techniques have been proven effective in the characterization of ground movements, both at the local (material level, 10^{-1} m) and global (structural level, 10^{1}-10^{2} m) scales. The main challenges in adopting these techniques lie in the evaluation of accuracy of the obtained 3D models, the computational time required to construct the point clouds, the accurate positioning in space of such point clouds (i.e., the geotagging operations) and sensor fusion capabilities to provide easier access to the spatial information (e.g., the RGB information for each recorded point).

One of the main objectives in the LiDAR surveying of horizontal infrastructure is to capture local and global deformation modes over time (i.e., under different conditions and throughout the undermining operations). To this extent, it is of vital importance to perform accurate scans prior to any expected ground movement, in order to define a baseline to compare subsequent scans to. It is therefore advisable to use easy-to-detect targets attached to salient features to detect (e.g., inner and outer shoulders, guide rails) to guide the feature recognition and segmentation operations.

Additional challenges regard the different spatial resolution obtained in the LiDAR depth maps across a scene, as a result of the fact that the car hosting the sensor usually only spans the mid-section of the Interstate. This results in portions of the scene to be consistently further away from the sensor (e.g., the shoulders and guide rails), yielding lower resolutions in these areas which are often times the ones of greater interest for the deformation quantification. The addition of targets to both the shoulders and guide rails can alleviate this problem, but it is also suggested that the scans are performed on "grids" rather than "lines" to increase the quality of the point clouds.

Gathering still pictures of the surveyed area is common in practice, but it brings the disadvantage of large datasets to be analyzed which contain disjointed information (i.e., the RGB information obtained from the pictures is not readily linked to the 3D point cloud). This yields severe drawbacks in the data manipulation operations, either because of the loss of potentially relevant information or a substantial increase in the post-processing cost and time. To this extent, recent advances in 3D imaging and reconstructions allow for the contextual, quasi-real time construction of hybrid LiDAR-RGB point clouds, by gathering the LiDAR depth information (in the form of a point cloud) and establishing a correspondence map with the RGB information (in the form of RGB matrices) by means of polar-grid mapping representations or Structure from Motion (SfM) techniques. In such a way, the dense point clouds (>10 points/sq.ft.) obtained through a LiDAR sensor can also retain the RGB information obtained by the camera sensor(s). This operation requires additional information, namely the position and 3D orientation of the scanner to be obtained by a GPS and an Inertial Measurement Unit (IMU). These techniques bring the appealing feature of readily available scans that leverage data fusion techniques to retain information that helps the post-processing operations. Advanced hybrid (LiDAR + RGB) reconstructions can, in fact, be used to increase the quality and efficiency of segmentation and feature extraction techniques on the 3D point clouds. This can ultimately allow for faster processing of the data, clearer outputs and (partially or entirely) automated 3D processing of the deformation fields (e.g., through semantic segmentation of the ground targets).

2.0 Evaluate Methods to Assess the Structural Integrity of Assets Subjected to Subsidence Induced Movements

During the process of conducting this research study, deficiencies were identified in our current understanding as to how highway structures respond to a developing subsidence basin. A research effort is needed to study how pavements are adversely affected by differential vertical and horizontal movements. The impact of these adverse effects on the pavement's available life span can and should be determined. In addition to pavements, the performance of several other structures, including single span overpasses, concrete retaining walls, and buried culverts when subjected to longwall mining subsidence has not been adequately studied. If hazards develop within a subsiding single span overpass, it could threaten the traveling public. If instabilities develop within reinforced concrete culvert, water flow could be disrupted potentially creating new safety and environmental hazards.

Current techniques to assess the integrity of structures discussed above is limited to PennDOT and AASTHO standards and recommendation, none of which apply to the kinds of movements expected during longwall mining. A promising approach would be to instrument exemplar structures to monitor pre-mining performance, including strains and/or deflections when subjected to a standard vehicle loading. The changes to the structure could then be monitored through this same instrumentation post-mining. Lastly, the structure could be subjected to the standard vehicle loading again post-mining to evaluate its performance. The pre- and post-mining performance would allow for a benchmark to be established for estimating the life consumed/remaining life of a structure in such circumstances, while also facilitating/validating the development of an inverse analysis approach to predict the life of a structure based upon pre-mining monitoring data along with subsidence predictions and/or monitoring.

REFERENCES

Anon (2004a). Buried Structures and Tunnel Liners, AASHTO LRFD Load and Resistance Factor Design, Chapter 12 on Pipes and Buried Structures, 91 p.

Anon (2004b). Buried Structures and Tunnel Liners, AASHTO LRFD Bridge Design Specifications, Section 10: Foundations, 3rd ed., p. 113.

Anon (2019). "Structures, Procedures, Design, and Plans Presentation", PennDOT Design Manual, Part 4 (DM-4), PDT No., 15M, December 2019 ed., 1084 p.

Bain, D., DaCanal, T., Iannacchione, A., Kautz, A., Shirey, P., Tonsor, S. Copeland, M., Deglmann, J., Hill, M., Kandanarachchi, D., Trout, S. and Winn, R. (2019). "The Effects of Subsidence Resulting from Underground Bituminous Coal Mining in Pennsylvania, 2013-2018," 5th Five-Year Report, Bituminous Mine Subsidence and Land Conservation Act, Act 54 Amendments, PA Department of Environmental Protection, submitted by the University of Pittsburgh, August 31, 2019, vol. 1 and vol. 2, p.

Gutierrez, J., Vallejo, L., and Lin, J-S. (2010). "A Study of Highway Subsidence due to Longwall Mining using Data Collected from I-79," Final Report for PennDOT Contract #510601, WO#015, 426 p.

Hebblewhite, B. and Gray R. (2014). "Non-Conventional Subsidence Behavior and Impacts – Ryerson State Park Dam, Pennsylvania USA Case Study," Proceedings of the 9th Triennial Conference on Mine Subsidence, pp. 51-60.

Hood, M., Ewy, R., and Riddle, L. (1981). "Empirical Methods of Subsidence Prediction – A Case Study," Proceedings Workshop on Surface Subsidence Due to Underground Mining, S. Peng, ed., West Virginia University, Morgantown, WV, pp. 100-123.

Iannacchione, A., Tonsor, S., Witkowski, M., Benner, J., Hale, A., and Shendge, M. (2011). "The Effects of Subsidence Resulting from Underground Bituminous Coal Mining on Surface Structures and Features and on Water Resources, 2003 to 2008," 3rd Five-Year Report, Bituminous Mine Subsidence and Land Conservation Act, Act 54 Amendments, PA Department of Environmental Protection, submitted by the University of Pittsburgh on January 10, 2011, 499 pages and 1 plate.

Iannacchione, A., Adelsohn, E., Buettner, N., Bumstead, J., DaCanal, T., and Donnelly, C. (2019). "Exploring Approaches to Managing Landslide Risk," Impactful Resilient Infrastructure Science and Engineering Technical Report, IRISE-19-P20-01-01, November 2019, 16 p.

Karmis, M., Goodman, G., and Hasenfus, G. (1984). "Subsidence Prediction Techniques for Longwall and Room and Pillar Panels in Appalachia," Proceedings of the 2nd International Conference on Stability in Underground Mining, University of Kentucky, Lexington, KY, August 6-8, 1984, pp. 541-553.

Luo, Y., and Peng, S. (1997). “Subsidence Prediction Influence Assessment and Damage Control,” Proceedings of the 16th International Conference on Ground Control in Mining, July, Morgantown, WV, pp. 360-366.

Mark, C., and T.P. Mucho, T.P. (1994). “Longwall Mine Design for Control of Horizontal Stress,” in New Technology for Longwall Ground Control: Proceedings of the USBM Technology Transfer Seminar, USBM Special Publication 94-01, pp. 53-76.

Mark, C., Agioutantis, Z. (2019). “Analysis of Coal Pillar Stability (ACPS): A New Generation of Pillar Design Software,” International Journal of Mining Science and Technology, https://doi.org/10.1016/j.ijmst.2018.11.007 - Also published in Proceedings of the 37th International Conference on Ground Control in Mining (2018), Morgantown, WV.

Miller, J.S. and Bellinger, W.Y. (2014). “Distress Identification Manual for the Long-Term Pavement Performance Program,” 4th edition, U.S. Department of Transportation, Federal Highway Administration, Report No. FHWA-HRT-13-092, 142 p.

Painter, R. (2020). Personal communication.

Peng S. and Cheng, S. (1981). “Predicting Surface Subsidence for Damage Preventions,” Coal Mining and Processing, May 1981, pp. 84-95.

Peng, S. S., Luo, Y, and Zhang, Z. M. (1995b). “Development of a Subsidence Database and Determination of Subsidence Parameters,” Proceedings of the 14th International Conference on Ground Control in Mining, West Virginia University, Morgantown, WV, August 1995, pp. 226-235.

Tonsor, S., Hale, A., Iannacchione, A., Bain, D., Keener, M., Pfeil-McCullough, E., and Garmire, K. (2014). “The Effects of Subsidence Resulting from Underground Bituminous Coal Mining, 2008-2013,” 4th Five-Year Report, Bituminous Mine Subsidence and Land Conservation Act, Act 54 Amendments, PA Department of Environmental Protection, submitted by the University of Pittsburgh on August 30, 2014, p.

Vallejo, L. (2020), Personal Communication.

Vallejo, L., and Lobo-Guerrero, S. (2005). "The Elastic Moduli of Clay with Dispersed Oversized Particles,” Engineering Geology, Vol. 78, 6.3, pp. 163-171.

Yancich, R. (1986). *Surface Subsidence in Longwall Mining – A Case Study.* Master’s Thesis, Department of Mining Engineering, West Virginia University.

Acknowledgement

The project team would like to thank members of PennDOT's staff, the administrators, engineers, scientists, geologists, and maintenance workers, for making this activity a rewarding experience for all those connected with it. In particular, we are grateful to Joseph Szczur and William Kovach, former and current District 12 Executives, for articulating the vision and need for the project. It was impressive to see how their staff prepared for the undermining of a major transportation artery and later brought this same section of highway back to normal operations. This was a large and complex effort and it came off in an admirable fashion. It is notable that these same individuals were always ready to search out answers for our inquiries. The one person we must personally recognize is Mr. Roy Painter, Geotechnical Engineer for District 12. Roy was our technical contact for this project and was invaluable to the project's success.

A special recognition to Pat Brown of Earth Inc and Joe Brennsteiner of SPK Engineering for sharing laboratory and surveying results and for their counsel throughout the project. During the study, West Virginia Department of Highways, E.L. Robinson Engineering, and Alliance Natural Resource's Tunnel Ridge Mine personnel, joined the project team with PennDOT and its contractors on a monthly basis to discuss important findings. These exchanges of information were beneficial for all parties.

There are many at the University of Pittsburgh that deserve special recognition. Both Dr. Radisav Vidic (Civil and Environmental Engineering Department Chair) and Ms. Amy Kapp (CEE Department Administrator) assisted with navigating this contract through the University's administration. Mark Magalotti and Keith Johnson, Co-Directors of the Center for Sustainable Transportation Infrastructure (CSTI), identified this research idea and worked to secure support and funding along with PennDOT's central office staff, Teresa Swisher and Shelley Scott.

What was perhaps most special for the project team was their participation in a vibrant research community at the University of Pittsburgh. This community consisted of not only the project team members but also the faculty, staff, and student body within the Civil and Environmental Engineering Department. In particular, two visiting graduate students, Jie Yanga and Qin Xiangnan from the University of Mining and Technology-Beijing, China, were invaluable in their assistance to help initiate subsidence modeling efforts. Taylor DaCanal, a graduate student working on a related research project, as well as Ethan Fisher, an undergraduate researcher on this project, assisted with planning, field work, and data analysis. The three graduate students assigned to the project, Mingzhou Li, Emily Adelsohn, and Robert Winn (Max) epitomized hard work and collegial cooperation. They were the ones responsible for doing the most meticulous and important work. A special thanks goes to Julie Vandenbossche whose knowledge in cement and concrete systems helped the team focus on the highway pavement, revealing some of the most unique data from this study. Lastly but not least, the project team thanks Luis Vallejo whose deep understanding of soil mechanics was critical in fully grasping the distinctive behavior of embankments subjected to subsidence.

To all of these individuals and organizations, you have our thanks and gratitude.

Anthony Iannacchione, Principal Investigator, University of Pittsburgh